

1 I am pleased to resubmit for publication the revised version of ACP paper acp-2014-
2 228. I have incorporated new figures, tables and text into the paper in response to the
3 reviewers' comments. The introduction and background sections have been combined
4 and condensed to better motivate the current study. The results section has been
5 condensed and restructured to frame the discussion of meteorological and other physical
6 and chemical processes through their effects on O₃ distributions. New analyses include
7 an evaluation of the simulated PBL depth and mean O₃ profiles calculated over broad
8 regions to facilitate comparison with other models. The revised paper includes
9 discussion of the potential implications of model biases in biogenic emissions and
10 clarifications of the implications of the aircraft-satellite-model O₃ intercomparison, and
11 numerous other clarifications and corrections to the text. Please find below my
12 responses to specific comments.

13 Reviewer #1

14 1. The major criticism I have of this paper is the lack of detailed information about the
15 process controlling chemical production of O₃ from the models. At present the model
16 results are compared against the observed O₃ but few details are given as to why the
17 model results agree or disagree with the observations from a chemical point of view.
18 There is some focus on the role of NO (from soil) and indeed comparisons are made to
19 NO profiles, but other important O₃ precursors (e.g. PAN) are neglected. Similarly
20 there is hardly any mention of the role of VOCs in the paper. For example, isoprene acts
21 as an important O₃ precursor. How sensitive are the model results to isoprene emissions
22 and chemistry? A cursory comparison of isoprene fluxes from observations and the
23 MEGAN model is included. But there is little to no discussion on the impacts biases in
24 isoprene oxidation may cause. A large amount of the model observation comparison
25 focuses on comparison with meteorological data. Whilst this is undoubtedly a key
26 component to the story I suggest perhaps some of this could be cut down and more
27 analysis on the O₃ budgets could be included. Or more links could be drawn between
28 the chemistry and meteorology. What impact does biases in temperature have on O₃?
29 The wet scavenging of soluble species should impact O₃ too, the effect of which can be
30 relatively easily tested in the model simulations.

31 We thank the reviewer for his/her comments. We have added the following text
32 discussing the possible model sensitivities to errors in emissions of isoprene and other
33 BVOCs (lines 567-576 in the Revised Manuscript):

34 "Emissions of BVOCs can increase O₃ production by the following mechanism.
35 Oxidation of BVOCs can lead to formation of HO₂ and RO₂•, which react with NO to
36 form NO₂. NO₂ in turn photolyzes to form O(³P), which reacts with O₂ to form O₃
37 (National Research Council, 1991). We expect the polluted east/south regions during

38 BARCA A to be VOC-sensitive and the clean west, north and around Manaus regions
39 during BARCA A and all regions in BARCA B to be NO_x-sensitive. Kuhn et al. (2010)
40 determined via aircraft transects in the Manaus urban plume that most of the VOC
41 reactivity was provided by isoprene emissions from the surrounding rainforest, and NO_x
42 emissions suppressed O₃ production close to urban sources, but stimulated it
43 downwind.”

44 One limitation of this study is that measurements of only a few gas phase species (CO,
45 O₃) are available from BARCA. Thus, it is not possible to evaluate other important O₃
46 precursors (PAN, VOCs) in the models using BARCA data. We also agree that wet
47 scavenging of soluble O₃ precursors should impact O₃ production. However, as
48 measurements of only relatively passive/insoluble species (CO, O₃) were taken during
49 BARCA, a detailed evaluation of the impact of wet scavenging falls outside the scope
50 of this study. The meteorological evaluation of the models has been shortened and
51 rewritten to emphasize how biases in meteorological variables (e.g. temperature) impact
52 O₃ (Section 4.2, lines 452-522).

53 References

54 National Research Council, 1991. Rethinking the Ozone Problem in Urban and
55 Regional Air Pollution. National Academy Press, Washington, DC, 500pp.

56 In general the manuscript is well written, however, I think the paper could benefit from
57 a number of changes, below, before being published in ACP.

58 General comments (line number, page and comment):

59 2. Line 1, page 14017: The authors have not included the role of VOCs (in particular
60 BVOCs) as O₃ precursors in the Amazon basin. Is this because they have no net effect
61 on O₃?

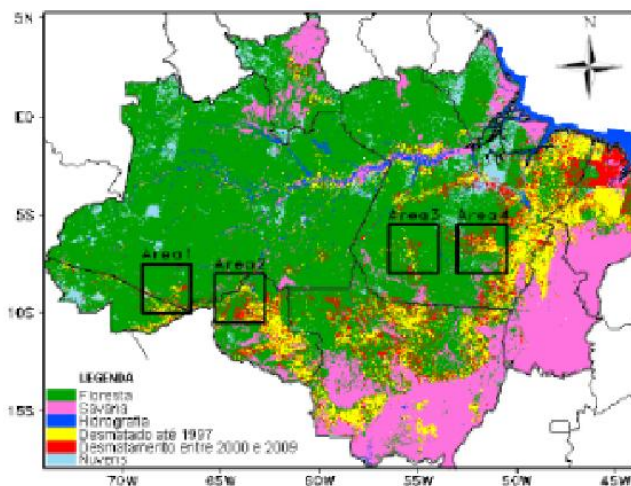
62 We chose to focus on NO_x as the primary O₃ precursor in the Amazon basin under clean
63 conditions based on the study of Jacob and Wofsy (1988), who found that O₃ production
64 in a photochemical model based on ABLE-2A was relatively insensitive to the amount
65 of VOCs present. This was because oxidation of CO provided sufficient HO_x to
66 generate background O₃ values of 20 ppb. Thus, the amount of additional O₃ produced
67 in the boundary layer depended on the amount of NO_x present. However, the polluted
68 regions during BARCA A may be VOC-sensitive, and we have added the following text
69 to discuss the possible implications (lines 760-764):

70 “In polluted, VOC-sensitive conditions, approximately the correct net amount of O₃ is
71 generated in the PBL. This suggests there is insufficient VOC reactivity in the models,
72 since the correct amounts of O₃ deposition velocities and NO_x emissions would both
73 decrease O₃ production.”

74 3. Line 20-27, page 14020: Are there likely to be any issues with using land use data
75 from c.a. 2000 when comparing to observations made in 2008/9?

76 Conversion of forest to pasture land cover reduces surface latent heat fluxes and
77 increases sensible heat fluxes, as shown in Figs. 6-7 using data from von Randow et al.
78 (2004). On a local scale, at least during the dry season, these changes decrease moisture
79 content and increase surface temperature and the depth of the convective boundary layer
80 over pasture areas (Fisch et al., 2004). Wang et al. (2009) found that deep convection
81 was stronger over forested areas due to the greater humidity, but that shallow
82 convection was enhanced over pasture areas.

83 The PROVEG dataset (years 2000-2001) was the most recent available for use in
84 regional models at the time of this study. However, deforestation from 2000-2009 (see
85 figure below) was minimal in the BARCA flight regions. Recently an updated
86 vegetation map based on MODIS observations in 2012 was produced for regional
87 models, and will be used in modeling studies going forward.



89 Figure 3.4 from Oliveira (2009): red areas were deforested from 2000-2009 according
90 to data from PRODES (Satellite Monitoring of the Brazilian Amazon) Project (2010,
91 <http://www.obt.inpe.br/prodes/>)

92 References:

93 Fisch, G., Tota, J., Machado, L. A. T., Silva Dias, M. A. F., Lyra, R. F. da F., Nobre, C.
94 A., Dolman, A. J., and Gash, J. H. C.: The convective boundary layer over pasture and
95 forest in Amazonia, *Theor. Appl. Climatol.* 78, 47–59, DOI 10.1007/s00704-004-0043-
96 x, 2004.

97 Oliveira, R. A., *Análise das Tendências da Precipitação sobre o Brasil e Impactos do*
98 *Desmatamento no Regime de Chuvas na Amazônia Legal*, Master's Thesis in

99 Meteorology, National Institute for Space Research (INPE), São José dos Campos,
100 Brazil, sid.inpe.br/mtc-m18/2011/12.08.10.56-TDI, 2009.

101 Wang, J., Chagnon, F. J. F., Williams, E. R., Betts, A. K., Renno, N. O., Machado, L.
102 A. T., Bisht, G., Knox, R., and Bras, R. L.: Impact of deforestation in the Amazon basin
103 on cloud climatology, P. Natl. Acad. Sci. USA, 106(10), 3670-3674,
104 doi:10.1073/pnas.0810156106, 2009.

105 4. Line 18, page 14022: Other modeling groups will, I hope, find the observations very
106 useful for model evaluation. As it may prove problematic to sample other models in the
107 manner the authors have could the authors comment on the biases from averaging the
108 observed O₃ in large areas compared to the sampling they perform in the current
109 manuscript (i.e. if they were to average the model O₃ from -3N to 4N, -58E to -68E
110 (roughly speaking the clean sector in Figure 2 (a), how would that compare to the
111 results presented in Figure 2(a)?).

112 Following the reviewer's suggestion, to facilitate other modeling groups' comparisons
113 with the data and modeling results of this study, a new figure has been added (Fig. 16)
114 which compares the mean observed profiles with large averaged area from the models
115 for: clean (West, North and around Manaus regions) and polluted (East and South
116 regions) regions during BARCA A and all regions during BARCA B.

117 The following text has been added (lines 350-361) explaining the methodology:

118 "To facilitate comparison of other models with the data presented in Fig. 2, mean
119 profiles from the large regions corresponding to clean (west, north and around Manaus
120 regions) and polluted (east and south regions) regions during BARCA A and all regions
121 during BARCA B are presented in Fig. 16. From the models, all horizontal grid points
122 falling within the corresponding region's longitude and latitude bounds for each flight
123 day (Table 6) and the closest model output times (12:00-18:00 UTC / 8:00-14:00 LT)
124 were averaged into 500 m vertical bins."

125 The following text has been added (lines 553-557) presenting the results:

126 "A similar model behavior is seen as in the mean profiles for individual regions. All
127 simulations over-estimate O₃ throughout the PBL and lower troposphere during clean
128 conditions in BARCA A, but under-estimate O₃ in polluted conditions. This is
129 especially true from 2-4 km where biomass burning plumes detrain O₃ precursors.
130 During BARCA B all simulations show good agreement."

131 5. Line 5, page 14023: The authors need to include the geographic extent that "west,
132 north etc." refer to in Figure 2 (and Figures 18-21).

133 A table has been added to include the geographic extents and dates encompassed by the
134 regions (lines 438-440):

135 “The longitude and latitude bounds and flight dates included in each geographic region
136 from BARCA A and BARCA B are listed in Table 6.”

137 6. Technical corrections (line number, page and comment):

138 Line 24, page 14013: Typo. “increased” should have “be” inserted before it.

139 Line 24, page 14015: Typo. “northem” should be “northern”.

140 Line 18, page 14030: Typo. Amazonia needs correcting.

141 We apologize for these errors, and we have made the suggested corrections in the text.

142

143 Reviewer #2

144 The paper describes an analysis of the temporal and spatial variability in ozone
145 concentrations, fluxes and controlling processes as observed during the BARCA
146 campaigns. This analysis is supported by model simulations done with the regional
147 chemistry transport modelling systems CCATT-BRAMS and WRF-CHEM. I deem this
148 being a very interesting analysis that aims to identify the role of chemical versus
149 physical and dynamical processes in O₃ over the Amazon forest for the contrasting
150 meteorological and chemical conditions of the wet and dry seasons. This analysis
151 combines the information gained from both detailed observations as well as model
152 analysis. As such it fits in very well with the scope of ACP but there are, according to
153 me, a number of major issues that must be resolved. For example, in the model
154 application there have been some processes not being considered/not well described
155 (anthrogenic emissions) but that are of potentially large relevance for O₃/photo-
156 chemistry over the Amazon forest (see detailed comments below). My most serious
157 concern is about the model application being used too much in a “black box” mode.
158 There are many statements including the term “may” expressing that the models are
159 somewhat being applied as a black box not really being able to really nail down the
160 reasons for the found discrepancies between model simulated and observed chemical
161 and meteorological properties. By the way, from the evaluation of the meteorological
162 parameters it becomes obvious that the model representation of the meteorology for the
163 Amazon region still poses a large limitation to properly simulate the atmospheric
164 chemistry being largely driven by these meteorological (and hydrological) drivers.

165 We thank the Reviewer for his/her general comments. Numerous modifications were
166 made that are detailed in the responses to the specific comments below.

167 1. Abstract: “However, O₃ simulated by the models was lower than both BARCA
168 observations in mid-levels and total tropospheric O₃ retrieved from OMI/MLS,
169 suggesting that the satellites are dominated by middle troposphere and long-range
170 processes and are not a good indication of O₃ conditions in the PBL.”; Satellites are
171 dominated?? This is apparently a very weird sentence that requires re-writing and re-
172 thinking. The observations should be all right but apparently the models do a relatively
173 poor job on representing the free troposphere-BL gradient in O₃.

174 We thank the reviewer for his/her comment. We did not intend to indicate that the
175 model-satellite discrepancy indicates an error in the satellite retrieval, and have altered
176 the text to specify that the models do a relatively poor job of representing the free
177 troposphere-BL gradient in O₃ compared with aircraft and satellite observations. The
178 new sentence (lines 31-37) now reads:

179 “In addition, O₃ simulated by the models was either within the error bars or lower than
180 BARCA observations in midlevels (3–5 km a.s.l.), and lower than total tropospheric O₃
181 retrieved from OMI/MLS, which is primarily comprised of middle troposphere O₃ and
182 thus reflects long-range transport processes. Therefore, the models do a relatively poor
183 job of representing the free troposphere-BL gradient in O₃ compared with aircraft and
184 satellite observations, which could be due to missing long-range and convective
185 transport of O₃ at mid-levels.”

186 2. Introduction; the paper starts straight away on the research questions to be addressed
187 in this paper but where it seems that first indicating why an improved
188 understanding/quantification of ozone temporal and spatial variability in the tropical
189 rainforest environment is important.

190 We agree with the reviewer that explaining the motivation for the study is important
191 before presenting the specific science questions. The introduction has been revised to
192 start with an explanation of why an improved understanding/quantification of ozone
193 temporal and spatial variability in the tropical rainforest environment is important,
194 followed by the statement of the scientific questions.

195 2. Introduction, line 65: “high availability of solar radiation”; rephrase to high solar
196 radiation levels

197 The sentence has been revised to include the reviewer’s suggestion.

198 The new sentence (lines 56-59) now reads:

199 “The Amazon Basin continues to rapidly urbanize, and urban emissions of O₃
200 precursors are also expected to grow. Emissions from cities in the tropics may have a
201 larger impact on the upper troposphere due to high solar radiation levels and intense
202 convective transport (Gallardo et al., 2010).”

203 3. Line 78; here it is stated that in-situ observations of cloud properties and chemical
204 species are the reason that we cannot constrain this system well ; I think it is much more
205 than only cloud properties and chemical species measurements; we need information on
206 many additional parameters; land use changes, boundary layer dynamics, cloud aerosol
207 interactions at the larger scale, etc.

208 We agree with the reviewer that many parameters/processes affect atmospheric
209 chemistry over Amazonia. The sentence has been revised to include the reviewer's
210 suggestion.

211 The new sentence (lines 96-98) now reads:

212 "In-situ data on cloud properties and chemical species, as well as observations of land
213 use changes, boundary layer dynamics and larger-scale cloud-aerosol interactions, are
214 scant in this region."

215 4. Line 90: "It is interesting to compare BARCA data to observations from the NASA
216 Amazon Boundary Layer Experiments ABLE campaigns (ABLE-2A and -2B), which
217 took place during the dry season of 1985 and wet-to-dry transition of 1987". I also think
218 this is interesting to do but then it should be stated what is expected from such a
219 comparison with these data from the 80's.

220 We agree that it is important to explain the purpose of comparing data from the current
221 campaign with one which took place three decades ago.

222 The following text has been added (lines 216-224) to reflect this suggestion from the
223 reviewer:

224 "Andreae et al. (2012) showed that CO mixing ratios were about 10 ppb higher during
225 ABLE-2B than in BARCA B everywhere except the southern region, reflecting the
226 global trend towards decreasing CO emissions since the 1980s, particularly in the
227 Northern Hemisphere. The CO comparison also showed a similar enhancement of 10–
228 20 ppb in the lowest 1 km above the surface, attributed to diffuse biogenic sources, and
229 also indicated that the much higher enhancements during the dry season in BARCA A
230 must be due to anthropogenic or biomass burning inputs. The O₃ comparison is
231 expected to yield information in long-term trends in O₃ production in the Amazon
232 Basin, as well as the relative importance of biogenic, urban and fire sources."

233 5. Line 134: "During BARCA A, coarse model aerosols were predominantly from
234 biogenic emissions and biomass burning, while fine mode aerosols consisted of biomass
235 smoke and some Secondary Organic Aerosol (SOA) from biogenic Volatile Organic
236 Compounds (VOCs)". I guess you refer here to coarse mode aerosols but how do you
237 know what the sources are of these coarse mode aerosols?

238 Numerous studies have focused on aerosol composition and origin in the Amazon
239 (Martin et al., 2010 provides a review). These studies show that the dominant coarse
240 mode source is primary biogenic emissions, while the main fine mode source is biomass
241 burning in the dry season and Secondary Organic Aerosol (SOA) from biogenic
242 Volatile Organic Compounds (bVOCs) in clean conditions. However, the aerosol size
243 distribution was not measured during BARCA, so the following sentence was removed:

244 “During BARCA A, coarse model aerosols were predominantly from biogenic
245 emissions and biomass burning, while fine mode aerosols consisted of biomass smoke
246 and some Secondary Organic Aerosol (SOA) from biogenic Volatile Organic
247 Compounds (VOCs).”

248 Reference:

249 Martin, S. T., Andreae, M. O., Artaxo, P., Baumgardner, D., Chen, Q., Goldstein, A. H.,
250 Guenther, A., Heald, C. L., Mayol-Bracero, O. L., McMurry, P. H., Pauliquevis, T.,
251 Pöschl, U., Prather, K. A., Roberts, G. C., Saleska, S. R., Dias, M. A. S., Spracklen, D.,
252 Swietlicki, E., and Trebs, I.: Sources and properties of Amazonian aerosol particles,
253 *Rev. Geophys.*, 48, RG2002, doi:10.1029/2008RG000280, 2010.

254 6. Line 142: “The mean contribution from biomass burning to total CO during BARCA-
255 A was about 31%, with a contribution from background (110 ppb) of about 61%”

256 First of all refer to all flights in a consistent way; BARCA-A (previously it was BARCA
257 A); Furthermore, the second part of the sentence reads weird; rephrase.

258 The sentence has been corrected to refer to the field campaigns in a consistent way
259 (BARCA A) and to explain the data more clearly.

260 The revised sentence (lines 161-163) now reads:

261 “According to analysis of tracer simulations, during BARCA A biomass burning
262 contributed on average about 56 ppb (31%) to the total CO of around 180 ppb, while the
263 background was 110 ppb (61%).”

264 7. Line 150: “Small boundary layer enhancements were attributed to a source from the
265 oxidation of biogenic VOCs”. Would be good to see some reference here.

266 The reference (Andreae et al., 2012) has been included at the end of this sentence (lines
267 170-171).

268 8. Line 152: “The simulated vertical CO profiles matched mean observed values, but
269 were overly vertical (too low near the surface and too high above 3 km), suggesting that
270 the models were overly diffusive or had too much convective transport”. Here you
271 already discuss a model result, one that is indicating a quite essential problem with the

272 models relevant for the presented analysis before you have even introduced in more
273 detail these models and their set-up.

274 The following sentence was added at the beginning of the paragraph (lines 172-175) to
275 indicate that the model results being discussed are from Andreae et al. (2012), not the
276 current study:

277 “Andreae et al. (2012) also showed simulated vertical CO profiles from CCATT-
278 BRAMS and WRF-Chem simulations, as well as the Stochastic Time Inverted
279 Lagrangian Transport (STILT) model with two different meteorological field inputs and
280 the WRF Greenhouse Gas Module (WRF-GHG).”

281 9. In the overview of the O₃ observations and role of different mechanisms explaining
282 this behavior I miss the references to studies that have demonstrated/explained the
283 behavior, e.g., line 181 on the role of convection in lofting O₃ and a chemical
284 production of 15 ppbv d⁻¹ over Brazil but also already at the beginning of the section on
285 the role of NO/BVOC emissions versus transport, on the observations collected in
286 Rondonia, etc.

287 We thank the reviewer for his/her suggestion on how to clarify the references in the text.
288 This portion of the background section has been condensed as follows (lines 76-79):

289 “Previous analyses of satellite ozone data have noted early-year O₃ maximums in the
290 tropical Southern Hemisphere primarily associated with cross-Atlantic transport of
291 biomass burning emissions from Africa (Fishman and Larson, 1987; Thompson et al.,
292 1996), Northern Hemisphere fires and lightning NO_x (Edwards et al., 2003).”

293 10. Lines 186-193; this is one example of extreme long sentences that make the paper
294 difficult to read; there are many more of those long sentences that require editing.

295 Numerous sentences were edited to make them shorter and easier to read.

296 11. Lines 218: “dry deposition in the region was a globally significant O₃ sink”, dry
297 deposition in the region provides a significant sink in the global O₃ budget.

298 Line 228; “aboard”, onboard (?)

299 The suggested changes have been made in the text.

300 12. Line 230; where the measurements collected at 1.5m above the soil surface or above
301 the canopy top? and what was the vertical extent over which the profiles were sample?
302 In the forest canopy there are large gradients especially during nighttime and then the
303 reference height becomes very important.

304 The sentence has been revised to clarify the height and vertical extent at which the
305 measurements were collected. The sentence (lines 208-213) now reads:

306 “As part of ABLE-2, near-continuous O₃ surface measurements (1.5 m above the soil
307 surface) showed daytime maximums of 3.7 ppb inside a forest and 5.7 ppb in a clearing
308 (typical standard deviations of 0.3 ppbv). Additionally, tower measurements at the
309 clearing site showed higher O₃ values of 6.7 ppb at 7 m above the soil surface and 6.9
310 ppb at 15 m above the soil surface (Kirchhoff et al., 1990).”

311 13. Line 281; I appreciate the overview of all the measurements that have informed us
312 about the typical features of O₃ and the photochemical and mixing/transport regimes
313 over the Amazon but at the end what can be concluded from this?? Because of the vast
314 amount of information it would be optimal to draw some conclusions about the main
315 findings.

316 Different O₃ measurement methods enable the observation of different physical and
317 chemical processes affecting O₃ variability in the Amazon, with satellites identifying
318 fire and lightning sources of precursors, ground measurements observing surface
319 processes, and aircraft in the location of convective transport. The following paragraph
320 was added to the Introduction (lines 90-96):

321 “Thus, satellite observations enable the attribution of tropical O₃ maxima to biomass
322 burning and lightning NO_x sources, while ground-based measurements allow the
323 identification of key surface processes in the Amazon Basin affecting O₃ amounts.
324 These processes include O₃ production from soil NO_x emissions and removal via dry
325 deposition to the forest canopy. Aircraft campaigns complete the suite of observations,
326 allowing the examination of convective lofting of surface emissions, with biomass
327 burning emissions of particular importance on the regional scale.”

328 14. Line 328; I think that indicating the location with 2 numbers behind the comma
329 suffices.

330 We have corrected the latitude/longitude locations to use two decimal places (lines 428-
331 432).

332 15. Line 387: “Anthropogenic emissions were estimated from the RETRO, GOCART
333 and EDGAR v4.0 global databases updated with South American inventories (Alonso et
334 al., 2010)”. It is rather easy to read over this quite essential part of the analysis. The
335 emissions, especially those of NO_x, will ultimately determine to a large extent the
336 photochemistry over the Amazon basin. Than having an estimate of the emissions based
337 on a selection of different emission inventories might introduce a large range in results.
338 I think it is essential to provide the emission inventory as used in this analysis and also
339 show how the numbers compare to the different alternatives; e.g., how do the RETRO
340 and EDGAR v4.0 compare for this domain and how does the actually applied inventory
341 compare to those global inventories for the domain?

342 In PREP-CHEM-SRC, the emissions are obtained from RETRO if available for that
343 species, then from EDGAR v4.0, otherwise from GOCART. The purpose of this is to
344 use the most consistent emissions inventory possible. The following sentence has been
345 added in order to clarify this point (lines 286-292):

346 “Emissions are obtained from RETRO if available for that species (CO, NO_x,
347 chlorinated hydrocarbons, acids, esters, alcohols, ethers, benzene, ketones, methanal,
348 other alkanals, other aromatics, C₂H₂, C₂H₄, C₂H₆, C₃H₆, C₃H₈, C₄H₁₀, C₅H₁₂, C₆H₁₄
349 plus higher alkanes, other VOCs, toluene, trimethylbenzenes, xylene), then from
350 EDGAR v4.0 (NMVOC, SO₄, CO₂, SF₆, N₂O), otherwise from GOCART (BC, OC,
351 SO₂, DMS), in order to use the most consistent emissions inventory possible.”

352 As the differences between the RETRO emissions and PREP-CHEM-SRC emissions
353 are documented and illustrated in Alonso et al. (2010), we do not feel it is necessary to
354 include another figure in the present paper.

355 16. I also realized, reading through the rest of the paper, that there is not reference at all
356 to how the atmosphere-biosphere NO_x exchange is treated, a component that is essential
357 for the analysis in all the areas without substantial anthropogenic influences.

358 Biogenic NO emissions were not included in these simulations as NO was not available
359 for the MEGAN 2000 climatology. Future simulations will include online MEGAN
360 emissions of NO and other biogenic species. The following sentence was added to the
361 model description section (lines 294-297) to make this clearer:

362 “The MEGAN 2000 climatology includes numerous biogenic species (acetaldehyde,
363 formaldehyde, other ketones, acetone, isoprene, propane, methane, propene, ethane,
364 methanol, sesquiterpenes, ethene, monoterpenes and toluene), but not soil NO
365 emissions.”

366 17. Line 410: “while in WRF-Chem, wet deposition and lightning production of NO_x
367 were not considered?”. Why?? I think this should be explained and then later on it will
368 be important to demonstrate/discuss the consequences of ignoring these quite essential
369 features in the presented analysis

370 The text was modified to explain why these processes were not included in the WRF-
371 Chem simulation:

372 (lines 320-322) On the other hand, no wet scavenging is included for cloud water and
373 precipitation resolved by the microphysics scheme, because this option is not currently
374 available in WRF-Chem for the RACM chemical mechanism.

375 (lines 331-333) “In WRF-Chem, lightning production of NO_x was not included, because
376 these parameterizations have not yet been evaluated for the Amazon region.”

377 The following text discusses the consequences of ignoring these processes:

378 (lines 322-326): “O₃ production in the upper troposphere is affected by the net
379 convective transport of soluble HO_x precursors (including hydrogen peroxide (H₂O₂),
380 methyl hydroperoxide (CH₃OOH) and formaldehyde (CH₂O)). However, uncertainties
381 remain about the scavenging efficiencies of these and other soluble species by deep
382 convective storms.”

383 (lines 333-337): “In the tropics, over continents, lightning production is comparable to
384 other sources of NO_x, including biomass burning and soil release, and it is the primary
385 source over oceans (Bond et al. 2002). Since lightning NO_x production peaks in the
386 upper troposphere, it could be an important contributor to ozone production.”

387 18. Line 480: “Especially in the case of WRF Chem, the excessive precipitation rate
388 may be due to a too sensitive deep convective trigger function or underestimated
389 shallow convection, leading to a more unstable atmosphere”; Would there be a way that
390 you could indeed confirm this explanation doing some sensitivity experiments?

391 We thank the reviewer for their suggestion. Sensitivity experiments on parameters of
392 the convective parameterization such as the trigger function would indeed be interesting
393 and provide useful information for tuning the convective parameterization for
394 Amazonia. However, we feel these tests fall outside the scope of this study. Simulations
395 for subsequent field campaigns will use updated versions of the convective schemes and
396 at that point it may be appropriate to tune the parameterizations.

397 19. In the discussion about the meteorological conditions I think it is essential to start
398 with the analysis of the shortwave radiation terms since if this parameter is off in the
399 models, then you would also not expect the latent and sensible heat fluxes to be
400 correctly simulated.

401 We agree that the shortwave radiation will affect the heat fluxes, and we have reordered
402 the text to reflect the reviewer’s suggestion (Section 4.2, lines 452-522).

403 20. Line 513; “The overestimated moisture in CCATT-BRAMS may be due to
404 overactive convective detrainment at midlevels, and could be associated with over-
405 active O₃ production”

406 Here you suggest with this sentence that O₃ is somehow responsible for the
407 overestimation of moisture in the model. I guess that you would like to express that the
408 issues on moisture representation in the model coincide with issues on the O₃
409 simulations due to issues on the convective transport.

410 We did not intend to suggest that overestimated O₃ production causes high moisture
411 bias in the models. Therefore we have altered this sentence to clarify that excessive
412 moisture may stimulate O₃ production (lines 507-510):

413 “The models generally show good agreement with soundings at Manaus (Figs. 8-9), but
414 excess moisture (positive dewpoint bias of 10 K) in CCATT-BRAMS above 500 hPa
415 may lead to increased photochemical production of O₃.”

416 21. Line 534; Overall the analysis of the meteorological parameters (measurements and
417 models) does not give a lot of confidence in this feature essential to a fair evaluation of
418 the chemistry. There appear to be substantial issues on the representation of some of the
419 key drivers of chemistry (solar radiation), tracer transport and removal processes. I also
420 think that the analysis is not very well structured going back and forth between all the
421 relevant meteorological parameters. Is there a more optimal way to structure this
422 description of the analysis of the meteorology?

423 We agree that accurate simulation of meteorological parameters in the Amazon
424 continues to be a challenge, and that these parameters will drive some of the main
425 processes that affect O₃ production and transport. We now state this at the beginning of
426 Section 3.2 (lines 452-454):

427 “Tropospheric O₃ distributions are driven by both chemical processes, including
428 chemistry and emissions of O₃ precursors, and meteorological ones, such as solar
429 radiation, tracer transport and removal.”

430 We also added a new paragraph (lines 477-485) that summarizes the key findings of the
431 model-data meteorological comparison and their implications for chemistry:

432 “Now we summarize the key findings of the model-data meteorological comparison and
433 their implications for the chemistry simulations. The models capture the seasonal spatial
434 distribution of precipitation over northern South America (Fig. 4), and the signs of NE-
435 SE differences are correctly modeled by both models during both seasons, i.e., the NE is
436 drier than the SE during November and vice-versa during May. For the Amazon,
437 CCATT-BRAMS slightly underestimates the precipitation rates in both seasons, but the
438 rate in WRF-Chem is about twice that of TRMM 3B43 (Table 2). This may lead to
439 errors in the strength and vertical distribution of convective transport and the amount of
440 convective wet removal.”

441 22. Line 551: “Typical model anthropogenic NO_x emissions values over the Amazon,
442 primarily from biofuel source..... (Garcia-Montiel et al., 2003).” Another example of a
443 way too long sentence.

444 This sentence was divided into four sentences to increase readability (lines 585-581):

445 “Typical model anthropogenic NO_x emissions values over the Amazon, primarily from
446 biofuel sources, were 0.008-13 μg N m⁻² hr⁻¹ N. These NO_x emissions included in the
447 models were less than one third of the mean values of 44 ± 14 μg N m⁻² h⁻¹ NO
448 measured by Kaplan et al. (1988) during ABLE-2A. This is considered a threshold
449 value for NO_x-driven O₃ production to be the dominant O₃ source in the PBL. The
450 model emissions were also much lower than the mean emissions from forest of 35.8 μg
451 N m⁻² h⁻¹ NO measured in the 1998 dry season (Garcia-Montiel et al., 2003).”

452 23. Line 727: “These discrepancies of models with observations may result from an
453 overly mixed (constant with altitude) profile due to overly active turbulent mixing from
454 1-2 km or too much downward convective transport of O₃ from 2 km to the surface, as
455 observed by Betts et al. (2002).”

456 This statement is an example of where I think that this analysis would benefit from
457 more in depth analysis of what really explains the observed discrepancies between the
458 models and the measurements. There are many statements including the term “may”
459 expressing that the models are somewhat being applied as a black box not really being
460 able to really nail down the reasons for the misrepresentations. On this particular topic I
461 think it would be very useful to see some analysis of the boundary layer (BL) depth,
462 how this compares to observations of the BL depth over tropical rainforest and also to
463 see, if the BL depth would be different, to what extent this is due to issues on the
464 surface energy balance representation, model representation of entrainment/detrainment
465 processes, etc.

466 We agree that we would like to better understand what explain the discrepancies
467 between the model and observations. For complex coupled meteorology-chemistry
468 models, with many feedbacks among processes, physical and chemical parameters and
469 input data sources, it is difficult to attribute an error to specific processes. In response to
470 the reviewer’s suggestion, we have included an analysis comparing the maximum CBL
471 depth from Fisch et al. (2004) with the models at forest and pasture sites for both
472 seasons. The text describing this analysis is as follows (lines 404-414):

473 “Fisch et al. (2004) found that in the dry season (14-25 August, 1994), higher sensible
474 heat fluxes over pasture increase the maximum height at 21 UTC (17 LT) of the
475 Convective Boundary Layer (CBL) from around 1100 m for forest (Rebio Jarú) to 1650
476 m over pasture (FNS). On the other hand, during the wet season (Jan.-Feb. 1999) the
477 height of the CBL is similar for both land types, around 1000 m. The simulated height
478 of the PBL at 21Z above the forest and pasture sites (Table 4) was analyzed from model
479 output using two different methods: *TKE*, the first level above the surface where the
480 Turbulent Kinetic Energy (TKE) from the PBL schemes dropped below 0.01 m² s⁻¹ and
481 *Theta*, the first level above the surface where theta exceeded theta of the level below by

482 0.6 K. In addition, *WRF MYNN* is the diagnostic from the WRF PBL scheme which
483 takes into account TKE as well as stability.”

484 Reviewer #3

485 1. Overall, the paper presents valuable results but would benefit from better
486 organization around the main science questions. For example, the introduction (Section
487 1) and Previous studies (Section 1.3) could be combined and condensed so that they
488 lead directly into the questions this study will address. Stronger links between the model
489 evaluation and the science questions would also be helpful.

490 We agree that the previous studies should be presented in order to justify the science
491 questions of this current study. Following the reviewer’s suggestion, the introduction
492 and previous studies sections have been combined and condensed, followed by the
493 science questions.

494 Specific Comments:

495 2. Abstract Line 15-18: There are a number of reasons ozone might be higher in
496 OMI/MLS than the model besides lack of PBL sensitivity in the satellite data.

497 We agree that in the scope of this study it is difficult to assess the accuracy of the
498 OMI/MLS data. The too-vertical nature of the model profiles could be due to missing
499 inputs from the boundary conditions and errors in the convective transport. This
500 sentence in the abstract (lines 31-37) has been modified to:

501 “In addition, O₃ simulated by the models was either within the error bars or lower than
502 BARCA observations in midlevels (3–5 km a.s.l.), and lower than total tropospheric O₃
503 retrieved from OMI/MLS, which is primarily comprised of middle troposphere O₃ and
504 thus reflects long-range transport processes. Therefore, the models do a relatively poor
505 job of representing the free troposphere-BL gradient in O₃ compared with aircraft and
506 satellite observations, which could be due to missing long-range and convective
507 transport of O₃ at mid-levels.”

508 3. P14010 Line 16: Please explain "The flights consisted of quasi-Lagrangian
509 measurement"

510 Lagrangian measurements involve following an air parcel as it moves through the
511 atmosphere in order to be able to constrain sources and sinks of chemical species found
512 within the parcel. As it is nearly impossible to do this with an aircraft, the term “quasi-
513 Lagrangian” is used to refer to sampling a parcel, then intercepting what is thought to be
514 the same parcel at a later time and location. The following paragraph (lines 130-138)
515 has been rephrased in order to clarify this terminology:

516 “In-situ measurements were made of carbon dioxide (CO₂), carbon monoxide (CO),
517 methane (CH₄), ozone (O₃), and aerosol number concentration and optical properties.
518 Flask samples were collected to determine CO₂, CH₄, sulfur hexafluoride (SF₆), CO,
519 nitrous oxide (N₂O), hydrogen, and the oxygen-nitrogen ratio (O₂/N₂). The flights
520 consisted of quasi-Lagrangian measurements, which attempt to sample an air parcel at
521 multiple locations along its path in order to constrain regional and basin-wide fluxes of
522 these species. The aircraft had a ceiling of 4500 m, and flights usually consisted of
523 ascending and descending vertical profiles separated by short (5–30 min) horizontal
524 legs.”

525 4. P14022 Line 26-28: What is the advantage of using the 16 boxes instead of just
526 sampling the model at the location of the observation?

527 The following sentence was inserted to explain this reasoning (lines 342-344):

528 “As the model output has a much coarser spatial and temporal resolution than the
529 aircraft measurements, the model value is interpolated to the observation time and
530 location.”

531 5. Section 3.3 1st Paragraph: Is this background information or findings of this study?
532 If it is background, please include citations.

533 This is background information to set up the analysis of the impact of seasonal
534 variations in meteorological and emissions conditions on the chemistry. The paragraph
535 has been edited to include references as follows:

536 (lines 454-456) “During the dry-to-wet transition season, increased actinic fluxes
537 stimulate the production of OH radicals from O₃ photolysis that can lead to net O₃
538 production (Seinfeld and Pandis, 2006).”

539 (lines 459-466) “On the other hand, in the wet-to-dry transition season, lower levels of
540 O₃ are largely associated with increased presence of convective clouds and
541 precipitation. Decreased surface temperatures and incident solar radiation due to
542 cloudiness suppress emissions of biogenic VOCs such as isoprene (Fall and
543 Wildermuth, 1998). In addition, higher surface humidity and precipitation decrease the
544 occurrence of fires (Morton et al., 2013; Chen et al., 2013) that emit NO_x and VOCs
545 (Freitas et al., 2007). O₃ precursors are further decreased by wet removal within the
546 storms (Barth et al., 2007a).”

547 References:

548 Barth, M. C., Kim, S.-W., Skamarock, W. C., Stuart, A. L., Pickering, K. E., and Ott, L.
549 E.: Simulations of the redistribution of formaldehyde, formic acid, and peroxides in the

550 July 10, 1996 STERAO deep convection storm, *J. Geophys. Res.*, 112, D13310,
551 doi:10.1029/2006JD008046, 2007.

552 Chen, Y., Velicogna, I., Famiglietti, J. S., and Randerson, J. T.: Satellite observations of
553 terrestrial water storage provide early warning information about drought and fire
554 season severity in the Amazon, *J. Geophys. Res. Biogeosci.*, 118, 495–504, doi:
555 10.1002/jgrg.20046, 2013.

556 Fall, R., and Wildermuth, M. C.: Isoprene Synthese: From Biochemical Mechanism to
557 Emission Algorithm, *J. Geophys. Res.*, 103(D19), 25599-25609, doi:
558 10.1029/98jd00808, 1998.

559 Morton, D. C., Le Page, Y., DeFries, R., Collatz, G. J., and Hurtt, G. C.: Understorey
560 fire frequency and the fate of burned forests in southern Amazonia, *Phil. Trans. R. Soc.*
561 *B*, 368(1619), doi: 10.1098/rstb.2012.0163, 2013.

562 Seinfeld, J. H. and Pandis, S. N.: *Atmospheric Chemistry and Physics: From Air*
563 *Pollution to Climate Change*, 2nd edition, J. Wiley, New York, 2006.

564 6. Page 14030 Lines 3-5: The second part of the sentence does not necessarily follow
565 from the first, since there could be errors in the model's vertical distribution of
566 ozone.

567 We agree with the reviewer that we cannot conclude that the satellite data is missing
568 PBL O₃. The tropospheric O₃ may be lower in the models than satellite due to missing
569 mid-level inflow and sources, as is also indicated by the comparison with the aircraft
570 observations and SHADOZ. This sentence has been revised as follows (lines 768-771):

571 “In addition, simulated O₃ was lower than both the OMI/MLS total tropospheric O₃ and
572 the BARCA observations in mid-levels, indicating that the models are missing sources
573 at mid-levels from long-range and convective transport.”

574 7. P14034 Lines 6-7: Better agreement than what?

575 Both sensitivity simulations agreed better with observations than the original
576 simulation. The sentence was revised and now reads (lines 739-741):

577 “Additional simulations with WRF-Chem showed that O₃ in the lower boundary layer
578 was about twice as sensitive to increases in O₃ deposition velocity as reductions in NO_x
579 emissions, but both simulations achieved better agreement with observations than the
580 base case simulation.”

581 8. P14034 Lines 9-10: Are there other possible sources of model error?

582 Yes, in clean (NO_x-sensitive) conditions, low ozone deposition and NO_x emissions can
583 contribute to the O₃ overestimate, while in polluted (VOC-sensitive) conditions these

584 errors may be compensated for by insufficient VOC reactivity. We have added the
585 following sentence to clarify this reasoning (lines 760-766):

586 “In polluted, VOC-sensitive conditions, approximately the correct net amount of O₃ is
587 generated in the PBL. This suggests there is insufficient VOC reactivity in the models,
588 since the correct amounts of O₃ deposition velocities and NO_x emissions would both
589 decrease O₃ production. Additionally, in clean, NO_x-sensitive conditions, proportionally
590 more O₃ is produced per unit NO_x emissions and the O₃ deposition velocities are still
591 too low, resulting in an overestimate.”

592 9. P14034 Line 24: Could insufficient ozone deposition also contribute?

593 Yes. See response to Comment #8.

594 10. P14035 Lines 1-4: While the lack of surface sensitivity in the satellite data is
595 known and is a potential factor in the model/obs mismatch, there can be many sources
596 of model error. This statement, here and in the abstract, needs to be re-worded; one
597 cannot conclude simply from the fact that simulated ozone was lower than OMI/MLS at
598 mid-levels that the O₃ observed by satellites is dominated by the mid-troposphere and
599 long-range transport.

600 These statements were revised as follows in the Abstract (lines 31-37):

601 “In addition, O₃ simulated by the models was either within the error bars or lower than
602 BARCA observations in midlevels (3–5 km a.s.l.), and lower than total tropospheric O₃
603 retrieved from OMI/MLS, which is primarily comprised of middle troposphere O₃ and
604 thus reflects long-range transport processes. Therefore, the models do a relatively poor
605 job of representing the free troposphere-BL gradient in O₃ compared with aircraft and
606 satellite observations, which could be due to missing long-range and convective
607 transport of O₃ at mid-levels.”

608 And in the Conclusions (lines 768-771):

609 “In addition, simulated O₃ was lower than both the OMI/MLS total tropospheric O₃ and
610 the BARCA observations in mid-levels, indicating that the models are missing sources
611 at mid-levels from long-range and convective transport.”

612 11. P14025 Lines 5-8: This sentence is confusing. Please re-word.

613 Following the suggestion of the reviewer, the sentence was re-worded to be clearer as
614 follows (lines 487-492):

615 “However, for the southern Amazon forest and pasture sites peak shortwave may be
616 overestimated (underestimated) by 50-100 W m⁻² by CCATT-BRAMS (WRF-Chem)
617 (Figs. 6-7), suggesting that there is insufficient (excessive) cloudiness in the models.”

618 12. Figure 2 Caption: What statistical test does Matlab use to determine outliers?

619 The following text was added to the Fig. 2 caption (lines 1157-1162) to include this
620 information:

621 “the whiskers extend to the most extreme data points not considered outliers and
622 outliers are plotted individually as red plusses. Values are drawn as outliers if their
623 values exceed $q_3 + w(q_3 - q_1)$ or are less than $q_1 - w(q_3 - q_1)$, where q_1 and q_3 are the
624 25th and 75th percentiles, respectively, and w is the maximum whisker length with the
625 default value of 1.5. For normally distributed data, the whiskers encompass from
626 approximately the 2.7 to 99.3 percentiles.”

627 Comments about organization:

628 13. P14008 Lines 8-13: This seems like a separate paragraph and should be moved
629 elsewhere.

630 A new paragraph was created after the Lelieveld et al. (2008) citation and the remainder
631 of the paragraph was reordered as follows (lines 56-68):

632 “The Amazon Basin continues to rapidly urbanize, and urban emissions of O_3
633 precursors are also expected to grow. Emissions from cities in the tropics may have a
634 larger impact on the upper troposphere due to high solar radiation levels and intense
635 convective transport (Gallardo, et al., 2010). In the upper troposphere, O_3 acts as a
636 greenhouse gas, increasing surface radiative forcing (IPCC, 2001). Inhalation of
637 elevated levels of ozone can irritate the lungs; aggravate asthma and cause emphysema,
638 bronchitis, and premature death (Schwela, 2000). High ozone concentrations can also
639 inhibit photosynthesis in plants and damage leaf tissue, harming wild ecosystems and
640 reducing crop productivity (Reich and Amundson, 1985). Thus, an improved
641 understanding/quantification of O_3 temporal and spatial variability in the tropical
642 rainforest environment is important for projecting future impacts of land use and
643 climate change in the Amazon Basin and other tropical rainforest regions worldwide on
644 their expanding human populations and significant biodiversity.”

645 14. P14009 Line 15: Description of BARCA seems like it should be a separate
646 paragraph

647 A separate section was created for the BARCA description (Section 2, lines 121-224)

648 15. Are sections 1.1-1.3 all subsections of the introduction? Section 1.3: This section
649 could potentially be combined with the introduction. It contains a lot of detail on
650 past studies, but it would be helpful to relate this information more strongly to the
651 goals of the current study and how the current study will advance our understanding.

652 Subsection 1.3 was condensed and integrated into the main body of the introduction to
653 create a more coherent justification of the current study.

654 16. Section 3.2: There is a lot of detail in this section that is difficult for the reader to
655 keep track of and relate to the main chemical processes. The last paragraph provides
656 a nice summary, so perhaps other portions of the text and the number of figures
657 could be reduced. Another possibility would be to combine sections 3.2 and 3.3 but
658 discuss each portion of the campaign separately.

659 Following the reviewer's suggestion, this section (now 4.2, lines 452-522) has been
660 condensed and reframed in terms of impacts on the chemical processes.

661

662 **Ozone production and transport over the Amazon**
663 **Basin during the dry-to-wet and wet-to-dry transition**
664 **seasons**

665

666 ***M. M. Bela^{1,*}, K. M. Longo², S. R. Freitas², D. S. Moreira², V.***
667 ***Beck³, S. C. Wofsy⁴, C. Gerbig³, K. Wiedemann⁴, M. O. Andreae⁵,***
668 ***P. Artaxo⁶***

669 [1] Center for Earth System Science (CCST), National Institute for Space Research
670 (INPE), São José dos Campos, Brazil

671 [2] Center for Weather Forecast and Climate Studies, National Institute for Space
672 Research (INPE), Cachoeira Paulista, Brazil

673 [3] Max Planck Institute for Biogeochemistry, Jena, Germany

674 [4] Division of Engineering and Applied Science/Department of Earth and Planetary
675 Science, Harvard University, Cambridge, MA, USA

676 [5] Biogeochemistry Department, Max Planck Institute for Chemistry, Mainz, Germany

677 [6] Institute of Physics, University of São Paulo, São Paulo, Brazil

678 [*] Now at Laboratory for Atmospheric and Space Physics, University of Colorado,
679 Boulder, USA

680 Correspondence to: M. M. Bela (megan.bela@colorado.edu)

681

Abstract

682 The Regional Carbon Balance in Amazonia (BARCA) campaign provided the first
683 Amazon Basin-wide aircraft measurements of O₃ during both the dry-to-wet (November
684 and December 2008) and wet-to-dry (May 2009) transition seasons. Extremely low
685 background values (< 20 ppb) were observed to the west and north of Manaus in both
686 seasons and in all regions during the wet-to-dry transition. On the other hand, elevated
687 O₃ levels (40-60 ppb) were seen during the dry-to-wet transition to the east and south of
688 Manaus, where biomass burning emissions of O₃ precursors were present. Chemistry
689 simulations with the CCATT-BRAMS and WRF-Chem models are within the error bars
690 of the observed O₃ profiles in the boundary layer (0-3 km a.s.l.) in polluted conditions.
691 However, the models overestimate O₃ in the boundary layer in clean conditions, despite
692 lacking the predominant NO source from soil. In addition, O₃ simulated by the models
693 was either within the error bars or lower than BARCA observations in midlevels (3–5
694 km a.s.l.), and lower than total tropospheric O₃ retrieved from OMI/MLS, which is
695 primarily comprised of middle troposphere O₃ and thus reflects long-range transport
696 processes. Therefore, the models do a relatively poor job of representing the free
697 troposphere-BL gradient in O₃ compared with aircraft and satellite observations, which
698 could be due to missing long-range and convective transport of O₃ at mid-levels.
699 Additional simulations with WRF-Chem showed that the model O₃ production is very
700 sensitive to both the O₃ deposition velocities and the NO_x emissions, which were both
701 about one half of observed values. These results indicate the necessity of more realistic
702 model representations of emissions, deposition and convective processes for accurate
703 monitoring and prediction of increases in O₃ production in the Amazon Basin as the
704 regional population grows.

Excluído: indicating that the models do not represent the free troposphere – boundary layer gradient in O₃. Total tropospheric O₃ retrieved from OMI/MLS was higher than that simulated by the models, suggesting that the satellite observations are dominated by the middle troposphere and long-range processes and are not a good indication of O₃ conditions in the PBL.

Excluído: , and the NO_x emissions

Excluído:

Excluído: have implications for the

718 **1 Introduction**

719 In the Amazon Basin, trace gases from biomass-burning, urban, and biogenic emissions
720 are important sources of ozone precursors, which are efficiently transported by intense
721 convective activity to the upper troposphere, where they can be dispersed over long
722 distances by regional and global circulations. Additionally, convective overshooting
723 may inject heat, moisture and trace gases into the tropical tropopause layer, impacting
724 stratospheric ozone and other aspects of global climate (Fueglistaler et al., 2009). In the
725 dry-to-wet transition season, regional smoke and haze plumes from biomass burning are
726 observed (Longo et al., 2009). On the other hand, in the wet-to-dry transition season,
727 biogenic emission of VOCs, particularly from the Amazon rainforest, may maintain the
728 atmospheric oxidative capacity for generating ozone and other photochemical pollutants
729 (Lelieveld et al., 2008).

730 The Amazon Basin continues to rapidly urbanize, and urban emissions of O₃ precursors
731 are also expected to grow. Emissions from cities in the tropics may have a larger impact
732 on the upper troposphere due to high solar radiation levels and intense convective
733 transport (Gallardo et al., 2010). In the upper troposphere, O₃ acts as a greenhouse gas,
734 increasing surface radiative forcing (IPCC, 2001). Inhalation of elevated levels of ozone
735 can irritate the lungs, aggravate asthma and cause emphysema, bronchitis, and
736 premature death (Schwela, 2000). High ozone concentrations can also inhibit
737 photosynthesis in plants and damage leaf tissue, harming wild ecosystems and reducing
738 crop productivity (Reich and Amundson, 1985). Thus, an improved understanding and
739 quantification of O₃ temporal and spatial variability in the tropical rainforest
740 environment is important for projecting future impacts of land use and climate change
741 in the Amazon Basin and other tropical rainforest regions worldwide on their expanding
742 human populations and significant biodiversity.

743 Analyses of satellite, aircraft and ground-based observations of O₃ over Amazonia since
744 the 1980s have demonstrated the influence of long-range transport of African biomass
745 burning and Northern Hemisphere inputs, local fire sources, NO soil and biogenic VOC
746 emissions, and convective transport on spatial and seasonal variability in O₃. In
747 particular, data from the ABLE-2B aircraft and ground campaign during the 1987 wet-
748 to-dry transition season and the BARCA observations offer the opportunity to compare
749 the regional O₃ distribution across decades.

750 Previous analyses of satellite ozone data have noted early-year O₃ maximums in tropical
751 Southern Hemisphere primarily associated with cross-Atlantic transport of biomass
752 burning emissions from Africa (Fishman and Larson, 1987; Thompson et al., 1996),
753 Northern Hemisphere fires, and lightning NO_x (Edwards et al., 2003). In the Amazon
754 region, ground-based and aircraft campaigns (e.g., Crutzen et al., 1985; Kirchhoff et al.,

Movido (inserção) [16]

Movido (inserção) [17]

Excluído: ;

Movido para cima [17]: In the upper troposphere, O₃ acts as a greenhouse gas, increasing surface radiative forcing (IPCC, 2001). The Amazon Basin continues to

Movido para cima [16]: The Amazon Basin continues to rapidly urbanize, and urban emissions of O₃ precursors are also expected to grow (Gallardo et al., 2010).

Excluído: A

Excluído: /

Movido para baixo [14]: Motivated by the impact of O₃ in the Amazon Basin on human and ecosystem health and global climate, we collected aircraft observations of O₃ during BARCA and conducted regional chemistry simulations in order to answer the following scientific questions: how does O₃ vary spatially and seasonally over the Amazon basin? What are the sources and sink of O₃ in this region? How well can state-of-the-art regional chemistry models reproduce O₃ distributions over the Amazon Basin? ¶

Excluído: the

1990; Browell et al., 1996; Kaufman et al., 1998; Longo et al., 1999, Andreae et al., 2001; Andreae et al., 2002; Zhou et al., 2002; Cordova et al., 2003; Rummel et al., 2007; Kuhn et al., 2010; Martin et al., 2010; Toon et al., 2010) have observed daytime background O₃ levels of 10-20 ppb, decreasing to very low values (~5 ppb) at night due to O₃ deposition to the forest. However, nighttime values can be increased up to 30 ppb due to convective downdrafts (Betts et al., 2002; Cordova et al., 2003). Elevated levels of 60-80 ppb are found due to production from regional fire emissions and recirculated urban pollution from SE Brazil, as well as evidence of deep convective transport of boundary layer air to the middle and upper troposphere.

Thus, satellite observations enable the attribution of tropical O₃ maxima to biomass burning and lightning NO_x sources, while ground-based measurements allow the identification of key surface processes in the Amazon Basin affecting O₃ amounts. These processes include O₃ production from soil NO_x emissions and removal via dry deposition to the forest canopy. Aircraft campaigns complete the suite of observations, allowing the examination of convective lofting of surface emissions, with biomass burning emissions of particular importance on the regional scale. In-situ data on cloud properties and chemical species, as well as observations of land use changes, boundary layer dynamics and larger-scale cloud-aerosol interactions, are scant in this region. Therefore, models are essential tools for monitoring and predicting atmospheric chemistry composition, weather, and climate at local, regional, and global scales. In turn, the observations help constrain uncertainties in the model representations of parameterized convection, turbulence, land surface and other subgrid scale processes that affect the simulated transport and chemical transformation of the atmospheric composition (Beck et al., 2013).

Motivated by the impact of O₃ in the Amazon Basin on human and ecosystem health and global climate, we collected aircraft observations of O₃ during BARCA and conducted regional chemistry simulations in order to answer the following scientific questions: how does O₃ vary spatially and seasonally over the Amazon basin? What are the sources and sinks of O₃ in this region? How well can state-of-the-art regional chemistry models reproduce O₃ distributions over the Amazon Basin?

The structure of this paper is as follows. In Section 2, the measurements taken during the BARCA aircraft campaign are presented, followed by the meteorological conditions and emissions regimes during the two phases of the campaign. The ABLE-2 campaigns from the 1980s are also described in this section. Sections 3.1-3.3 detail the aircraft observations, the setup of the CCATT-BRAMS and WRF-Chem simulations and the ground-based and remote sensing observations used in the analysis. In Section 4.1, the O₃ aircraft observations are presented, followed by the analysis of observed and

Excluído: Kirchhoff et al., 1990; Browell et al., 1996; Kaufman et al., 1998; Longo et al., 1999, Cordova et al., 2003; Andreae et al., 2001, 2002; Rummel et al., 2007; Kuhn et al., 2010; Martin et al., 2010; Toon et al., 2010

Excluído: both

Excluído: and e

Excluído: ¶

Movido para baixo [15]: In-situ data on cloud properties and chemical species, as well as observations of land use changes, boundary layer dynamics and larger-scale cloud-aerosol interactions, are scant in this region. Therefore, models are essential tools for monitoring and predicting atmospheric chemistry composition, weather, and climate at local, regional, and global scales. Uncertainties in the model representations of parameterized convection, turbulence, land surface and other subgrid scale processes lead to significant errors in simulated transport and chemical transformation of the atmospheric composition (Beck et al., 2013).

Movido (inserção) [15]

Excluído: ,

Excluído: U

Excluído: lead to significant errors in

Excluído: ¶

Movido (inserção) [14]

Excluído: ¶

Movido para baixo [11]: The Regional Carbon Balance in Amazonia (BARCA) Large-Scale Biosphere-Atmosphere (LBA) experiment, an aircraft campaign based in Manaus and conducted during the dry-to-wet (November and December 2008) and wet-to-dry (May 2009) transition seasons. BARCA was the first flight campaign to sample ozone and other trace gases on a regional scale in both transition seasons. It offers a unique opportunity, together with satellite observations and modeling studies, to understand the regional ozone distribution in the Amazon under different meteorological and emissions regimes.

Movido para baixo [13]: It is interesting to compare BARCA data ... [1]

Excluído: 1.1

Excluído: described

Excluído: in Sect. 1.2.

Excluído: Section 1.3 reviews previous observational and remote sensing stu ... [2]

Excluído: ,

Excluído: , as well as the setup of the CCATT-BRAMS and WRF-Chem ... [3]

Excluído: .

Excluído: 3

Excluído: results of the

909 modeled transition season meteorology in Section 4.2 and the findings from the O₃
910 simulations and process studies in Section 4.3. Final discussions and conclusions are
911 found in Section 5.

Excluído: meteorological and O₃ observations and simulations are presented, with f

912 2 BARCA aircraft campaigns

Excluído: in

Excluído: .

Excluído: 4

913 The Regional Carbon Balance in Amazonia (BARCA) Large-Scale Biosphere-
914 Atmosphere (LBA) experiment was an aircraft campaign based in Manaus and
915 conducted during the dry-to-wet (November and December 2008) and wet-to-dry (May
916 2009) transition seasons. BARCA was the first flight campaign to sample ozone and
917 other trace gases on a regional scale in both transition seasons. It offers a unique
918 opportunity, together with satellite observations and modeling studies, to understand the
919 regional ozone distribution in the Amazon under different meteorological and emissions
920 regimes.

Movido (inserção) [11]

Excluído: ,

921 The BARCA flights were conducted with the EMB 110 Bandeirante aircraft of the
922 Brazilian National Institute for Space Research (INPE). In-situ measurements were
923 made of carbon dioxide (CO₂), carbon monoxide (CO), methane (CH₄), ozone (O₃), and
924 aerosol number concentration and optical properties. Flask samples were collected to
925 determine CO₂, CH₄, sulfur hexafluoride (SF₆), CO, nitrous oxide (N₂O), hydrogen, and
926 the oxygen-nitrogen ratio (O₂/N₂). The flights consisted of quasi-Lagrangian
927 measurements, which attempt to sample an air parcel at multiple locations along its path
928 in order to constrain regional and basin-wide fluxes of these species. The aircraft had a
929 ceiling of 4500 m, and flights usually consisted of ascending and descending vertical
930 profiles separated by short (5-30 min) horizontal legs. A detailed description of the
931 aircraft measurements can be found in Andreae et al. (2012). Figure 1 shows a map of
932 the flight tracks from BARCA A and B. Both experiment periods included flights to the
933 north, south and east of Manaus, as well as local flights near Manaus. Only BARCA A
934 included flights to the west of Manaus, because intense convective activity in that
935 region during BARCA B precluded flying. During BARCA B, fire activity was low
936 throughout the Amazon region due to heavy precipitation, while during BARCA A,
937 intense fire activity occurred on the northern coast of Brazil and scattered fires were
938 present throughout the southeastern Amazon.

Excluído: <#>BARCA aircraft campaigns¶

Excluído: The flights consisted of quasi-Lagrangian measurements of

Excluído: s, and were designed to constrain basin-wide fluxes, understand distributions and sources of these species

Movido (inserção) [12]

Excluído: EMB 110 Bandeirante INPE

Excluído: In-situ measurements were made of CO₂, CH₄, CO, O₃, aerosol number concentration and optical properties.

Movido para cima [12]: Flask samples were collected to determine CO₂, CH₄, sulfur hexafluoride (SF₆), CO, nitrous oxide (N₂O), hydrogen, and the oxygen-nitrogen ratio (O₂/N₂).

939 Andreae et al. (2012) summarized the BARCA campaign, meteorological background,
940 carbon monoxide and aerosol observations and CO results from several regional
941 transport and chemistry models. These included the CCATT-BRAMS and WRF-Chem
942 simulations analyzed in greater detail in this paper. Meteorological analysis showed that
943 during BARCA A, when the Inter-Tropical Convergence Zone (ITCZ) was to the north
944 of the Amazon Basin, inflow to the Amazon was primarily from the Southern
945 Hemisphere. During BARCA B, the ITCZ extended to 20° S and air at low levels was

Excluído: <#>Transition season meteorology and emissions¶

971 of Northern Hemisphere origin, including some smoke from West African fires. On the
972 other hand, the mid-tropospheric air was of mixed origin.

Excluído:

973 The highest CO levels were observed on the flights on 25-27 November in the
974 southeastern Amazon, influenced by regional biomass burning, since maximum values
975 were observed from 1-3 km. These are typical of injection heights of smoke plumes
976 from savanna fires (Freitas et al., 2007). The excess CO from biomass burning was
977 between about 30 and 200 ppb, increasing from north to south across the Basin.

Excluído: as

978 According to analysis of tracer simulations, during BARCA A biomass burning
979 contributed on average about 56 ppb (31%) to the total CO of around 180 ppb, while the
980 background was 110 ppb (61%). Biomass burning influence was indicated by CO
981 mixing ratios up to 300 ppb, Condensation Nuclei (CN) approaching 10000 cm⁻³, and a
982 low CN to CO ratio ($\Delta\text{CN}/\Delta\text{CO}$) signifying aged smoke. This influence was highest in
983 the southern Amazon from 1-3 km. Manaus back trajectories at 500 and 4000 m came
984 from eastern Amazon fires rather than the intense African fires occurring at the same
985 time. During BARCA B, little biomass burning influence was observed. CN counts
986 were 300-500 cm⁻³ and a CO enhancement of ~10 ppb above the mixing ratios in air
987 entering the Basin from the Atlantic was seen. Small boundary layer enhancements
988 were attributed to a source from the oxidation of biogenic VOCs (Andreae et al., 2012).

Excluído: The mean contribution from biomass burning to total CO during BARCA A was about 31%, with a contribution from

Excluído: (

Excluído:) of about

Excluído: indicating

989 Andreae et al. (2012) also showed simulated vertical CO profiles from CCATT-
990 BRAMS and WRF-Chem simulations, as well as the Stochastic Time Inverted
991 Lagrangian Transport (STILT) model with two different meteorological field inputs and
992 the WRF Greenhouse Gas Module (WRF-GHG). The simulated CO profiles matched
993 mean observed values, but were overly vertical (too low near the surface and too high
994 above 3 km). This suggested that the models had too much convective transport or
995 vertical mixing from the PBL schemes. However, the probability densities were
996 consistent with observations in the boundary layer, indicating that horizontal dispersion
997 was reasonable. Beck et al. (2013) evaluated different CH₄ wetland emissions schemes
998 and maps using WRF-GHG. They found the best agreement with BARCA CH₄ data for
999 days where convective transport, as evaluated by comparison of upstream TRMM and
1000 WRF precipitation amounts, was well represented in the model. This indicates that
1001 proper representation of convective transport in models is essential for prediction of
1002 vertical distributions of pollutants in the Amazon Basin.

1003 It is interesting to compare BARCA data to observations from the NASA Amazon
1004 Boundary Layer Experiments ABLE campaigns (ABLE-2A and -2B), which took place
1005 during the dry season of 1985 and wet-to-dry transition of 1987. During the dry season
1006 (July-August 1985), the Amazon Boundary Layer Experiment (ABLE-2A) integrated
1007 aircraft, ground-based and satellite observations to study the processes affecting the

Movido (inserção) [13]

1017 chemical composition in mixed layer over Amazonia (Harriss et al., 1988). Jacob and
1018 Wofsy (1988) used a photochemical model of the Amazonian boundary layer to study
1019 the diurnal cycle of isoprene, NO_y and O₃ during ABLE-2A. They found that
1020 photochemical production spurred by NO emissions from soils increased daytime O₃ to
1021 about 20 ppb. However, at night, dry deposition to the forest caused O₃ to drop below 5
1022 ppb. Model results were consistent with the NO values of 25-60 ppt observed in the
1023 lower boundary layer over central Amazonia (Torres and Buchan, 1988). Isoprene
1024 emissions were found to have little effect on O₃ levels, as the oxidation of CO would
1025 produce sufficient HO_x to generate 20 ppb of O₃. However, O₃ production in the model
1026 was highly sensitive to NO_x emissions, and downward transport from the free
1027 troposphere became the dominant source of O₃ in the PBL when NO emissions were
1028 decreased below the average value of $44 \pm 14 \mu\text{g N m}^{-2} \text{h}^{-1}$ NO measured by Kaplan et
1029 al. (1988). Lidar observations during ABLE-2A showed highly variable O₃ levels, with
1030 some small regions with up to 30-40 ppb, attributed to variable NO flux from the
1031 canopy (Browell et al., 1988). ABLE-2B was conducted during the wet-to-dry transition
1032 season (April-May 1987) (Harriss et al., 1990). Periodic inputs from the Northern
1033 Hemisphere were found to be a pollution source over Amazonia, and dry deposition in
1034 the region provided a significant sink in the global O₃ budget. As part of ABLE-2, near-
1035 continuous O₃ surface measurements (1.5 m above the soil surface) showed daytime
1036 maximums of 3.7 ppb inside a forest and 5.7 ppb in a clearing (typical standard
1037 deviations of 0.3 ppb). Additionally, tower measurements at the clearing site showed
1038 higher O₃ values of 6.7 ppb at 7 m above the soil surface and 6.9 ppb at 15 m above the
1039 soil surface (Kirchhoff et al., 1990). Furthermore, 20 ozonesondes launched in the
1040 clearing showed typical mixing ratios of 40 ppb from 500-300 hPa, with values about
1041 10 ppb lower in the wet than dry season.

1042 Andreae et al. (2012) showed that CO mixing ratios were about 10 ppb higher during
1043 ABLE-2B than in BARCA B everywhere except the southern region, reflecting the
1044 global trend towards decreasing CO emissions since the 1980s, particularly in the
1045 Northern Hemisphere. The CO comparison also showed a similar enhancement of 10–
1046 20 ppb in the lowest 1 km above the surface, attributed to diffuse biogenic sources, and
1047 also indicated that the much higher enhancements during the dry season in BARCA A
1048 must be due to anthropogenic or biomass burning inputs. The O₃ comparison is
1049 expected to yield information in long-term trends in O₃ production in the Amazon
1050 Basin, as well as the relative importance of biogenic, urban and fire sources.

1051 3 Data and Methods

1052 3.1 BARCA aircraft measurements

1053 During the BARCA campaign, in-situ measurements of O₃ were conducted aboard the
1054 EMB 110 Bandeirante INPE aircraft using a dual-cell, UV Photometric analyzer (Ozone
1055 Analyzer, Model 49i, Thermo Fisher Scientific, United States). During BARCA A, 1
1056 minute averages of the original 1 second data were taken, while during BARCA B 1
1057 second data were stored. The detection limit for both campaigns was 1 ppb. The intake
1058 for O₃ was forward-facing, located 185 mm from the fuselage on the lower fuselage in
1059 front of the propellers to minimize effects of turbulence. The inlet lines consisted of
1060 stainless steel tubes with a bend radius of 100 mm and an inner diameter of 11.5 mm.
1061 The sample air was not heated or dried before measurement, so reported values are
1062 molar mixing ratios, nmol mol⁻¹, abbreviated 'ppb', with respect to ambient humid air
1063 (Andreae et al., 2012).

1064 3.2 Model description and simulation setup

1065 Simulations of BARCA A and B were conducted with the Chemistry Coupled Aerosol-
1066 Tracer Transport model to the Brazilian developments on the Regional Atmospheric
1067 Modeling System (CCATT-BRAMS; Longo et al., 2013; Freitas et al., 2009) and
1068 Weather Research and Forecasting with Chemistry (WRF-Chem; Grell et al., 2005)
1069 coupled chemistry and meteorology models. The model physics and chemistry options
1070 that were used are listed in Table 1. Both models used a two-way nested grid
1071 configuration, with a 140 km grid covering Africa and South America (southwest
1072 corner: 60°S, 100°W, northeast corner: 20°N, 50°W), to encompass the cross-Atlantic
1073 transport of biomass burning emissions from Africa, and a 35 km resolution grid
1074 covering most of South America (southwest corner: 35°S 85°W, northeast corner: 15°N,
1075 30°W), as depicted in Fig. 3.

1076 The simulations were initialized on 1 October 2008 00:00 UTC and 1 April 2009 00:00
1077 UTC for BARCA A and B, respectively. Boundary conditions and analysis nudging on
1078 the outer domain were given by the NCEP GFS analysis
1079 (<http://rda.ucar.edu/datasets/ds083.2/>) with a 6 hourly time resolution and 1° × 1°
1080 spatial resolution. Chemistry initial and boundary conditions were provided by 6 hourly
1081 analyses from the Model of Atmospheric Chemistry at Large Scale (Modélisation de la
1082 Chimie Atmosphérique Grande Echelle, MOCAGE) global model (Peuch et al., 1999)
1083 with a T42 (~ 2.8°) spatial resolution. Sea surface temperature was provided by the
1084 NOAA Optimum Interpolation (OI) Sea Surface Temperature (SST) V2 (available at
1085 <http://www.esrl.noaa.gov/psd/data/gridded/data.noaa.oisst.v2.html>) with 1° × 1° spatial
1086 resolution. Soil moisture was initialized with the TRMM-based soil moisture
1087 operational product (GPNR) developed by Gevaerd and Freitas (2006).

Excluído: <#>¶
<#>Previous studies of O₃ in the Amazon¶
<#>Analyses of satellite, aircraft and ground-based observations of O₃ over Amazônia since the 1980s have demonstrated the influence of long-range transport of African biomass burning and Northern Hemisphere inputs, local fire sources, NO soil and biogenic VOC emissions, and convective transport on spatial and seasonal variability in O₃. In particular, data from the ABLE-2B aircraft and ground campaign during the 1987 wet-to-dry transition season offers the opportunity to compare the regional O₃ distribution across decades.¶
<#>Several studies of satellite data have reported a seasonal O₃ maximum in the tropical Southern Hemisphere, largely associated with long-range transport of African fire emissions or lightning NO_x sources. Fishman and Larsen (1987) combined data from 1979-1980 from the Total Ozone Mapping Spectrometer (TOMS) and the Stratospheric Aerosol and Gas Experiment (SAGE) instruments to construct a climatology of tropospheric O₃ from 15°N to 15°S. They attributed the most elevated O₃ from 60°W to 60°E to biomass burning sources. Thompson et al. (1996) integrated TOMS satellite O₃ data with observations from the Transport and Atmospheric Chemistry near the Equator-Atlantic (TRACE-A) and the southern African Fire-Atmosphere Research Initiative (SAFARI) 1992 experiments. They showed a seasonal maximum in tropospheric O₃ in the south Atlantic, with the highest values (> 90 ppb) between 0-25°S. Back and forward trajectories attributed this elevated O₃ to transport of O₃ from fires in southern Africa by mid-level easterlies or recirculations, with little South American contribution. In Brazil, O₃ was seen to be lofted by deep convective transport, and then transported by high-level westerlies. However, from 0-10°S most of the O₃ was from Africa, since there was a delay of 1-2 months from peak African biomass burning to the O₃ maximum at the coastal site of Natal. O₃ production from the surface to 4 km was estimated to be 15 ppb O₃ per day, with a lower but nonzero rate in the upper troposphere. Using remote sensing observations of fire and lightning flash counts and NO₂, Edwards et al. (2003) identified ... [4]

- Excluído: -
- Excluído: -
- Excluído: . On the other hand,
- Excluído: -
- Excluído: , and t
- Movido (inserção) [10]
- Excluído: -

1249 The PBL parameterization in CCATT-BRAMS is based on Mellor and Yamada (1982),
1250 while in WRF-Chem the Mellor-Yamada-Janjic (MYJ; Janjić, 1994) scheme was used.
1251 In CCATT-BRAMS, shallow and deep convection are parameterized based on the
1252 mass-flux approach of Grell and Dévényi (2002). CCATT-BRAMS also uses the
1253 Turbulent Kinetic Energy (TKE) from the Planetary Boundary Layer (PBL) scheme to
1254 determine if convection will be triggered within a grid cell. In WRF-Chem the Grell 3D
1255 (G3) scheme was used, which includes shallow convection and subsidence spreading of
1256 convective outflow into neighboring grid cells. The Noah land surface model (Koren et
1257 al., 1999) was used in WRF-Chem and the Land Ecosystem-Atmosphere Feedback
1258 model v.2 (LEAF-2; Walko et al., 2000) was utilized in CCATT-BRAMS. Land use
1259 was provided by the United States Geological Survey (USGS) global 1 km vegetation
1260 dataset, updated with a land cover map for the Brazilian Legal Amazon Region for use
1261 in meteorological models (PROVEG) (Sestini et al., 2003). PROVEG is based on
1262 the Thematic Mapper (TM) Landsat images with spatial resolution of 90 m × 90 m
1263 from the year 2000 and deforestation data from the Amazon Deforestation Monitoring
1264 Program (PRODES) for the year 1997. For WRF-Chem, albedo and greenness fraction
1265 were calculated offline using the updated vegetation dataset, Moderate Resolution
1266 Imaging Spectroradiometer (MODIS) Normalized Difference Vegetation Index (NDVI)
1267 data from the years 2001-2002 and vegetation parameters from the LEAF-2 land surface
1268 model as implemented in CCATT-BRAMS.

Excluído: 2

1269 Emissions were generated with PREP-CHEM-SRC (Freitas et al., 2011) Version 1.2.
1270 Fire emissions were estimated from GOES, AVHRR and MODIS fire count data using
1271 the Brazilian Biomass Burning Emission Model (3BEM; Longo et al., 2009).
1272 Anthropogenic emissions were estimated from the RETRO, GOCART and EDGAR
1273 v4.0 global databases updated with South American inventories (Alonso et al., 2010).
1274 Emissions are obtained from RETRO if available for that species (CO, NO_x, chlorinated
1275 hydrocarbons, acids, esters, alcohols, ethers, benzene, ketones, methanal, other alkanals,
1276 other aromatics, C₂H₂, C₂H₄, C₂H₆, C₃H₆, C₃H₈, C₄H₁₀, C₅H₁₂, C₆H₁₄ plus higher
1277 alkanes, other VOCs, toluene, trimethylbenzenes, xylene), then from EDGAR v4.0
1278 (NMVOC, SO₄, CO₂, SF₆, N₂O), otherwise from GOCART (BC, OC, SO₂, DMS), in
1279 order to use the most consistent emissions inventory possible. Biogenic emissions were
1280 provided by a monthly climatology for the year 2000 produced with the Model of
1281 Emissions of Gases and Aerosols from Nature (MEGAN; Guenther et al., 2006). The
1282 MEGAN 2000 climatology includes numerous biogenic species (acetaldehyde,
1283 formaldehyde, other ketones, acetone, isoprene, propane, methane, propene, ethane,
1284 methanol, sesquiterpenes, ethene, monoterpenes and toluene), but not soil NO
1285 emissions. In WRF-Chem, the same Gaussian diurnal cycle with peak at 15:00 UTC
1286 (11:00 LT) is applied to both anthropogenic and biogenic emissions, while in CCATT-

1288 BRAMS the diurnal cycle of biogenic emissions follows the solar radiation cycle. In
1289 both models, the biomass burning daily cycle peaks at 18:00 UTC (15:00 LT).

1290 In both CCATT-BRAMS and WRF-Chem, the Regional
1291 Atmospheric Chemistry Mechanism (RACM) was used (Stockwell et al., 1997). In
1292 WRF-Chem, the Goddard Chemistry Aerosol Radiation and Transport (GOCART; Chin
1293 et al., 2002) aerosol scheme was used with aerosol direct radiative effects. CCATT-
1294 BRAMS has a smoke aerosol scheme with intensive optical properties (extinction
1295 efficiency, single scattering albedo and asymmetry parameter) calculated in an offline
1296 Mie code based on observations of climatological size distribution and complex
1297 refractive index from AERONET sites in the southern Amazon (Rosario et al., 2011,
1298 2013).

1299 CCATT-BRAMS includes scavenging of soluble species in the convective scheme
1300 following Berge (1993), as described in Freitas et al. (2005), where the wet removal
1301 rates are a function of the precipitation rate, liquid water content and precipitable water.
1302 In the cloud microphysics scheme the wet deposition follows Barth et al. (2001),
1303 whereby low solubility species partition into the liquid phase according to Henry's Law
1304 and high solubility species by diffusion-limited mass transfer. In WRF-Chem, at the
1305 convective-parameterizing scale, a constant fraction of gas and aerosol species in
1306 convective updrafts are removed (complete removal for sulfur dioxide – SO₂, sulfate –
1307 H₂SO₄, ammonium – NH₃, nitric acid – HNO₃ and sea salt; no removal for hydrophobic
1308 organic (OC) and black carbon (BC) and dimethyl sulfide (DMS); and 50% removal for
1309 all other aerosol species). On the other hand, no wet scavenging is included for cloud
1310 water and precipitation resolved by the microphysics scheme, because this option is not
1311 currently available in WRF-Chem for the RACM chemical mechanism. O₃ production
1312 in the upper troposphere is affected by the net convective transport of soluble HO_x
1313 precursors (including hydrogen peroxide (H₂O₂), methyl hydroperoxide (CH₃OOH) and
1314 formaldehyde (CH₂O)). However, uncertainties remain about the scavenging
1315 efficiencies of soluble species by deep convective storms. Simulations of an idealized
1316 thunderstorm by several cloud-resolving models yielded varying results for CH₂O, H₂O₂
1317 and HNO₃ in convective outflow due to differing microphysics and assumptions about
1318 retention of chemical species during cloud drop freezing (Barth et al., 2007).

1319 The CCATT-BRAMS simulations employ a lightning NO_x parameterization based on
1320 convective cloud top height (Stockwell et al., 1999). In WRF-Chem, lightning
1321 production of NO_x was not included, because these parameterizations have not yet been
1322 evaluated for the Amazon region. In the tropics, over continents, lightning production is
1323 comparable to other sources of NO_x, including biomass burning and soil release, and it
1324 is the primary source over oceans (Bond et al. 2002). Since lightning NO_x production

Excluído: also

Excluído: wet deposition and

Excluído: ere

Excluído: considered

Excluído: Uncertainties remain about the scavenging efficiencies of soluble species by deep convective storms. Simulations of an idealized thunderstorm by several cloud-resolving models yielded varying results for CH₂O, H₂O₂ and HNO₃ in convective outflow due to differing microphysics and assumptions about retention of chemical species during cloud drop freezing (Barth et al., 2007).

1339 peaks in the upper troposphere, it could be an important contributor to ozone
1340 production. The roles of wet deposition and lightning NO_x production will be more
1341 closely examined in future modeling studies of tropospheric chemistry in the Amazon.

1342 For model results evaluation, the mean vertical O₃ profiles for observations, CCATT-
1343 BRAMS and WRF-Chem were calculated for the regions to the west, north, south, east,
1344 and around Manaus. Horizontal flight legs were excluded from analysis to eliminate the
1345 influence of plumes in the boundary layer. As the model output has a much coarser
1346 spatial and temporal resolution than the aircraft measurements, the model value is
1347 interpolated to the observation time and location. To calculate the mean simulated
1348 profiles, the four grid points closest in latitude and longitude to each observation were
1349 determined at the two model hours that bracket the observations. At each of these grid
1350 points and hours, vertical profiles were extracted from the model output and then
1351 linearly interpolated to the observed GPS height. The four points from each time were
1352 averaged, weighting by the inverse distance to the observed longitude and latitude.
1353 Finally, the prior and posterior hour values were averaged with appropriate weights.
1354 Thus, 16 model points were used with spatial and temporal weights to obtain each
1355 model value for comparison to observations. The observed and model time series were
1356 then separated into five regions to the west, north, east, and south of Manaus, and in the
1357 region of Manaus itself. The mean value and standard deviation were calculated for
1358 each region and 500 m vertical bin. To facilitate comparison of other models with the
1359 data presented in Fig. 2, mean profiles from the large regions corresponding to clean
1360 (west, north and around Manaus regions) and polluted (east and south regions) regions
1361 during BARCA A and all regions during BARCA B are presented in Fig. 16. From the
1362 models, all horizontal grid points falling within the corresponding region's longitude
1363 and latitude bounds for each flight day (Table 6) and the closest model output times
1364 (12:00-18:00 UTC / 8:00-14:00 LT) were averaged into 500 m vertical bins.

1365 **3.3 Meteorological and satellite and ground-based O₃ data**

1366 Monthly mean precipitation over the Amazon region was obtained from the 3B43
1367 Tropical Rainfall Monitoring Mission (TRMM) and Other Data Precipitation Product at
1368 a spatial resolution of 0.25° × 0.25° (obtained from <http://trmm.gsfc.nasa.gov/>)
1369 (Kummerow et al., 1998; Kawanishi et al., 2000). TRMM 3B43 is derived from
1370 retrievals of 3-hourly precipitation amount from the Precipitation Radar (PR), TRMM
1371 Microwave Imager (TMI), and Visible and Infrared Scanner (VIRS) aboard the TRMM
1372 satellite, merged with rain gauge data from Climate Anomaly Monitoring System
1373 (CAMS) and the Global Precipitation Climatology Project (GPCP). Satellite estimates
1374 of precipitation are used for model evaluation due to their more complete spatial and
1375 temporal coverage compared to rain gauge data. Buarque et al. (2011) found that mean

Excluído: ¶

Excluído: S

Excluído: and meteorological

Excluído: In addition to the in-situ O₃ data, the model results were compared with OMI/MLS monthly mean tropospheric ozone mixing ratios and total column ozone (http://acd-ext.gsfc.nasa.gov/Data_services/cloud_slice/#pub) (Ziemke et al., 2006). Tropospheric values were estimated by subtracting the stratospheric contribution from total column measurements. A cloud-slicing method was used to detect O₃ inside optically thick clouds. This method was able to detect elevated O₃ levels of around 50 ppb in the upper parts of convective clouds over South America and Africa, comparable to background cloud-free levels in the tropics (Ziemke et al., 2009). The model total tropospheric O₃ column and mean tropospheric O₃ mixing ratio were calculated by summing O₃ mixing ratios, weighted by the model level air density, from the first model level to the level below the tropopause. The tropopause level was determined by the World Meteorological Organization (WMO) definition of a temperature lapse rate less than 2 K km⁻¹ (Logan, 1999). ¶
The models were also compared with soundings measuring O₃, temperature, and relative humidity conducted at sites in Paramaribo, Surinam (5.8°N, 55.2°W) and Natal, Brazil (5.4°S, 5.4°W) during the BARCA periods as part of the Southern Hemisphere Additional OZonesondes (SHADOZ) network (<http://croc.gsfc.nasa.gov/shadoz/>) (Thompson et al., 2003a, b, 2007). ¶

1416 annual rainfall from Brazilian rain gauge and TRMM 3B42 3-hourly data at 488 sites in
 1417 the Amazon Basin for the years 2003-2005 agreed within 5%. Other characteristics of
 1418 the rainfall distribution, such as the number of days with rainfall, differed more
 1419 substantially. Mean precipitation during the dry-to-wet (Nov. 2008) and wet-to-dry
 1420 (May 2009) transition seasons was calculated for the TRMM 3B43 data and the
 1421 CCATT-BRAMS and WRF-Chem models for three regions: the Amazon (15°S – 10°N,
 1422 50°W – 80°W), northeast Brazil (15°S – 0°N, 35°W – 50°W), and southeast South
 1423 America (15°S – 35°S, 35°W – 65°W). The values are listed in Table 2. The mean
 1424 precipitation on the 35 km resolution domain for the two months is shown in Fig. 4, as
 1425 well as the delineations of the subregion boxes.

1426 Surface downward shortwave radiation (Level 1.5) obtained with a Kipp and Zonen
 1427 CM-21 pyranometer (305-2800 nm) were obtained from the Solar Radiation Network
 1428 (SolRad-Net) site at Manaus (2.56°S, 60.04°W, 93 m a.s.l.)
 1429 (http://aeronet.gsfc.nasa.gov/cgi-bin/bamgommas_interactive) (Fig. 5).

1430 Mean daily cycles of fluxes of sensible and latent heat and radiation were obtained from
 1431 flux tower measurements for the wet (February - March 1999, January - March 2000)
 1432 and dry (July - September 1999-2000) seasons at forest (Rebio Jarú, 10.08°S, 61.93°W,
 1433 145 m a.s.l.) and pasture (Fazenda Nossa Senhora, 10.75°S, 62.37°W, 293 m a.s.l.)
 1434 tower sites (von Randow et al., 2004) (Figs. 6-7).

1435 Surface meteorological station data was obtained for the BARCA region for October -
 1436 November 2008 and April - May 2009 from 52 SYNOP (INMET) and 26 METAR
 1437 (airport) stations, the locations of which are depicted in Fig. 10. The models were also
 1438 evaluated against TRMM 3B42 3-hourly precipitation rates at the 78 surface station
 1439 locations in the Amazon. Mean observations and values of Root Mean Squared Error
 1440 (RMSE) and bias for the CCATT-BRAMS and WRF-Chem simulations are shown in
 1441 Table 3.

1442 Meteorological soundings from the Manaus airport (3.15°S, 59.98°W) were conducted
 1443 at 00:00 UTC (12 in October-November 2008, 60 in April-May 2009) and 12:00 UTC
 1444 (49 in October - November 2008, 60 in April - May 2009). During BARCA A, 13
 1445 additional soundings were conducted at 18:00 UTC from 18 November – 1 December
 1446 2008 (Figs. 8-9).

1447 Fisch et al. (2004) found that in the dry season (14-25 August, 1994), higher sensible
 1448 heat fluxes over pasture increase the maximum height at 21:00 UTC (17:00 LT) of the
 1449 Convective Boundary Layer (CBL) from around 1100 m for forest (Rebio Jarú) to 1650
 1450 m over pasture (FNS). On the other hand, during the wet season (January-February
 1451 1999) the height of the CBL was similar for both land types, around 1000 m. The
 1452 simulated height of the PBL at 21:00 UTC above the forest and pasture sites (Table 4)

Excluído: .

Excluído: Z

Excluído: Z

Excluído: Z 18

Excluído: <#>Model description and simulation setup¶

Movido para cima [10]: Simulations of BARCA A and B were conducted with the Chemistry Coupled Aerosol-Tracer Transport model to the Brazilian developments on the Regional Atmospheric Modeling System (CCATT-BRAMS; Longo et al., 2013; Freitas et al., 2009) and Weather Research and Forecasting with Chemistry (WRF-Chem; Grell et al., 2005) coupled chemistry and meteorology models. The model physics and chemistry options that were used are listed in Table 1. Both models used a two-way nested grid configuration, with a 140 km grid covering Africa and South America (southwest corner: 60°S, 100°W, northeast corner: 20°N, 50°W), to encompass the cross-Atlantic transport of biomass burning emissions from Africa, and a 35-km resolution grid covering most of South America (southwest corner: 35°S 85°W, northeast corner: 15°N, 30°W), as depicted in Fig. 3.¶
 The simulations were initialized on 1 October 2008 00:00 UTC and 1 April 2009 00:00 UTC for BARCA A and B, respectively. Boundary conditions and analysis nudging on the outer domain were given by the NCEP GFS analysis (<http://rda.ucar.edu/datasets/ds083.2/>) with a 6 hourly time resolution and 1° □ 1° spatial resolution. Chemistry initial and boundary conditions were provided by 6 hourly analyses from the Model of Atmospheric Chemistry at Large Scale (Modélisation de la Chimie Atmosphérique Grande Echelle, MOCAGE) global model (Peuch et al., 1999) with a T42 (~ 2.8°) spatial resolution. Sea surface temperature was provided by the NOAA Optimum Interpolation (OI) Sea Surface Temperature (SST) V2 (available at <http://www.esrl.noaa.gov/psd/data/gridded/data.noaa.oisst.v2.html>) with 1° □ 1° spatial resolution. Soil moisture was initialized with the TRMM-based soil moisture operational product (GPNR) developed by Gevaerd and Freitas (2006). ¶
 The PBL parameterization in CCATT-BRAMS is based on Mellor and Yamada (1982), while in WRF-Chem the Mellor-Yamada-Janjic (MYJ; Janjic, 1994) scheme was used. In CCATT-BRAMS, shallow and deep convection are parameterized based on the mass-flux approach of Grell and Dévényi (2002). CCATT-BRAMS also uses the Turbulent Kinetic Energy (TKE) from the Planetary Boundary Layer (PBL) scheme to determine if convection will be triggered within a grid cell. In WRF-Chem the Grell 3D (G3) scheme was used, which includes subsidence spreading of convective outflow into neighboring grid cells. The Noah land surface model (Koren et al., 1999) was used in WRF-Chem... [5]

1615 was analyzed from model output using two different methods: *TKE*, the first level above
1616 the surface where the Turbulent Kinetic Energy (TKE) from the PBL schemes dropped
1617 below $0.01 \text{ m}^2 \text{ s}^{-1}$ and *Theta*, the first level above the surface where theta exceeded theta
1618 of the level below by 0.6 K. In addition, *WRF MYNN* is the diagnostic from the WRF
1619 PBL scheme which takes into account TKE as well as stability.

1620 In addition to the in-situ O_3 data, the model results were compared with OMI/MLS
1621 monthly mean tropospheric ozone mixing ratios and total column ozone (http://acd-ext.gsfc.nasa.gov/Data_services/cloud_slice/#pub) (Ziemke et al., 2006) (Fig. 20-21). In
1622 this product, the tropospheric values are estimated by subtracting the stratospheric
1623 contribution from total column measurements. A cloud-slicing method is used to detect
1624 O_3 inside optically thick clouds. This method is able to detect elevated O_3 levels of
1625 around 50 ppb in the upper parts of convective clouds over South America and Africa,
1626 comparable to background cloud-free levels in the tropics (Ziemke et al., 2009). In this
1627 study, the model total tropospheric O_3 column and mean tropospheric O_3 mixing ratio
1628 were calculated by summing O_3 mixing ratios, weighted by the model level air density,
1629 from the first model level to the level below the tropopause. The tropopause level was
1630 determined by the World Meteorological Organization (WMO) definition of a
1631 temperature lapse rate less than 2 K km^{-1} (Logan, 1999).
1632

1633 The models were also compared with soundings measuring O_3 , temperature, and
1634 relative humidity conducted at sites in Paramaribo, Surinam (5.8°N , 55.2°W) and Natal,
1635 Brazil (5.4°S , 5.4°W) during the BARCA periods as part of the Southern Hemisphere
1636 ADditional OZonesondes (SHADOZ) network (<http://croc.gsfc.nasa.gov/shadoz/>)
1637 (Thompson et al., 2003a, b, 2007) (Fig. 22).

1638 **4 Results and discussion**

1639 **4.1 BARCA O_3 Observations**

1640 The vertical distributions of O_3 measured by the aircraft during BARCA A and B are
1641 depicted in Fig. 2. Observations during the dry-to-wet transition (BARCA A) are
1642 plotted separately for clean (west, north and around Manaus regions) and fire-influenced
1643 polluted (east and south regions) conditions. [The longitude and latitude bounds and flight dates included in each geographic region from BARCA A and BARCA B are listed in Table 6.](#) The O_3 distributions are similar during BARCA A in the clean regions
1644 and BARCA B, with median values ranging from 10-25 ppb. However, there is more
1645 variability, as measured by the difference between the 25th and 75th percentiles, in the
1646 BARCA A data. This may be due to downward mixing of O_3 transported long-range
1647 from fires in Africa or recirculated from the polluted southeast Brazil region. In the fire-
1648 influenced regions during BARCA A, medians range from 25-45 ppb, peaking at a
1649 typical plume injection height for savanna fires of 2-3 km. The highest variability is
1650
1651

1652 seen in polluted conditions during BARCA A, particularly at 2-3 km, indicating the
1653 influence of small-scale fire plumes. This variability of O₃ in the PBL presents a
1654 challenge to the regional models, since the effects of small-scale processes such as
1655 plume rise and convection are parameterized and averaged across the grid cell.

1656 4.2 Observed and Simulated Meteorology

1657 Tropospheric O₃ distributions are driven by both chemical processes, including
1658 chemistry and emissions of O₃ precursors, and meteorological ones, such as solar
1659 radiation, tracer transport and removal. During the dry-to-wet transition season,
1660 increased actinic fluxes stimulate the production of OH radicals from O₃ photolysis that
1661 can lead to net O₃ production (Seinfeld and Pandis, 2006). In November 2008, a band of
1662 increased precipitation extended, in TRMM 3B43 observations from the northwest
1663 Amazon to southeast Brazil but the northern Amazon between Manaus and Belém was
1664 relatively dry (Fig. 4a). On the other hand, in the wet-to-dry transition season, lower
1665 levels of O₃ are largely associated with increased presence of convective clouds and
1666 precipitation. Decreased surface temperatures and incident solar radiation due to
1667 cloudiness suppress emissions of biogenic VOCs such as isoprene (Fall and
1668 Wildermuth, 1998). In addition, higher surface humidity and precipitation decrease the
1669 occurrence of fires (Morton et al., 2013; Chen et al., 2013) that emit NO_x and VOCs
1670 (Freitas et al., 2007). O₃ precursors are further decreased by wet removal within the
1671 storms (Barth et al., 2007a). In May 2009, increased precipitation as observed by
1672 TRMM 3B43 extended, from the western Amazon to the northeast coast of Brazil (Fig.
1673 4b). In radiosoundings at Manaus, a more pronounced decrease in dew point
1674 temperature from 0:00 UTC to 12:00 UTC is observed in May 2009 (Fig. 9) than Nov.
1675 2008 (Fig. 8) in upper levels (300-400 hPa), likely due to more precipitation.

1676 Land cover also impacts surface heat and moisture exchange and can thus affect
1677 convective triggering. In both transition seasons, surface sensible heat fluxes are higher
1678 and latent heat fluxes are lower at the pasture compared to forest sites (Figs. 6a-b and
1679 7a-b). However, incident solar radiation and thereby peak sensible heat flux (Fig. 7) are
1680 lower in the wet-to-dry than dry-to-wet transitions (Fig. 6) for both forest and pasture
1681 sites.

1682 Now we summarize the key findings of the model-data meteorological comparison and
1683 their implications for the chemistry simulations. The models capture the seasonal spatial
1684 distribution of precipitation over northern South America signs of NE-SE differences
1685 are correctly modeled by both models during both seasons, i.e., the NE is drier than the
1686 SE during November, and vice-versa during May. For the Amazon, CCATT-BRAMS
1687 slightly underestimates the precipitation rates in both seasons, but the rate in WRF-
1688 Chem is about twice that of TRMM 3B43 (Table 2). This may lead to errors in the

Excluído: In addition to surface emissions and chemical sources and sinks of O₃, several meteorological processes are key drivers of tropospheric O₃ distributions, including solar radiation, tracer transport and removal. Thus, first we evaluate the ability of the models to represent these processes and their seasonalities.¶

Excluído: In

Excluído: ,

Excluído: s

Excluído: , and precipitation is also intense in the ITCZ at 10°N (Fig. 4)

Excluído: In

Excluído: s

Excluído: 5

Movido (inserção) [9]

Excluído: from 0 to 12 or 18Z

Excluído: , more pronounced in the wet-to-dry transition season (Figs. 9 and 10).

Excluído: Incident solar radiation is higher in the dry than wet season for both sites (Figs. 6-8). At the forest and pasture sites, peak sensible heat flux is higher in the dry-to-wet than wet-to-dry transition seasons, and higher at forest than pasture sites for both seasons, while latent heat flux is higher in the wet-to-dry than dry-to-wet transition seasons for both sites, and higher at the pasture site for both seasons (Figs. 7 and 8).

Movido para cima [9]: In radiosoundings, a decrease in dew point temperature is observed in upper levels (300-400 hPa) from 0 to 12 or 18Z, likely due to precipitation, more pronounced in the wet-to-dry transition season (Figs. 9 and 10).

Excluído: Mean precipitation during the dry-to-wet (November 2008) and wet-to-dry (May 2009) transition seasons was calculated for the TRMM 3B43 data and the CCATT-BRAMS and WRF-Chem models for three regions: the Amazon (15°S – 10°N, 50°W – 80°W), northeast Brazil (15°S – 0°N, 35°W – 50°W), and southeast South America (15°S – 35°S, 35°W – 65°W). The values are listed in Table 2. The mean precipitation on the 35-km resolution domain for the two months is shown in Figs. 3 and 4, respectively, as well as the delineations of the subregion boxes. The signs of NE-SE differences are correctly modeled by both models during both seasons, i.e., the NE is drier than the SE during November, and vice-versa during May. For the Amazon, CCATT-BRAMS slightly underestimates the precipitation rates in both seasons, but the rate in WRF-Chem is about twice that of TRMM ... [6]

Movido (inserção) [8]

Excluído: , although the mean precipitation rates are slightly lower (CCATT-BRAMS) and substantially ... [7]

Excluído: indicate

1786 [strength and vertical distribution of convective transport and the amount of convective](#)
1787 [wet removal.](#)

1788 [Peak surface shortwave radiation during the dry-to-wet transition at Manaus is within](#)
1789 [the error bars of the observations for both models \(Fig. 5\). However, for the southern](#)
1790 [Amazon forest and pasture sites peak shortwave may be overestimated \(underestimated\)](#)
1791 [by 50-100 W m⁻² by CCATT-BRAMS \(WRF-Chem\) \(Figs. 6-7\), suggesting that there](#)
1792 [is insufficient \(excessive\) cloudiness in the models. This will increase \(decrease\) surface](#)
1793 [temperature and evaporation, and therefore increase \(decrease\) O₃ production from](#)
1794 [photolysis.](#)

1795 [In the dry-to-wet transition season \(Fig. 7\), the observed Bowen ratio \(sensible/latent](#)
1796 [heat flux\) is lower at the forest site than the pasture site \(0.23-0.38 vs. 0.8\). However, in](#)
1797 [WRF-Chem, the Bowen ratio at 13:00 LT shows a smaller contrast between the forest](#)
1798 [and pasture sites \(0.40 vs. 0.51\), due to underestimated sensible heat flux at the pasture](#)
1799 [site. In the wet-to-dry transition season \(Fig. 8\), the observed Bowen ratio is lower at](#)
1800 [both forest and pasture sites for this season \(0.18-0.39 vs. 0.33-0.59\). On the other hand,](#)
1801 [in WRF-Chem, latent and sensible heat flux and thus the Bowen ratio are nearly](#)
1802 [constant at the forest and pasture sites \(0.39 vs. 0.38\). This indicates that the Noah land](#)
1803 [surface model is not properly representing the impact of conversion of forest to pasture](#)
1804 [and the resulting increase in sensible heat flux.](#)

1805 [At the surface stations \(Table 3\), both models overestimate precipitation on average,](#)
1806 [Dew point temperature is underestimated by 1-2 K and temperature is underestimated in](#)
1807 [all cases by 0.1 - 2.4 K except by CCATT-BRAMS during BARCA A, which](#)
1808 [overestimated temperature by about 1 K. All of these biases will decrease](#)
1809 [photochemical O₃ production at the surface. The models generally show good](#)
1810 [agreement with soundings at Manaus, but excess moisture \(positive dewpoint bias of 10](#)
1811 [K\) in CCATT-BRAMS above 500 hPa may lead to increased O₃ production at mid-](#)
1812 [levels.](#)

1813 [Next we compare the CBL heights for wet and dry seasons reported by Fisch et al.](#)
1814 [\(2004\) with the simulated PBL heights in the dry-to-wet and wet-to-dry transitions](#)
1815 [\(Table 4\). The models represent the pattern of lower PBL heights in the wet-to-dry than](#)
1816 [dry-to-wet transitions, and similar PBL heights at the forest and pasture sites. However,](#)
1817 [for the dry-to-wet transition, the PBL heights are indistinguishable between forest and](#)
1818 [pasture sites for both models, and generally closer to the observed forest \(1.1 km\) than](#)
1819 [pasture \(1.65 km\) values. Additionally, for the wet-to-dry transition, the mean PBL](#)
1820 [height for all models and diagnostics except Theta for CCATT-BRAMS are lower than](#)
1821 [observed \(1 km\). Overall the models underestimate the PBL depth, which may](#)
1822 [contribute to an overestimate of O₃ near the ground. Despite these limitations, the](#)

Movido (inserção) [7]

Excluído: Peak shortwave radiation is slightly overestimated by both models, which may be related to low cloudiness (convection is triggering too early) or AOD (too much aerosol wet removal). This will increase O₃ production from photolysis, as well as increase surface temperature and evaporation. Although biogenic emissions are not coupled with meteorology in these simulations, this may increase biogenic emissions in future studies that include online biogenic emissions. WRF-Chem predicts a nearly constant Bowen ratio at forest and pasture sites. This indicates that the Noah land surface model is not properly representing the impact of conversion of forest to pasture and the resulting increase in sensible heat flux. ¶

In the dry-to-wet transition season, for both CCATT-BRAMS and WRF-Chem, the mean daily cycle of surface incident shortwave radiation calculated for the Manaus AERONET site for October–November 2008, falls within one standard deviation of the mean AERONET observations (Fig. 6), but is closer to the upper limit, possibly due to underestimated cloudiness or AOD in the models. For the forest and pasture sites, both models represent the daily cycles of incident ... [8]

Excluído: peak latent heat flux at 13:00 LT is higher at the forest site than at the pasture site (460 W m⁻² vs. 268 W m⁻²) whereas the sensible heat flux shows ... [9]

Movido para cima [7]: Both models represent the daily cycles of incident shortwave and incoming and outgoing longwave radiation, although incident ... [10]

Excluído: as for the dry-to-wet transition, peak latent heat flux at 13:00 LT is higher at the forest site than at the pasture site (401 W m⁻² vs. 324 W m⁻²). However, the ... [11]

Excluído: Mean vertical profiles at Manaus from radiosoundings, CCATT-BRAMS and WRF-Chem for October - November 2008 at 0, 12 and 18Z at ... [12]

Excluído: B

Excluído: , with a RMSE of 2.4 - 3.0 mm h⁻¹ and bias of 0.3-3.5 mm h⁻¹ for CCATT-BRAMS, and RMSE of 4.5 - 7.1 mm h⁻¹ and bias of 3.5-5.8 mm h⁻¹ for WRF-Chem

Excluído: surface pressure is underestimated by 1 - 2 hPa. Wind speed is underestimated by CCATT-BRAM ... [13]

Movido (inserção) [6]

Excluído: stimulate

Excluído: excess

Excluído: ¶

Movido para cima [8]: Now we summarize the key findings of the model-data meteorological comparison and their implications for the chemistry simu ... [14]

Movido para cima [6]: The models generally show good agreement with soundings, but excess moisture in ... [15]

2038 models are able to capture the meteorological contrast between the dry-to-wet and wet-
2039 to-dry transition seasons.

2040 4.3 Observed and Simulated Chemistry

2041 4.3.1 Mean O₃ Profiles

2042 An example of observed and simulated O₃ during the flight legs between Manaus and
2043 Belém in BARCA A and B is shown in Fig. 17. While the models capture the pattern of
2044 increasing O₃ values with height, the models underestimate elevated O₃ values from 2.5-
2045 4.5 km, and overestimate low values near the surface (1-1.5 km). The models also do
2046 not reproduce the variability in the high values, likely due to the aircraft intersection of
2047 biomass burning plumes. This is expected given the coarse horizontal grid resolution.
2048 Thus, mean profiles are analyzed in order to study differences among the regions and
2049 seasons and to assess the models' abilities to capture the impacts of such small-scale
2050 processes on regional O₃ distributions.

2051 The mean vertical O₃ profiles for observations, CCATT-BRAMS and WRF-Chem for
2052 the regions to the west, north, south, east and around Manaus are shown for BARCA A
2053 and B in Figs. 12 and 14, respectively, and NO profiles corresponding to the aircraft
2054 tracks are depicted in Figs. 13 and 15, respectively. Mean profiles from longitudinal
2055 surveys over Amazonia of O₃ during ABLE-2A (Browell et al., 1988) and ABLE-2B
2056 (Harriss et al., 1990) and NO during ABLE-2A (Torres and Buchan, 1988) are included
2057 for comparison. In BARCA B, O₃ values were at or near background values in all
2058 regions, ranging from 8 - 15 ppb at the surface to 2 - 15 ppb at 4 - 4.5 km, and the
2059 models are generally within 5 - 10 ppb of the observations. During BARCA A, while
2060 the W region still had low O₃ values (5 ppb at the surface to 20 ppb at 4 - 4.5 km), the
2061 N, S and M regions ranged from 15 - 20 ppb at the surface to 30 - 35 ppb at 4 - 4.5 km,
2062 and the E region presented the most elevated values, from 25 - 55 ppb. ABLE-2A O₃
2063 profiles are similar in all regions, ranging from 15 - 20 ppb near the surface to 30 - 40
2064 ppb from 4 - 6 km, so that the BARCA values are higher in the fire-influenced east and
2065 south regions, lower in the north and west regions, and very similar around Manaus.
2066 The profiles from ABLE-2B are within one standard deviation of the BARCA B
2067 measurements, except for the north region, where they are lower (5-15 ppb). These
2068 results suggest an increasing influence of fire emissions to the east and south of
2069 Manaus, but that O₃ in clean regions has not changed much.

2070 A similar model behavior is seen in the broad regional mean profiles (Fig. 16). All
2071 simulations over-estimate O₃ throughout the PBL and lower troposphere during clean
2072 conditions in BARCA A, but under-estimate O₃ in polluted conditions. This is
2073 especially true from 2-4 km where biomass burning plumes detrain O₃ precursors.
2074 During BARCA B all simulations show good agreement.

Movido (inserção) [5]

Excluído: Lower levels of O₃ in the rainy season are largely associated with increased presence of convective clouds and precipitation. Decreased surface temperatures and incident solar radiation due to cloudiness suppress emissions of biogenic VOCs such as isoprene. In addition, higher surface humidity and precipitation decrease the occurrence of fires that emit NO_x and VOCs. O₃ precursors are further decreased by wet removal within the storms. On the other hand, during the dry-to-wet transition season, increased solar radiation, latent heat and temperature stimulate the production of OH and other HO_x radicals that can stimulate net O₃ production. ¶

Movido para cima [5]: Lower levels of O₃ in the rainy season are largely associated with increased presence of convective clouds and precipitation. Decreased surface temperatures and incident solar radiation due to cloudiness suppress emissions of biogenic VOCs such as isoprene. In addition, higher surface humidity and precipitation decrease the occurrence of fires that emit NO_x and VOCs. O₃ precursors are further decreased by wet removal within the storms. On the other hand, during the dry-to-wet transition season, increased solar radiation, latent heat and temperature stimulate the production of OH and other HO_x radicals that can stimulate net O₃ production.

Movido (inserção) [4]

Excluído: However, the BARCA observations are generally lower than the models in the boundary layer, indicating that the satellites appear here to be dominated by the middle troposphere and long-range transport.

Excluído: 8

Excluído: 20

Excluído: 9

Excluído: 2

Excluído: 6

Excluído: ¶
Both models generally overestimate O₃ from 1-2 km and underestimate O₃ from 3-4.5 km. As seen in the CO results shown in Andreae et al. (2012), the model profiles have steeper slopes than the observations, except in the polluted south, possibly due to excessive vertical mixing of precursors. In addition, the models may be missing sources of O₃ and/or precursors at 3-4.5 km in the model inflow boundary conditions. In general the models overestimate O₃ in the PBL compared to aircraft measurements, but underestimate the total column values relative to the OMI/MLS satellite product. This suggests that the total column values in Amazonia are dominated by global pollution from Africa, rather than local O₃ production from biomass burning. ¶

2139 In order to understand the possible sources of model error, we now individually
2140 examine the contributions of different chemical sources and sinks, including surface
2141 emissions and deposition, boundary inflow and chemistry within the PBL.

2142 **4.3.2 Emissions**

2143 The relative sensitivities of O₃ production to NO_x or BVOC emissions depend upon the
2144 relative amounts of VOCs and NO_x present. Under clean conditions with a high
2145 VOC:NO_x ratio, O₃ production is NO_x sensitive, whereby increases in NO_x will lead to
2146 increases in O₃ while increased VOCs will have little impact. On the other hand, in
2147 polluted areas with a high NO_x:VOC ratio, the system is VOC-sensitive, that is,
2148 increased VOCs contribute to O₃ production but an increase in NO_x actually depletes
2149 O₃. Emissions of BVOCs can increase O₃ production by the following mechanism.
2150 Oxidation of BVOCs can lead to formation of HO₂ and RO₂•, which react with NO to
2151 form NO₂. NO₂ in turn photolyzes to form O(³P), which reacts with O₂ to form O₃
2152 (National Research Council, 1991). We expect the polluted east/south regions during
2153 BARCA A to be VOC-sensitive and the clean west, north and around Manaus regions
2154 during BARCA A and all regions in BARCA B to be NO_x-sensitive. Kuhn et al. (2010)
2155 determined via aircraft transects in the Manaus urban plume that most of the VOC
2156 reactivity was provided by isoprene emissions from the surrounding rainforest, and NO_x
2157 emissions suppressed O₃ production close to urban sources, but stimulated it downwind.

2158 For BARCA, the simulated mean monthly emission rates for two O₃ precursors, NO_x
2159 (anthropogenic and biomass burning) and isoprene (biogenic) are shown in Fig. 17. In
2160 Nov. 2008, elevated NO_x emission rates of up to $5 \times 10^{-5} \text{ kg m}^{-2} \text{ day}^{-1}$ are seen from an
2161 area of intense biomass burning in the northeast Amazon, as well as from more
2162 scattered fires in the southeast Amazon. These are both regions that were overflowed by
2163 the aircraft (Fig. 1). In May 2009, the Amazon region is largely free of fire. Because
2164 biogenic NO emissions (e.g., from soil) were not included in the MEGAN climatology
2165 used in this study, background NO emissions (in absence of fire) are likely too low.
2166 Typical model anthropogenic NO_x emissions values over the Amazon, primarily from
2167 biofuel sources, were 0.008-13 $\mu\text{g N m}^{-2} \text{ hr}^{-1}$. This NO_x emissions included in the
2168 models were less than one third of the mean values of $44 \pm 14 \mu\text{g N m}^{-2} \text{ h}^{-1}$ NO
2169 measured by Kaplan et al. (1988) during ABLE-2A. This is considered a threshold
2170 value for NO_x-driven O₃ production to be the dominant O₃ source in the PBL. The
2171 model emissions were also much lower than the mean emissions from forest of $35.8 \mu\text{g}$
2172 $\text{N m}^{-2} \text{ h}^{-1}$ NO measured in the 1998 dry season (Garcia-Montiel et al., 2003). Wetting
2173 the forest soil resulted in small pulses of NO and therefore the mean emissions are
2174 expected to be higher in the wet season than dry season.

Excluído: 2

Excluído: 2

2177 Isoprene emissions are highest in the western and southern Amazon, reaching 15×10^{-5}
2178 $\text{kg m}^{-2} \text{d}^{-1}$ in November 2008 and $5-10 \times 10^{-5} \text{kg m}^{-2} \text{d}^{-1}$ in the aircraft sampling region.
2179 Due to decreased surface temperature and incident solar radiation in the rainy season,
2180 isoprene emissions in the Amazon Basin are much lower during BARCA B, $3-5 \times 10^{-5}$
2181 $\text{kg m}^{-2} \text{d}^{-1}$. The MEGAN emissions are consistent with isoprene emission measurements
2182 above the Amazonian canopy: a normalized flux of $5.76 \times 10^{-5} \text{kg m}^{-2} \text{d}^{-1}$ in July 2000 at
2183 the end of the rainy season (Rinne et al., 2002) and an average noontime flux of $18.7 \pm$
2184 $5.5 \times 10^{-5} \text{kg m}^{-2} \text{d}^{-1}$ in September 2004 during the dry season (Karl et al., 2007).

Excluído: .

2185 4.3.3 Deposition

2186 Figures 18 and 19 show the average O_3 dry deposition flux and median daytime
2187 deposition velocity, respectively, as simulated on the 35 km resolution domain by the
2188 CCATT-BRAMS and WRF-Chem models for November 2008 and May 2009. In the
2189 Amazon Basin, O_3 deposition fluxes are higher in the dry-to-wet transition season, with
2190 values reaching $3.5 \text{ nmol m}^{-2} \text{ s}^{-1}$ for CCATT-BRAMS and $6 \text{ nmol m}^{-2} \text{ s}^{-1}$ for WRF-
2191 Chem in the northeast Amazon, near the region of concentrated biomass burning. These
2192 values are also seen along the northern Andes and Southeast Brazil, due to recirculation
2193 of O_3 -rich air. In the wet-to-dry transition season, O_3 deposition is at a minimum in the
2194 western Amazon, with values of $0.5-1 \text{ nmol m}^{-2} \text{ s}^{-1}$ for CCATT-BRAMS and 2 nmol m^{-2}
2195 s^{-1} for WRF-Chem. For both models, deposition velocities are higher over the rainforest
2196 than in the savanna to the east or south of the Amazon Basin, and higher in the wet-to-
2197 dry transition than in the dry-to-wet transition. These patterns are also seen in the tower
2198 observations in Table 5.

Excluído: 3

Excluído: 4

Excluído: 4

2199 O_3 surface fluxes and dry deposition velocities predicted by the models were compared
2200 with observations from several field campaigns (Table 5). These include during the dry
2201 (May 1999) and wet (September–October 1999) seasons at Reserva Biológica Jarú
2202 (RBJ, forest) and Fazenda Nossa Senhora (FNS, pasture) from LBA-EUSTACH
2203 (Rummel et al., 2009; Kirkman et al., 2002) and during the wet season at Reserva
2204 Ducke (RD, forest tower near Manaus, 2.95°S , 59.95°W) from ABLE 2B (April–May
2205 1987) (Fan et al., 1990) and at FNS from LBA-TRMM (January - February 1999) (Sigler
2206 et al., 2002). For the observations, the means of the hourly (WRF-Chem) and 3-hourly
2207 (CCATT-BRAMS) O_3 dry deposition fluxes ($\text{nmol m}^{-2} \text{ s}^{-1}$) and the medians of the
2208 daytime (11:00 – 21:00 UTC) hourly mean deposition velocities (cm s^{-1}) are shown.
2209 The values were extracted from the grid points closest to the tower locations. In the
2210 observations, O_3 fluxes are larger in the dry season, due to higher O_3 mixing ratios.
2211 However, deposition velocities are higher in the wet season, and O_3 deposition to the
2212 Amazon forest constitutes a globally significant O_3 sink (Rummel et al., 2009). Both
2213 models capture these patterns, but the models underestimate the deposition velocities by

Excluído: 4

2219 15-75%, which may be partially responsible for the low O₃ fluxes at the Jarú forest site
2220 in both seasons and the pasture site in the dry season.

2221 4.3.4 Boundary Conditions

2222 The mean tropospheric and total tropospheric column O₃ from OMI/MLS, CCATT-
2223 BRAMS and WRF-Chem for November 2008 and May 2009 are shown in Figs. 20, and
2224 21, respectively. The models significantly underestimate the total columns from satellite
2225 and middle altitudes from BARCA. For both BARCA A and B, the models represent
2226 the pattern of lower O₃ over the Amazon and higher values over northeast Brazil
2227 (BARCA A only) and at 30°S, although the values are strongly underestimated. In
2228 November 2008, OMI/MLS mean tropospheric O₃ concentrations show an inflow of
2229 elevated O₃ (mean ca. 55 ppb, total 40-45 DU) on the northeast Brazilian coast due to
2230 cross-Atlantic transport from biomass burning in southern and sub-Saharan Africa.
2231 Additionally, a band of elevated O₃ (mean 55-60 ppb, total 35-40 DU) passes over the
2232 South American continent at around 30°S, also from cross-Atlantic transport. During
2233 this month, Northern Hemisphere O₃ levels to the north of South America are relatively
2234 low (mean 35-40 ppb, total 25-30 DU). On the other hand, the tropospheric ozone
2235 distribution in May 2009 (Fig. 16) is characterized by a band of low ozone extending
2236 over the Amazon Basin and northeast Brazil between 10°S and 10°N (mean 25-35 ppb,
2237 total 20-25 DU). In addition, slightly elevated values at around 30°S, primarily over the
2238 oceans (40-55 ppb, 30-35 DU) and higher ozone in the Northern Hemisphere (mean 50-
2239 55 ppb, total 35-40 DU north of 10°N). Both models capture the overall distribution
2240 (inflow in NE Brazil in Nov. 2008, lower values over the Amazon Basin, elevated at
2241 30°S) but values are underestimated relative to OMI/MLS. In general the models
2242 overestimate O₃ in the PBL compared to aircraft measurements, but underestimate the
2243 total column values relative to the OMI/MLS satellite product. This suggests that the
2244 total column values in Amazonia are dominated by global pollution from Africa, rather
2245 than local O₃ production from biomass burning. A typical OMI averaging kernel (cloud-
2246 free ocean conditions) shows maximum sensitivity from 594-416 hPa (Zhang et al.,
2247 2010). Therefore, OMI may not be detecting O₃ in the PBL from local sources, but
2248 rather primarily seeing global pollution from Africa.

2249 Above the boundary layer, from 3-4 km a.g.l., chemical inflow at the eastern boundary
2250 of South America may contribute to O₃ elevated above background. In order to evaluate
2251 the model representation of this inflow, vertical profiles from SHADOZ soundings on
2252 the northeast coast of South America during the BARCA A and B periods were
2253 compared with CCATT-BRAMS and WRF-Chem (Fig. 22). In addition, 120 h back
2254 trajectories from the sounding locations at heights of 1500 m, 6000 and 9000 m above
2255 ground level (gal) were calculated with the HYSPLIT model

Movido para baixo [3]: <#>The mean tropospheric and total tropospheric column O₃ from OMI/MLS, CCATT-BRAMS and WRF-Chem for November 2008 and May 2009 are shown in Figs. 15 and 16, respectively. The models significantly underestimate the total columns from satellite and middle altitudes from BARCA. For both BARCA A and B, the models represent the pattern of lower O₃ over the Amazon and higher values over northeast Brazil (BARCA A only) and at 30°S, although the values are strongly underestimated. In November 2008, OMI/MLS mean tropospheric O₃ concentrations show an inflow of elevated O₃ (mean ca. 55 ppb, total 40-45 DU) on the northeast Brazilian coast due to cross-Atlantic transport from biomass burning in southern and sub-Saharan Africa. Additionally, a band of elevated O₃ (mean 55-60 ppb, total 35-40 DU) passes over the South American continent at around 30°S, also from cross-Atlantic transport. During this month, Northern Hemisphere O₃ levels to the north of South America are relatively low (mean 35-40 ppb, total 25-30 DU). On the other hand, the tropospheric ozone distribution in May 2009 (Fig. 16) is characterized by a band of low ozone extending over the Amazon Basin and northeast Brazil between 10°S and 10°N (mean 25-35 ppb, total 20-25 DU). In addition, slightly elevated values at around 30°S, primarily over the oceans (40-55 ppb, 30-35 DU) and higher ozone in the Northern Hemisphere (mean 50-55 ppb, total 35-40 DU north of 10°N). Both models capture the pattern of... [16]

Movido para cima [4]: <#>However, the BARCA observations are generally lower than the models in the boundary layer, indicating that the satellites appear here to be dominated by the middle troposphere and long-range transport. An example of observed and simulated O₃ during the flight legs between Manaus and Belém in BARCA A and B is shown in Fig. 17. While the models capture the pattern of... [17]

Movido (inserção) [3]

Excluído: 15

Excluído: 16

Movido para baixo [2]: The excess O₃ in the PBL in the models could be due to either a low deposition sink, as O₃ dry deposition velocities in the models are about half of observed values, or excessive model sensitivity to NO_x emissions, or both. Two additional simulations were conducted with WRF-Chem to evaluate the model sensitivity to these processes: (1) doubling the calculated deposition velocity for O₃ only (2DEPVEL) and (2) halving the NO_x surface emission rates (0.5ENOX). ... [18]

2534 (<http://ready.arl.noaa.gov/hypub-bin/trajtype.pl?runtime=archive>) using meteorological
2535 data from the NCEP/NCAR global reanalysis. Inflow at Paramaribo originated either in
2536 the Caribbean or the tropical Atlantic, while at Natal, air parcels came from anti-
2537 cyclonic recirculation from southeastern Brazil or the tropical Atlantic. Both models
2538 generally represent the SHADOZ O₃ profiles up to 600 hPa, but do not capture layers of
2539 elevated O₃ above 500 hPa. These are likely to be either from pollution recirculated
2540 from southeast Brazil or possibly from African biomass burning. The models also do
2541 not reproduce thinner layers of high O₃ below 600 hPa. For example, at Natal on 7
2542 November 2008 (Fig. 22c, air of African origin at ~850 hPa and ~470 hPa) and 19
2543 November 2008 (Fig. 22d, air from the central African coast at ~850 hPa and
2544 recirculation from southeastern Brazil at ~470 hPa and ~310 hPa) and at Paramaribo on
2545 11 May 2009 (Fig. 22f, air of tropical Atlantic origin at all three levels), both models
2546 underestimate O₃ above 500 hPa by 40-60 ppb (model values of 30-50 ppb versus
2547 observations maximum values of 80-100 ppb). A previous analysis of ozone soundings
2548 and aircraft measurements at Natal suggested that increases in tropospheric ozone in the
2549 Southern Hemisphere springtime may be due to stratospheric intrusion (Logan, 1985).
2550 This is consistent with the November 2008 profiles at Natal; the models may not be
2551 capturing the intrusion of stratospheric air masses seen in the observations, indicated by
2552 upper tropospheric (> 500 hPa) layers with elevated O₃ and very low relative humidity
2553 (< 20%). On the other hand, at Paramaribo on 6 November 2008 and 25 November 2008 and
2554 at Paramaribo on 4 May 2009, when air masses at all levels were of Northern
2555 Hemisphere origin, the models reproduced the nearly constant with altitude O₃ values of
2556 30-40 ppb.

Excluído: 7,

Excluído: 19,

Excluído: 11,

Excluído: s

Excluído: 6

Excluído: 25,

2557 4.3.5 Chemistry

2558 The excess O₃ in the PBL in the models could be due to either a low deposition sink, as
2559 O₃ dry deposition velocities in the models are about half of observed values, or
2560 excessive model sensitivity to NO_x emissions, or both. Two additional simulations were
2561 conducted with WRF-Chem to evaluate the model sensitivity to these processes: (1)
2562 doubling the calculated deposition velocity for O₃ only (2DEPVEL) and (2) halving the
2563 NO_x surface emission rates (0.5ENOX). The O₃ profiles corresponding to BARCA
2564 flights for these two simulations are also included in Figs. 12 and 14. The corresponding
2565 NO profiles from all model simulations as well as a mean profile over Amazônia from
2566 ABLE-2A are depicted in Figs. 13 and 14. The 0.5ENOX simulation reduces O₃ more
2567 than 2DEPVEL throughout the entire profile. In the dry-to-wet transition, 2DEPVEL
2568 reduces O₃ in the lower PBL by about 25%, while 0.5ENOX decreases O₃ by around
2569 40%, and in the wet-to-dry-transition the reductions are about 10% and 30%,
2570 respectively. In general the 0.5ENOX O₃ profiles are lower than observed in the first 500
2571 m above the surface, but they provide the best representation of the data for the north

Formatado: articletitle, Justificado,
Espaço Antes: 6 pt, Depois de: 6 pt,
Espaçamento entre linhas: Pelo menos
18 pt, Vários níveis + Nível: 3 + Estilo
da numeração: 1, 2, 3, ... + Iniciar em:
2 + Alinhamento: Esquerda + Alinhado
em: 0 cm + Recuar em: 1.27 cm,
Manter com o próximo

Movido (inserção) [2]

Formatado: Heading 21, Espaço
Antes: 6 pt

Excluído: 8

Excluído: 20

Excluído: 9

Excluído: 21

2582 and west regions in the dry-to-wet transition. They also provide a similarly good fit as
2583 2DEPVEL for the east, Manaus and south regions, while in the wet-to-dry transition
2584 0.5ENOX is closer to the observed value from 0-500 m in all regions except the north.
2585 During BARCA A, NO in all WRF-Chem simulations in the north, west, and Manaus
2586 regions is 10-15 ppt from 0-500 m above the surface, increasing to a maximum of 20-50
2587 ppt at 2 km a.g.l., and is generally lower than the ABLE-2A observations in the PBL. In
2588 the east and south, where biomass burning influence was seen, NO in 0-500 m a.g.l.
2589 increased from 20-50 ppt in the base simulation to 35-60 ppt in 2DEPVEL due to
2590 decreased O₃ and conversion of NO to NO₂, and was generally within one standard
2591 deviation of the ABLE-2A measurements in the PBL. In BARCA B, NO simulated by
2592 WRF-Chem is very low, 5-10 ppt in the entire profile, except for the west region, where
2593 a mean NO of 30 ppt is seen from 0-500 m a.g.l. This is again due to very low O₃, and
2594 for the Manaus region, where anthropogenic NO_x sources may have contributed to NO
2595 values of 20 ppt. These results suggest that adjustment of dry deposition
2596 parameterizations are needed to increase O₃ deposition velocities by about a factor of
2597 two in agreement with ground observations. Future research will compare simulated
2598 NO_x fields with observations from more recent field campaigns, as the results of these
2599 simulations also suggest that O₃ in WRF-Chem is very sensitive to NO_x emissions.

Excluído: ¶

Formatado: Fonte: (Padrão) Times
New Roman, Alemão (Alemanha)

2600 In summary, chemistry simulations of the BARCA periods with CCATT-BRAMS and
2601 WRF-Chem overestimated O₃ in the PBL by 5-10 ppb in the wet-to-dry transition
2602 (BARCA B), with background levels observed (10-20 ppb) in all regions. In the dry-to-
2603 wet transition (BARCA A), the models generally reproduced elevated O₃ levels in the
2604 northeast and southeast Amazon where biomass burning emissions of precursors led to
2605 significant enhancements of ambient O₃. However, the models overestimate O₃ in the
2606 PBL by 5-10 ppb, whereas from 2-4 km the modeled values are generally lower than
2607 observations. These discrepancies of models with observations may result from an
2608 overly-mixed (constant with altitude) profile due to overly active turbulent mixing from
2609 1-2 km or too much downward convective transport of O₃ from 2 km to the surface, as
2610 observed by Betts et al. (2002). In addition, the models may be missing sources of O₃
2611 and/or precursors at 3-4.5 km in the model inflow boundary conditions. The surface
2612 sink of O₃ (dry deposition) may be too low, or overestimation of NO_x sources may
2613 produce too much O₃. In the lower boundary layer, the surface sink of O₃ (dry
2614 deposition) may be too low, or overestimation of NO_x sources may produce too much
2615 O₃. Additional simulations with WRF-Chem showed that O₃ in the lower boundary
2616 layer was about twice as sensitive to increases in O₃ deposition velocity as reductions in
2617 NO_x emissions, but both simulations achieved better agreement with observations.
2618 Although NO emissions over the forest were less than half of observed values, likely
2619 due to the lack of inclusion of soil emissions, sufficient O₃ production occurred to match

Excluído: T

Excluído: In the lower boundary layer, t

2623 or exceed aircraft observations, suggesting that the model chemistry is overly NO_x-
2624 sensitive.

2625 5 Conclusions

2626 The BARCA campaign offered the first regional aircraft survey of O₃ in the Amazon
2627 Basin in both the dry-to-wet and wet-to-dry transition seasons. In both seasons,
2628 extremely low background O₃ values (< 20 ppb) were observed to the west and north of
2629 Manaus, and in the wet-to-dry transition low O₃ was also measured to the east and south
2630 and in the region around Manaus. These background values are the lowest observed on
2631 Earth, due to a combination of isolation from anthropogenic and biomass burning NO_x
2632 sources and O₃ deposition to the forest canopy, and the ecosystem and atmospheric
2633 chemistry is adjusted to these very low values. According to the models, the chemistry
2634 in the Amazon is very sensitive to NO_x emissions from soils, so that even a small
2635 overestimate of NO_x emissions generates too much O₃ in the PBL. However, it is likely
2636 that the model chemistry is incorrect in the PBL, because the models have about the
2637 right amount of NO_x but far too much O₃ in the PBL. Further simulations with WRF-
2638 Chem showed that the model O₃ production is very sensitive to both the O₃ deposition
2639 velocities, which were about one half of observed values, and the NO_x emissions. In
2640 polluted, VOC-sensitive conditions, approximately the correct net amount of O₃ is
2641 generated in the PBL. This suggests there is insufficient VOC reactivity in the models,
2642 since the correct amounts of O₃ deposition velocities and NO_x emissions would both
2643 decrease O₃ production. Additionally, in clean, NO_x-sensitive conditions, proportionally
2644 more O₃ is produced per unit NO_x emissions and the O₃ deposition velocities are still
2645 too low, resulting in an overestimate. Therefore, we conclude that the current model
2646 chemistry produces much more O₃ per unit NO_x than the atmosphere at very low NO_x,
2647 but may be about right in polluted conditions. In addition, simulated O₃ was lower than
2648 both the OMI/MLS total tropospheric O₃ and the BARCA observations in mid-levels,
2649 indicating that the models are missing sources at mid-levels from long-range and
2650 convective transport.

Movido (inserção) [1]

Movido para cima [1]: Further simulations with WRF-Chem showed that the model O₃ production is very sensitive to both the O₃ deposition velocities, which were about one half of observed values, and the NO_x emissions.

Excluído: the O₃ retrieved by satellites is dominated by the middle troposphere and long-range transport and does not represent well boundary layer O₃ values

2651 As the regional population grows in the Amazon basin, leading to increases in both
2652 urban and fire NO_x sources, this is indeed a big concern because PBL O₃ is lower in
2653 clean areas than the models predict, so that the change to polluted conditions is larger,
2654 and that the chemistry to define the path to higher NO_x conditions is poorly represented.
2655 Future modeling studies can include more complete organic chemistry and biogenic
2656 emissions, including NO emissions from soil, as well as improved representation of
2657 lightning NO_x production, dry deposition, convective transport and wet scavenging
2658 processes, to address this NO_x sensitivity. Additionally, future field campaigns in the
2659 Amazon that include aircraft observations of nitrogen oxides and hydrocarbons and

2670 ground-based measurements of NO flux from the forest canopy may allow better
2671 constraints on the Amazonian O₃ budget.

2672

2673

Acknowledgements

2674 The authors are grateful to the entire BARCA team, including E. Gottlieb, V.Y. Chow,
2675 M.D.P. Longo, G.W. Santoni, F. Morais, A.C. Ribeiro, N. Jürgens, J. Steinbach, H.
2676 Chen, O. Kolle, L.V. Gatti, J.B. Miller, and the two INPE Bandeirante airplane pilots, P.
2677 Celso and D. Gramacho. We would also like to thank the GMAI group at INPE for
2678 indispensable support with the modeling and analysis, including [M. Alonso](#), [R. Braz](#), [D.](#)
2679 [Franca](#), [H. Lopez](#), [R. Mello](#), [R. Oliveira](#), [V. Oliveira](#), [M. Sanchez](#), [F. Santos](#) and [R.](#)
2680 [Stockler](#). Many thanks to Anne Thompson, Neusa Paes Leme, Rinus Scheele, and
2681 Francis J. Schmidlin for the SHADOZ ozone sounding data. We thank B. Holben for his
2682 effort in establishing and maintaining the Manaus AERONET site. This work was
2683 supported by an IIE Fulbright Scholarship and PCI CNPQ, and the flight campaign was
2684 supported by the Max Planck Society, NASA grants NASA NNX08AP68A and NASA
2685 NNX10AR75G, FAPESP thematic project AEROCLIMA 2008/58100-2, CNPq
2686 Millennium Institute of the Large Scale Biosphere – Atmosphere Experiment in
2687 Amazonia (LBA) (CNPq Project 477575/2008-0), and MCT and INPE. [Finally, we](#)
2688 [would like to express our gratitude to the three anonymous reviewers for their generous](#)
2689 [comments and revisions which greatly improved the manuscript.](#)

Excluído: F. Santos, R. Stockler, R. Mello, M. Alonso, M. Sanchez, D. Franca, R. Braz, H. Lopez, and V. Oliveira

2693

References

- 2694 Alonso, M. F., Longo, K., Freitas, S., Fonseca, R., Marecal, V., Pirre, M., and Klenner,
2695 L.: An urban emissions inventory for South America and its application in numerical
2696 modeling of atmospheric chemical composition at local and regional scales, *Atmos.*
2697 *Environ.*, 44, 5072–5083, 2010.
- 2698 Andreae, M. O., Artaxo, P., Fischer, H., Freitas, S. R., Grégoire, J.-M., Hansel, A.,
2699 Hoor, P., Kormann, R., Krejci, R., Lange, L., Lelieveld, J., Lindinger, W., Longo, K.,
2700 Peters, W., de Reus, M., Scheeren, B., Silva Dias, M. A. F., Stroem, J., van Velthoven,
2701 P. F. J., and Williams, J.: Transport of biomass burning smoke to the upper troposphere
2702 by deep convection in the equatorial region, *Geophys. Res. Lett.*, 28, 951–954, 2001.
- 2703 Andreae, M. O., Artaxo, P., Brandão, C., Carswell, F. E., Ciccioli, P., da Costa, A. L.,
2704 Culf, A. D., Esteves, J. L., Gash, J. H. C., Grace, J., Kabat, P., Lelieveld, J., Malhi, Y.,
2705 Manzi, A. O., Meixner, F. X., Nobre, A. D., Nobre, C., Ruivo, M. d. L. P., Silva-Dias,
2706 M. A., Stefani, P., Valentini, R., von Jouanne, J., and Waterloo, M. J.: Biogeochemical
2707 cycling of carbon, water, energy, trace gases, and aerosols in Amazonia: The LBA-
2708 EUSTACH experiments, *J. Geophys. Res.*, 107(D20), 8066,
2709 doi:10.1029/2001JD000524, 2002.
- 2710 Andreae M. O., Rosenfeld, D., Artaxo, P., Costa, A. A., Frank, G. P., Longo, K. M.,
2711 Silva Dias, M. A. F.: Smoking rain clouds over the Amazon, *Science*, 303, 1337, 2004.
- 2712 Andreae, M. O., Artaxo, P., Beck, V., Bela, M., Freitas, S., Gerbig, C., Longo, K.,
2713 Munger, J. W., Wiedemann, K. T., and Wofsy, S. C.: Carbon monoxide and related
2714 trace gases and aerosols over the Amazon Basin during the wet and dry-to-wet
2715 transition seasons, *Atmos. Chem. Phys.*, 12, 6041–6065, doi:10.5194/acp-12-6041-2012,
2716 2012.
- 2717 Avery, M., Twohy, C., McCabe, D., Joiner, J., Severance, K., Atlas, E., Blake, D., Bui,
2718 T. P., Crouse, J., Dibb, J., Diskin, G., Lawson, P., McGill, M., Rogers, D., Sachse, G.,
2719 Scheuer, E., Thompson, A. M., Trepte, C., Wennberg, P., Ziemke, J.: Convective
2720 distribution of tropospheric ozone and tracers in the Central American ITCZ region:
2721 Evidence from observations during TC4, *J. Geophys. Res.*, 115, D00J21,
2722 doi:[10.1029/2009JD013450](https://doi.org/10.1029/2009JD013450), 2010.
- 2723 Barth, M. C., Stuart, A. L., and Skamarock, W. C.: Numerical simulations of the July 10
2724 STERAO/Deep Convection storm: Redistribution of soluble tracers, *J. Geophys. Res.*,
2725 106, 12 381–12 400, 2001.
- 2726 Barth, M. C., Kim, S.-W., Wang, C., Pickering, K. E., Ott, L. E., Stenchikov, G.,
2727 Leriche, M., Cautenet, S., Pinty, J.-P., Barthe, Ch., Mari, C., Helsdon, J. H.,

2728 Farley, R. D., Fridlind, A. M., Ackerman, A. S., Spiridonov, V., and Telenta, B.: Cloud-
2729 scale model intercomparison of chemical constituent transport in deep convection,
2730 *Atmos. Chem. Phys.*, 7, 4709-4731, doi:10.5194/acp-7-4709-2007, 2007.

2731 Beck, V., Gerbig, C., Koch, T., Bela, M. M., Longo, K. M., Freitas, S. R., Kaplan, J. O.,
2732 Prigent, C., Bergamaschi, P., and Heimann, M.: WRF-Chem simulations in the Amazon
2733 region during wet and dry season transitions: evaluation of methane models and wetland
2734 inundation maps, *Atmos. Chem. Phys.*, 13, 7961-7982, doi:10.5194/acp-13-7961-2013,
2735 2013.

2736 Berge, E.: Coupling of wet scavenging of sulphur to clouds in a numerical weather
2737 prediction model, *Tellus*, 45B, 1-22, 1993.

2738 Betts, A. K., L. V. Gatti, A. M. Cordova, M. A. F. Silva Dias, and J. D. Fuentes,
2739 Transport of ozone to the surface by convective downdrafts at night, *J. Geophys. Res.*,
2740 107(D20), 8046, doi:10.1029/2000JD000158, 2002.

2741 Bond, D.W., Steiger, S., Zhang, R., Tie, X.X. and Orville, R.E.: The importance of NO_x
2742 production by lightning in the tropics, *Atmos. Environ.*, 36, 1509-1519,
2743 doi:[10.1016/S1352-2310\(01\)00553-2](https://doi.org/10.1016/S1352-2310(01)00553-2), 2002.

2744 Browell, E. V., Gregory, G. L., Harriss, R. C., and Kirchhoff, V. W. J. H.: Tropospheric
2745 ozone and aerosol distributions across the Amazon Basin, *J. Geophys. Res.*, 93(D2),
2746 1431-1451, doi:[10.1029/JD093iD02p01431](https://doi.org/10.1029/JD093iD02p01431), 1988.

2747 Browell, E. V., Fenn, M. A., Butler, C. F., Grant, W. B., Clayton, M. E., Fishman, J.,
2748 Bachmeier, A. S., Anderson, B. E., Gregory, G. L., Fuelberg, H. E., Bradshaw, J. D.,
2749 Sandholm, S. T., Blake, D. R., Heikes, B. G., Sachse, G. W., Singh, H. B., and Talbot,
2750 R. W., Ozone and aerosol distributions and air mass characteristics over the South
2751 Atlantic Basin during the burning season, *J. Geophys. Res.*, 101, 24,043-24,068, 1996.

2752 Buarque, D. C., de Paiva, R. C. D., Clarke, R. T., and Mendes, C. A. B.: A comparison
2753 of Amazon rainfall characteristics derived from TRMM, CMORPH and the Brazilian
2754 national rain gauge network, *J. Geophys. Res.*, 116, D19105,
2755 doi:[10.1029/2011JD016060](https://doi.org/10.1029/2011JD016060), 2011.

2756 [Chen, Y., Velicogna, I., Famiglietti, J. S., and Randerson, J. T.: Satellite observations of
2757 terrestrial water storage provide early warning information about drought and fire
2758 season severity in the Amazon, *J. Geophys. Res. Biogeosci.*, 118, 495-504, doi:
2759 \[10.1002/jgrg.20046\]\(https://doi.org/10.1002/jgrg.20046\), 2013.](#)

2760 Chin, M., Ginoux, P., Kinne, S., Holben, B. N., Duncan, B. N., Martin, R. V., Logan, J.
2761 A., Higurashi, A., and Nakajima, T.: Tropospheric aerosol optical thickness from the

2762 GOCART model and comparisons with satellite and sunphotometer measurements, J.
2763 Atmos. Sci. 59, 461-483, 2002.

2764 Cordova Leal, A. M.: Gases Traço na Amazônia: Variabilidade Sazonal e Temporal de
2765 O₃, NO_x e CO em Ambientes de Pastagem e Floresta, Tese de Doutorado, Instituto de
2766 Astronomia, Geofísica e Ciências Atmosféricas da Universidade de São Paulo, 2003.

2767 Crutzen, P. J., Delany, A. C., Greenberg, J. P., Haagenson, P., Heidt, L., Lueb, R.,
2768 Pollock, W., Seiler, W., Wartburg, A. F., and Zimmerman, P. R.: Tropospheric chemical
2769 composition measurements in Brazil during the dry season: J. Atmos. Chem., 2, 233-
2770 256, 1985.

2771 Ebben, C. J., Martinez, I. S., Shrestha, M., Buchbinder, A. M., Corrigan, A. L.,
2772 Guenther, A., Karl, T., Petäjä, T., Song, W. W., Zorn, S. R., Artaxo, P., Kulmala, M.,
2773 Martin, S. T., Russell, L. M., Williams, J., and Geiger, F. M.: Contrasting organic
2774 aerosol particles from boreal and tropical forests during HUMPPA-COPEC-2010 and
2775 AMAZE-08 using coherent vibrational spectroscopy, Atmos. Chem. Phys., 11, 10317-
2776 10329, doi:10.5194/acp-11-10317-2011, 2011.

2777 Fall, R., and Wildermuth, M. C.: Isoprene Synthase: From Biochemical Mechanism to
2778 Emission Algorithm, J. Geophys. Res., 103(D19), 25599-25609, doi:
2779 10.1029/98jd00808, 1998.

2780 Fan, S. M., Wofsy, S. C., Bakwin, P. S., Jacob, D. J., and Fitzjarrald, D. R.:
2781 Atmosphere-biosphere exchange of CO₂ and O₃ in the central Amazon forest, J.
2782 Geophys. Res., 95(D10), 16 851–16 864, 1990.

2783 Fishman, J., and Larsen, J. C., The distribution of total ozone and stratospheric ozone in
2784 the tropics: Implications for the distribution of tropospheric ozone, J. Geophys. Res., 92,
2785 6627-6634, 1987.

2786 Fueglistaler S., Dessler, A. E., Dunkerton, T. J., Folkins, I., Fu, Q., and Mote, P. W.:
2787 Tropical tropopause layer, Rev. Geophys., 47, RG1004, doi:10.1029/2008RG000267,
2788 2009.

2789 Freitas, S. R., Silva Dias, M. A. F., Silva Dias, P. L., Longo, K. M., Artaxo, P., Andreae,
2790 M. O., and Fischer, H.: A convective kinematic trajectory technique for low-resolution
2791 atmospheric models, J. Geophys. Res., 105, D19, 24, 375-24, 386,
2792 doi:10.1029/2000JD900217, 2000.

2793 Freitas, S., Longo, K., Silva Dias, M., Silva Dias, P., Chatfield, R., Prins, E., Artaxo, P.,
2794 Grell, G. and Recuero, F.: Monitoring the transport of biomass burning emissions in
2795 South America, Environ. Fluid Mech., DOI: 10.1007/s10652-005-0243-7, 5(1-2), 135-
2796 167, 2005.

2797 Freitas, S. R., Longo, K. M., Chatfield, R., Latham, D., Silva Dias, M. A. F.,
2798 Andreae, M. O., Prins, E., Santos, J. C., Gielow, R., and Carvalho Jr., J. A.: Including
2799 the sub-grid scale plume rise of vegetation fires in low resolution atmospheric transport
2800 models, *Atmos. Chem. Phys.*, 7, 3385-3398, doi:10.5194/acp-7-3385-2007, 2007.

2801 Freitas, S. R., Longo, K. M., Silva Dias, M. A. F., Chatfield, R., Silva Dias, P., Artaxo,
2802 P., Andreae, M. O., Grell, G., Rodrigues, L. F., Fazenda, A., and Panetta, J.: The
2803 Coupled Aerosol and Tracer Transport model to the Brazilian developments on the
2804 Regional Atmospheric Modeling System (CATT-BRAMS) - Part 1: Model description
2805 and evaluation, *Atmos. Chem. Phys.*, 9, 2843-2861, 2009.

2806 Freitas, S. R., Longo, K. M., Alonso, M. F., Pirre, M., Marecal, V., Grell, G., Stockler,
2807 R., Mello, R.F., Sanchez Gacita, M.: PREP-CHEM-SRC-1.0: a preprocessor of trace
2808 gas and aerosol emission fields for regional and global atmospheric chemistry models,
2809 *Geosci. Model Dev.*, 4, 419-433, 2011.

2810 Gallardo, L., Alonso, M., Andrade, M. F., Carvalho, V. S. B., Behrentz, E.,
2811 Vasconcellos, P. C., D'Angiola, A., Dawidowski, L., Freitas, S., Gómez, D., Longo, K.
2812 M., Martins, M., Mena, M., Matus, P., Osses, A., Osses, M., Rojas, N., Saide, P.,
2813 Sánchez-Ccoyllo, O., and Toro, M. V.: South America, in *IGAC Report on Megacity*
2814 *Air Pollution and Climate*, 2010.

2815 Garcia-Montiel, D. C., Steudler, P. A., Piccolo, M., Neill, C., Melillo, J., Cerri, C. C.:
2816 Nitrogen oxide emissions following wetting of dry soils in forest and pastures in
2817 Rondônia, Brazil, *Biogeochemistry*, 64(3), 319-336, 2003.

2818 Gevaerd, R.: Estudo da Redistribuição 3-D de Gases e Aerossóis de Queimadas em
2819 Roraima 1998, Master's thesis, University of São Paulo, 2005.

2820 Gevaerd, R. and S. R. Freitas: Estimativa operacional da umidade do solo para iniciação
2821 de modelos de previsão numérica da atmosfera. Parte I: Descrição da metodologia e
2822 validação. *Revista Brasileira de Meteorologia*, 21(3), 59-73, 2006.

2823 Gevaerd, R., Freitas, S., and Longo, K.: Numerical simulation of biomass burning
2824 emission and transport during 1998 Roraima fires, in: *International Conference on*
2825 *Southern Hemisphere Meteorology and Oceanography (ICSHMO)*, 8, Proceedings, Foz
2826 do Iguaçu, INPE, São José dos Campos, 2006, 883-889, CD-ROM, ISBN 85-17-00023-
2827 4, 2006.

2828 Guenther, A., Karl, T., Harley, P., Wiedinmyer, C., Palmer, P. I., and Geron, C.:
2829 Estimates of global terrestrial isoprene emissions using MEGAN (Model of Emissions
2830 of Gases and Aerosols from Nature), *Atmos. Chem. Phys.*, 6, 3181-3210,
2831 doi:10.5194/acp-6-3181-2006, 2006.

2832 Grell, G. A., and D. Dévényi, A generalized approach to parameterizing convection
2833 combining ensemble and data assimilation techniques, *Geophys. Res. Lett.*, 29(14),
2834 doi:[10.1029/2002GL015311](https://doi.org/10.1029/2002GL015311), 2002.

2835 Grell, G. A., Peckham, S. E., Schmitz, R., McKeen, S. A., Frost, G., Skamarock, W. C.,
2836 and Eder, B.: Fully coupled online chemistry within the WRF model, *Atmos. Environ.*,
2837 39, 6957– 6975, 2005.

2838 Harriss, R. C., et al.: The Amazon Boundary Layer Experiment (ABLE 2A): dry season
2839 1985, *J. Geophys. Res.*, 93(D2), 1351–1360, doi:[10.1029/JD093iD02p01351](https://doi.org/10.1029/JD093iD02p01351), 1988.

2840 Harriss, R. C., Garstang, M., Wofsy, S. C., Beck, S. M., Bendura, R. J., Coelho, J. R. B.,
2841 Drewry, J. W., Hoell, J. M., Matson, P. A., McNeal, R. J., Molion, L. C. B., Navarro, R.
2842 L., Rabine, V., and Snell, R. L.: The Amazon Boundary Layer Experiment: Wet Season
2843 1987, *J. Geophys. Res.*, 95, 16721–16736, 1990.

2844 Jacob, D. J., and Wofsy, S. C.: Photochemistry of biogenic emissions over the Amazon
2845 forest, *J. Geophys. Res.*, 93(D2), 1477–1486, doi:[10.1029/JD093iD02p01477](https://doi.org/10.1029/JD093iD02p01477), 1988.

2846 Janjić, Z. I.: The step-mountain eta coordinate model: further developments of the 445
2847 convection, viscous sublayer and turbulence closure schemes, *Mon. Wea. Rev.*, 122,
2848 446 927-945, 1994.

2849 Kaplan, W. A., Wofsy, S. C., Keller, M., and Da Costa, J. M.: Emission of NO and
2850 deposition of O₃ in a tropical forest system, *J. Geophys. Res.*, 93(D2), 1389–1395,
2851 doi:[10.1029/JD093iD02p01389](https://doi.org/10.1029/JD093iD02p01389), 1988.

2852 Karl, T., Guenther, A., Yokelson, R. J., Greenberg, J., Potosnak, M., Blake, D.R., and
2853 Artaxo, P.: The tropical forest and fire emissions experiment: Emission, chemistry, and
2854 transport of biogenic volatile organic compounds in the lower atmosphere over
2855 Amazonia, *J. Geophys. Res.* 112, D18302, 2007.

2856 Kaufman, Y., Hobbs, P. V., Kirchhoff, V. W., Artaxo, P., Remer, L., Holben, B. N.,
2857 King, M. D., Prins, E. M., Ward, D. E., Longo, K. M., Mattos, L. F., Nobre, C. A.,
2858 Spinhirne, J., Thompson, A. M., Gleason, J. F., and Christopher, S. A.: Smoke, Clouds,
2859 and Radiation-Brazil (SCAR-B) experiment, *J. Geophys. Res.*, 103(D24), 31783–
2860 31808, doi:[10.1029/98JD02281](https://doi.org/10.1029/98JD02281), 1998.

2861 Kawanishi, T., Kuroiwa, H., Kojima, M., Oikawa, K., Kozu, T., Kumagai, H.,
2862 Okamoto, K., Okumura, M., Nakatsuka, H., and Nishikawa, K.: TRMM precipitation
2863 radar, *Remote Sens. Appl.: Earth Atmos. Oceans*, 25, 969–972, 2000.

2864 Kirchhoff, V. W. J. H., da Silva, I. M. O., and Browell, E. V., Ozone measurements in
2865 Amazonia: Dry season versus wet season: *J. Geophys. Res.*, 95, 16,913-16,926, 1990.

2866 Kirkman, G. A., Gut, A., Ammann, C., Gatti, L. V., Cordova, A. M., Moura, M. A. L.,
2867 Andreae, M. O., and Meixner, F. X.: Surface exchange of nitric oxide, nitrogen dioxide,
2868 and ozone at a pasture in Rondonia, Brazil, *J. Geophys. Res.*, 107(D20), 8083,
2869 doi:10.1029/2001JD000523, 2002.

2870 Koren, V., Schaake, J., Mitchell, K., Duan, Q.-Y. and Chen, F.: A parameterization of
2871 snowpack and frozen ground intended for NCEP weather and climate models. *J.*
2872 *Geophys. Res.*, 104, 19569-19585, 1999.

2873 Kuhn, U., Ganzeveld, L., Thielmann, A., Dindorf, T., Welling, M., Sciare, J., Roberts,
2874 G., Meixner, F. X., Kesselmeier, J., Lelieveld, J., Ciccioli, P., Lloyd, J., Trentmann, J.,
2875 Artaxo, P., and Andreae, M. O., Impact of Manaus City on the Amazon Green Ocean
2876 atmosphere: Ozone production, precursor sensitivity and aerosol load, *Atmos. Chem.*
2877 *Phys.*, 10, 9251–9282, 2010.

2878 Kummerow, C., Barnes, W., Kozu T., Shiue, J., and Simpson, J.: The Tropical Rainfall
2879 Measuring Mission (TRMM) sensor package, *J. Atmos. Ocean. Tech.*, Boston, 15(3),
2880 809–816, 1998.

2881 Lelieveld, J., Butler, T. M., Crowley, J. N., Dillon, T. J., Fischer, H., Ganzeveld, L.,
2882 Harder, H., Lawrence, M. G., Martinez, M., Taraborrelli, D., and Williams, J.:
2883 Atmospheric oxidation capacity sustained by a tropical forest, *Nature*, 452, 737-740,
2884 2008.

2885 Logan, J.A.: Tropospheric ozone: Seasonal behavior, trends, and anthropogenic
2886 influence, *J. Geophys. Res.*, 90, 10463-10482, 1985.

2887 Logan, J. A.: An analysis of ozonesonde data for the troposphere: Recommendations for
2888 testing 3-D models and development of a gridded climatology for tropospheric ozone, *J.*
2889 *Geophys. Res.*, 104, 16,115– 16,149, 1999.

2890 Longo, K. M., Thompson, A. M., Kirchhoff, V. W. J. H., Remer, L. A., de Freitas, S.
2891 R., Dias, M. A. F. S., Artaxo, P., Hart, W., Spinhirne, J. D., and Yamasoe, M. A.:
2892 Correlation between smoke and tropospheric ozone concentration in Cuiabá during
2893 Smoke, Clouds, and Radiation-Brazil (SCAR-B), *J. Geophys. Res.*, 104(D10), 12113–
2894 12129, doi:10.1029/1999JD900044, 1999.

2895 Longo, K. M., Freitas, S. R., Andreae, M. O., Yokelson, R., Artaxo, P., Biomass
2896 burning in Amazonia: emissions, long-range transport of smoke and its regional and
2897 remote impacts, in Keller, M., Bustamante, M., Gash, J., and Silva Dias, P., ed.,
2898 Amazonia and Global Change, AGU Geophysical Monograph Series, Washington,
2899 D.C., v. 186, 2009.

2900 Longo, K. M., Freitas, S. R., Pirre, M., Marécal, V., Rodrigues, L. F., Panetta, J.,
2901 Alonso, M. F., Rosário, N. E., Moreira, D. S., Gácita, M. S., Arteta, J., Fonseca, R.,
2902 Stockler, R., Katsurayama, D. M., Fazenda, A., and Bela, M.: The chemistry CATT–
2903 BRAMS model (CCATT–BRAMS 4.5): a regional atmospheric model system for
2904 integrated air quality and weather forecasting and research, *Geosci. Model Dev.*, 6,
2905 1389-1405, doi:10.5194/gmd-6-1389-2013, 2013.

2906 Martin, S. T., Andreae, M. O., Althausen, D., Artaxo, P., Baars, H., Borrmann, S.,
2907 Chen, Q., Farmer, D. K., Guenther, A., Gunthe, S. S., Jimenez, J. L., Karl, T.,
2908 Longo, K., Manzi, A., Müller, T., Pauliquevis, T., Petters, M. D., Prenni, A. J.,
2909 Pöschl, U., Rizzo, L. V., Schneider, J., Smith, J. N., Swietlicki, E., Tota, J., Wang, J.,
2910 Wiedensohler, A., and Zorn, S. R.: An overview of the Amazonian Aerosol
2911 Characterization Experiment 2008 (AMAZE-08), *Atmos. Chem. Phys.*, 10, 11415–
2912 11438, doi:10.5194/acp-10-11415-2010, 2010.

2913 Mellor, G. L. and Yamada, T.: Development of a turbulence closure model for
2914 geophysical fluid problems, *Rev. Geophys. Space Phys.*, 20, 851–875, 1982.

2915 [Morton, D. C., Le Page, Y., DeFries, R., Collatz, G. J., and Hurtt, G. C.: Understorey](#)
2916 [fire frequency and the fate of burned forests in southern Amazonia, *Phil. Trans. R. Soc.*](#)
2917 [B, 368\(1619\), doi: 10.1098/rstb.2012.0163, 2013.](#)

2918 [National Research Council, 1991. Rethinking the Ozone Problem in Urban and](#)
2919 [Regional Air Pollution. National Academy Press, Washington, DC, 500pp.](#)

2920 Reich, P. B. and Amundson, R. G.: Ambient levels of ozone reduce net photosynthesis
2921 in tree and crop species, *Science*, 230, 566–570, doi:10.1126/science.230.4725.566,
2922 1985.

2923 Rinne, H. J. I., Guenther, A.B., Greenberg, J.P., and Harley, P.C.: Isoprene and
2924 monoterpene fluxes measured
2925 above Amazonian rainforest and their dependence on light and tempera-
2926 ture, *Atmos. Environ.*, 36(14), 2421–2426, doi:10.1016/S1352-2310(01)
2927 00523-4, 2002.

2928 Rosário, N. M. E. Variability of aerosol optical properties over South America and the
2929 impacts of direct radiative effect of aerosols from biomass burning. 2011. Thesis (PhD).
2930 Institute of Astronomy, Geophysics and Atmospheric Sciences, University of São
2931 Paulo, São Paulo, 2011 (in Portuguese).

2932 Rosário N. E., K. M. Longo, S. R. Freitas, M. A. Yamasoe, and R. M. Fonseca.
2933 Modeling South America regional smoke plume: aerosol optical depth variability and
2934 shortwave surface forcing, *Atmos. Chem. Phys.*, 13, 2923-2938, doi:10.5194/acp-13-
2935 2923-2013, 2013.

2936 Rummel, U., Ammann, C., Kirkman, G. A., Moura, M. A. L., Foken, T., Andreae, M.
2937 O., and Meixner, F. X., Seasonal variation of ozone deposition to a tropical rainforest in
2938 southwest Amazonia, *Atmos. Chem. Phys.*, 7, 5415-5435, 2007.

2939 Seinfeld, J. H. and Pandis, S. N.: *Atmospheric Chemistry and Physics: From Air*
2940 *Pollution to Climate Change*, 2nd edition, J. Wiley, New York, 2006.

2941 Sestini, M., Reimer, E., Valeriano, D., Alvalá, R., Mello, E., Chan, C., and Nobre, C.:
2942 Mapa de cobertura da terra da Amazônia legal para uso em modelos meteorológicos,
2943 *Anais XI Simpósio Brasileiro de Sensoriamento Remoto*, 2901–2906, 2003.

2944 Sigler, J. M., Fuentes, J. D., Heitz, R. C., Garstang, M., and Fisch, G.: Ozone dynamics
2945 and deposition processes at a deforested site in the Amazon Basin, *Ambio*, 31(1), 21–
2946 27, 2002.

2947 Silva, C. M. S., Freitas, S.R., Gielow, R., and Barros, S.S.: Evaluation of high-
2948 resolution precipitation estimate over the Amazon Basin, *Atmos. Sci. Let.*, 10, 273–278,
2949 2009.

2950 Silva, C. M. S., Freitas, S. R., and Gielow, R.: Numerical simulation of the diurnal cycle
2951 of rainfall in SW Amazon Basin during the 1999 rainy season: the role of convective
2952 trigger function, *Theor. Appl. Climatol.*, 109, 473, 2012.

2953 Stockwell, D. Z., Giannakopoulos, C., Plantevin, P.-H., Carver, G. D., Chipperfield, M.
2954 P., Law, K. S., Pyle, J. A., Shallcross, D. E., and Wang, K.-Y.: Modeling NO_x from
2955 lightning and its impact on global chemical fields, *Atmos. Environ.*, 33(27), 4477-
2956 4493, 1999.

2957 Stockwell, W. R., Kirchner, F., and Kuhn, M.: A new mechanism for regional chemistry
2958 modeling, *J. Geophys. Res.*, 102, 25847–25879, 1997.

2959 Thompson, A. M., Pickering, K. E., McNamara, D. P., Schoeberl, M. R., Hudson, R. D.,
2960 Kim, J. H., Browell, E. V., Kirchhoff, V. W. J. H., and Nganga, D.: Where did
2961 tropospheric ozone over southern Africa and the tropical Atlantic come from in October
2962 1992? Insights from TOMS, GTE TRACE A, and SAFARI 1992, *J. Geophys. Res.*,
2963 101(D19), 24251–24278, doi:[10.1029/96JD01463](https://doi.org/10.1029/96JD01463), 1996.

2964 Thompson, A.M., Witte, J. C., McPeters, R. D., Oltmans, S. J., Schmidlin, F. J., Logan,
2965 J. A., Fujiwara, M., Kirchhoff, V. W. J. H., Posny, F., Coetzee, G. J. R., Hoegger, B.,
2966 Kawakami, S., Ogawa, T., Johnson, B. J., Vömel, H., and Labo, G.: Southern
2967 Hemisphere Additional Ozonesondes (SHADOZ) 1998-2000 tropical ozone
2968 climatology 1. Comparison with Total Ozone Mapping Spectrometer (TOMS) and
2969 ground-based measurements, *J. Geophys. Res.*, 108, 8238, doi:[10.1029/2001JD000967](https://doi.org/10.1029/2001JD000967),
2970 2003.

2971 Thompson, A.M., Witte, J. C., Oltmans, S. J., Schmidlin, F. J., Logan, J. A., Fujiwara,
2972 M., Kirchhoff, V. W. J. H., Posny, F., Coetzee, G. J. R., Hoegger, B., Kawakami, S.,
2973 Ogawa, T., Fortuin, J. P. F., and Kelder, H. M.: Southern Hemisphere Additional
2974 Ozonesondes (SHADOZ) 1998-2000 tropical ozone climatology 2. Tropospheric
2975 variability and the zonal wave-one, *J. Geophys. Res.*, 108, 8241,
2976 doi:10.1029/2002JD002241, 2003.

2977 Thompson, A. M., Witte, J.C., Smit, H.G.J., Oltmans, S.J., Johnson, B.J., Kirchhoff,
2978 V.W.J H., and Schmidlin, F.J.: Southern Hemisphere Additional Ozonesondes
2979 (SHADOZ) 1998-2004 tropical ozone climatology: 3. Instrumentation, station-to-station
2980 variability, and evaluation with simulated flight profiles, *J. Geophys. Res.*, 112,
2981 D03304, doi:10.1029/2005JD007042, 2007.

2982 Toon, O. B., Starr, D. O., Jensen, E. J., Newman, P. A., Platnick, S., Schoeberl, M.
2983 R., Wennberg, P. O., Wofsy, S. C., Kurylo, M. J., Maring, H., Jucks, K. W., Craig, M.
2984 S., Vasques, M. F., Pfister, L., Rosenlof, K. H., Selkirk, H. B., Colarco, P. R., Kawa, S.
2985 R., Mace, G. G., Minnis, P., and Pickering, K. E.: Planning, implementation, and first
2986 results of the Tropical Composition, Cloud and Climate Coupling Experiment (TC4), *J.*
2987 *Geophys. Res.*, 115, D00J04, doi:[10.1029/2009JD013073](https://doi.org/10.1029/2009JD013073), 2010.

2988 Torres, A. L., and Buchan, H.: Tropospheric nitric oxide measurements over the
2989 Amazon Basin, *J. Geophys. Res.*, 93(D2), 1396–1406, doi:[10.1029/JD093iD02p01396](https://doi.org/10.1029/JD093iD02p01396),
2990 1988.

2991 [von Randow, C., Manzi, A. O., Kruijt, B., de Oliveira, P. J., Zanchi, F. B., Silva, R. L.,](#)
2992 [Hodnett, M. G., Gash, J. H. C., Elbers, J. A. Waterloo, M. J., Cardoso, F. L., and Kabat,](#)
2993 [P.: Comparative measurements and seasonal variations in energy and carbon exchange](#)
2994 [over forest and pasture in South West Amazonia, *Theor. Appl. Climatol.*, 78, 5–26](#)
2995 [\(2004\), DOI 10.1007/s00704-004-0041-z, 2004.](#)

2996 Walko, R. L., Band, L. E., Baron, J., Kittel, T.G.F., Lammers, R., Lee, T. J., Ojima, D.,
2997 Pielke, R. A., Taylor, C., Tague, C., Tremback, C. J., and Vidale, P.L.: Coupled
2998 atmosphere-biophysics hydrology models for environmental modeling, *J. Appl.*
2999 *Meteor.*, 39, 931-944, 2000.

3000 Wesley, M. L.: Parameterization of surface resistance to gaseous dry deposition in
3001 regional numerical models, *Atmos. Environ.*, 16, 1293–1304, 1989.

3002 Zhang, L., Jacob, D. J., Liu, X., Logan, J. A., Chance, K., Eldering, A., and
3003 Bojkov, B. R.: Intercomparison methods for satellite measurements of atmospheric
3004 composition: application to tropospheric ozone from TES and OMI, *Atmos. Chem.*
3005 *Phys.*, 10, 4725-4739, 2010.

3006 Zhou, J., Swietlicki, E., Hansson, H. C., and Artaxo, P.: Submicrometer aerosol particle
3007 size distribution and hygroscopic growth measured in the Amazon rain forest during the
3008 wet-to-dry transition season, *J. Geophys. Res.*, 107(D20), 8055,
3009 doi:10.1029/2000JD000203, 2002.

3010 Ziemke, J. R., Chandra, S., Duncan, B. N., Froidevaux, L., Bhartia, P. K., Levelt, P. F.
3011 and Waters, J. W.: Tropospheric ozone determined from Aura OMI and MLS:
3012 Evaluation of measurements and comparison with the Global Modeling Initiative's
3013 Chemical Transport Model, *J. Geophys. Res.*, 111, D19303,
3014 doi:10.1029/2006JD007089, 2006.

3015 Ziemke, J. R., Joiner, J., Chandra, S., Bhartia, P. K., Vasilkov, A., Haffner, D. P., Yang,
3016 K., Schoeberl, M. R., Froidevaux, L., and Levelt, P. F.: Ozone mixing ratios inside
3017 tropical deep convective clouds from OMI satellite measurements, *Atmos. Chem. Phys.*,
3018 9, 573–583, 2009.

	CCATT-BRAMS	WRF-Chem
Short/longwave radiation	Based on CARMA	RRTMG
Cloud microphysics	Single moment bulk	WSM-5
Deep/shallow convection	Grell and Dévényi (GD)	Grell 3D
Trace gas chemistry	RACM	RACM
Photolysis	F-TUV	F-TUV
Aerosol scheme	Smoke aerosol	GOCART
Wet deposition	convective and grid scales	convective scale only

3019 Table 1. CCATT-BRAMS and WRF-Chem physics and chemistry options for the
3020 BARCA simulations.

3021

Region	Nov. 2008		May 2009			
	TRMM 3B43	CCATT- BRAMS	WRF- Chem	TRMM 3B43	CCATT- BRAMS	WRF- Chem
Amazon	0.24	0.22	0.51	0.20	0.15	0.40
Northeast	0.12	0.07	0.08	0.37	0.23	0.49
Southeast	0.19	0.11	0.24	0.10	0.06	0.07

3022 Table 2. Monthly mean precipitation (mm h^{-1}) for TRMM 3B43, CCATT-BRAMS and
3023 WRF-Chem models for three regions: the Amazon ($15^{\circ}\text{S} - 10^{\circ}\text{N}$, $50^{\circ}\text{W} - 80^{\circ}\text{W}$),
3024 northeast Brazil ($15^{\circ}\text{S} - 0^{\circ}\text{N}$, $35^{\circ}\text{W} - 50^{\circ}\text{W}$), and southeast South America ($15^{\circ}\text{S} -$
3025 35°S , $35^{\circ}\text{W} - 65^{\circ}\text{W}$).

		Oct-Nov 2008		May-Apr 2009	
		CCATT- BRAMS	WRF- Chem	CCATT- BRAMS	WRF- Chem
T (K)	<i>Mean Obs.</i>	295.97		293.89	
	RMSE	2.30	2.81	1.70	2.44
	Bias	1.04	-2.42	-0.06	-2.28
T_d (K)	<i>Mean Obs.</i>	289.26		288.49	
	RMSE	2.68	1.72	1.76	1.67
	Bias	-1.92	-0.81	-0.99	-0.83
Wind Spd. (m s⁻¹)	<i>Mean Obs.</i>	3.00		2.59	
	RMSE	1.41	1.33	1.15	1.00
	Bias	-0.60	0.16	-0.51	0.07
Sfc. Press. (hPa)	<i>Mean Obs.</i>	1013.17		1016.09	
	RMSE	2.16	1.43	1.09	1.34
	Bias	-2.01	-1.02	-0.79	-1.17
Precip. TRMM (mm h⁻¹)	<i>Mean Obs.</i>	0.49		0.62	
	RMSE	2.42	4.50	3.03	7.12
	Bias	0.28	3.47	0.25	5.84

3027 Table 3. Values of RMSE and bias for CCATT-BRAMS and WRF-Chem simulations
3028 for 26 METAR and 52 SYNOP stations in the Amazon Basin for BARCA A (October-
3029 November 2008) and BARCA B (April-May 2009).

		Forest			Pasture			
PBL Height (km)		Method	TKE	Theta	WRF MYNN	TKE	Theta	WRF MYNN
BARCA A (Nov. 2008)	CCATT- BRAMS	Mean	1.103	1.610	---	1.143	1.636	---
		Std.						
		Dev.	0.621	0.646	---	0.581	0.640	---
	WRF- Chem	Mean	1.211	1.131	0.983	1.258	1.087	0.991
		Std.						
		Dev.	0.655	0.390	0.423	0.665	0.470	0.455
BARCA B (May 2009)	CCATT- BRAMS	Mean	0.628	1.067	---	0.669	1.049	---
		Std.						
		Dev.	0.515	0.554	---	0.527	0.564	---
	WRF- Chem	Mean	0.828	0.922	0.815	0.845	0.933	0.766
		Std.						
		Dev.	0.443	0.336	0.288	0.432	0.282	0.272

3030 Table 4. PBL height at 21:00 UTC (17:00 LT) estimated from CCATT-BRAMS and
3031 WRF-Chem using methods based on Turbulent Kinetic Energy (TKE) and theta (θ) and
3032 the diagnostic from the WRF MYNN PBL scheme.

		Dry Season			Wet Season		
Site		Observed	CCATT- BRAMS	WRF- Chem	Observed	CCATT- BRAMS	WRF- Chem
		RBJ (forest)	Flux	-5.69	-2.43	-3.25	-2.93
	v_d	0.6	0.3	0.5	1.2	0.4	0.8
FNS (pasture)	Flux	-4.68	-3.06	-2.49	-2.04	-2.07	-2.04
	v_d	0.6	0.4	0.4	0.7	0.4	0.7
RD (forest)	Flux				-1.82	-1.63	-2.68
	v_d				1.6	0.4	0.6

Excluído: 4

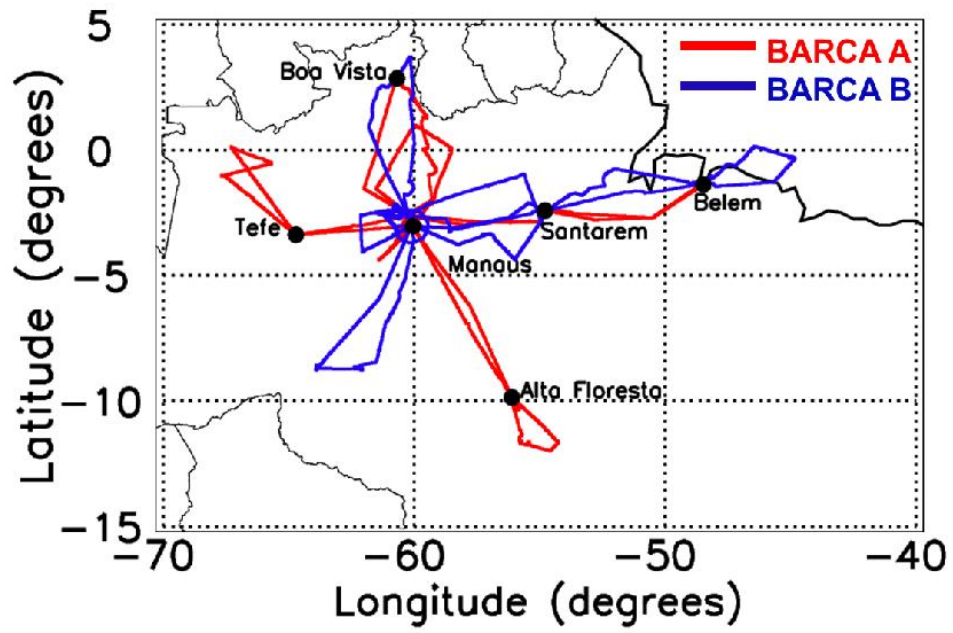
3033 Table 5. Average O₃ dry deposition flux (nmol m⁻² s⁻¹) and daytime (11:00-21:00 UTC)
3034 median deposition velocity (cm s⁻¹) in the dry and wet seasons (Rummel et al., 2007),
3035 and WRF-Chem and CCATT-BRAMS simulations from November 2008 (dry-to-wet
3036 transition) and May 2009 (wet-to-dry transition) for Reserva Biológica Jarú (RBJ),
3037 Fazenda Nossa Senhora (RNS) and Reserva Ducke (RD).

3039

Region	<i>BARCA A (Nov. 2008)</i>				<i>BARCA B (May 2009)</i>			
	Longitude	Latitude	Days	Longitude	Latitude	Days		
west	-60.06	-54.24 -12.00	-3.03 29, 30	-61.16	-59.46 -3.71	-2.39 28		
north	-62.00	-59.11 -3.04	2.89 23	-61.81	-60.00 -3.04	3.71 19		
around Manaus	-61.52	-58.50 -4.39	1.00 16, 22	-62.14	-60.00 -4.07	-2.16 15, 17		
east	-108.73	-48.45 -3.04	-1.33 18, 19	-60.34	-44.82 -4.39	0.14 23, 26		
south	-67.69	-60.01 -3.40	0.12 25, 26	-63.93	-60.01 -8.77	-3.04 27		

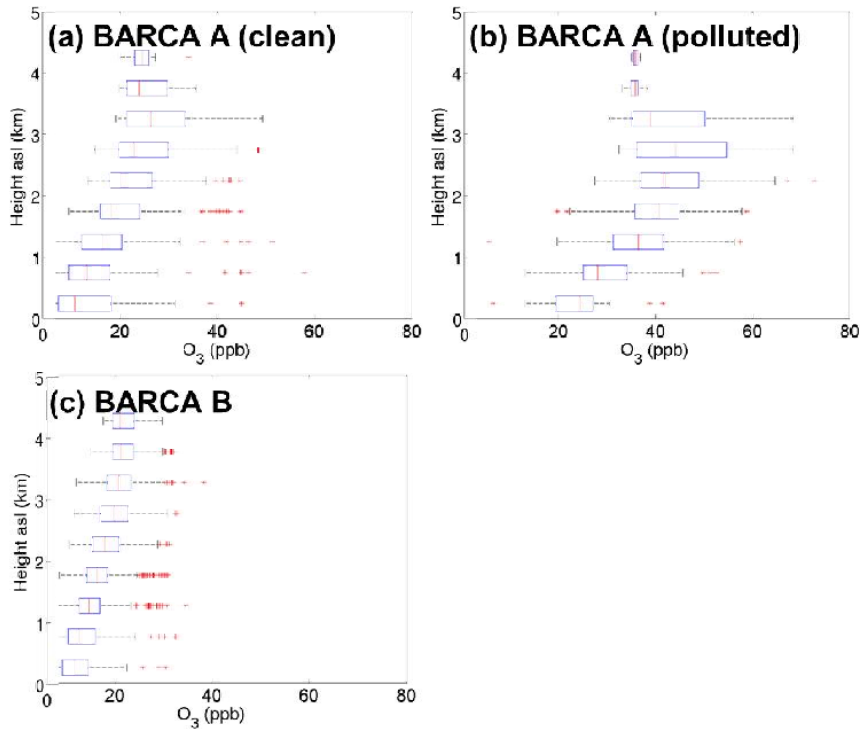
3040 Table 6. Longitude and latitude bounds and dates for each region of the BARCA A and
 3041 B campaigns.

3042



3043

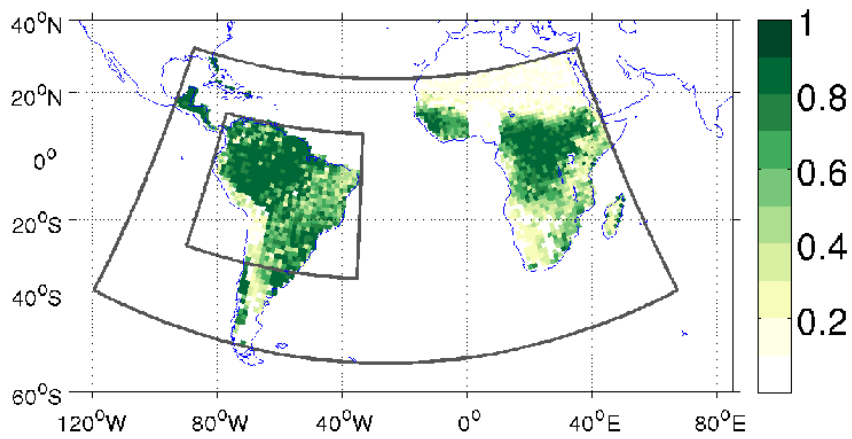
3044 Figure 1. Flight tracks during BARCA.



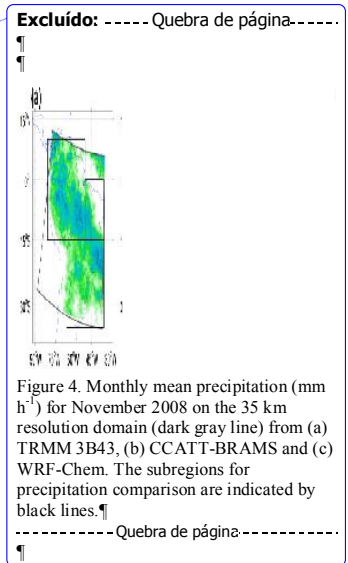
3046

3047 Figure 2. O₃ observations during (a) BARCA A, clean conditions (W_{est}, N_{orth} and
 3048 around Manaus regions), (b) BARCA A, polluted conditions (E_{ast} and S_{outh} regions)
 3049 and (c) BARCA B. The central mark is the median, the edges of the box are the 25th
 3050 and 75th percentiles, the whiskers extend to the most extreme data points not considered
 3051 outliers (as defined by Matlab) and outliers are plotted individually as red pluses.
 3052 Values are drawn as outliers if their values exceed $q_3 + w(q_3 - q_1)$ or are less than $q_1 -$
 3053 $w(q_3 - q_1)$, where q_1 and q_3 are the 25th and 75th percentiles, respectively, and w is the
 3054 maximum whisker length with the default value of 1.5. For normally distributed data,
 3055 the whiskers encompass from approximately the 2.7 to 99.3 percentiles.

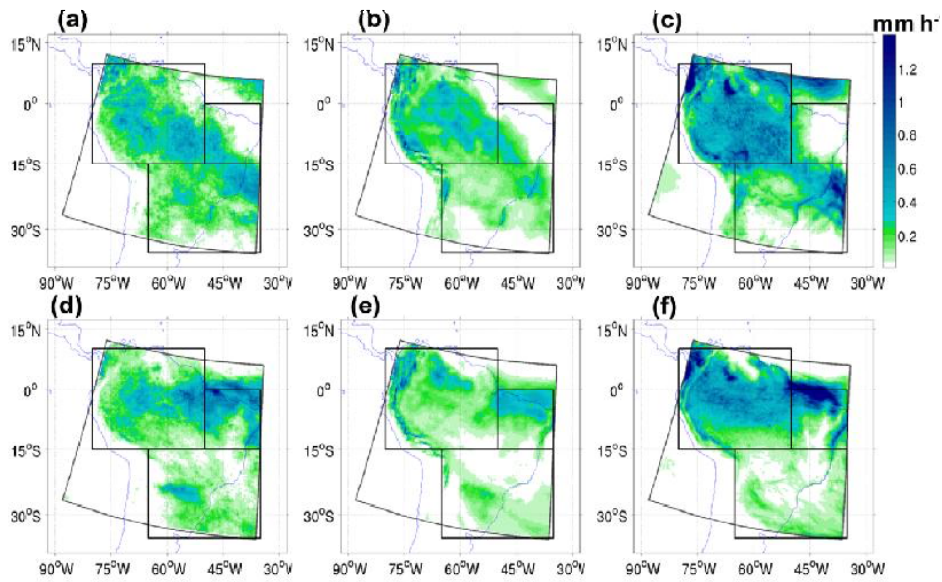
- Excluído: w
- Excluído: n
- Excluído: e
- Excluído: s



3060
 3061 Figure 3. Land surface albedo (fraction) and locations of the coarse (140 km resolution)
 3062 and nested (35 km resolution) domains for WRF-Chem simulations.



3076



3077

3078

3079

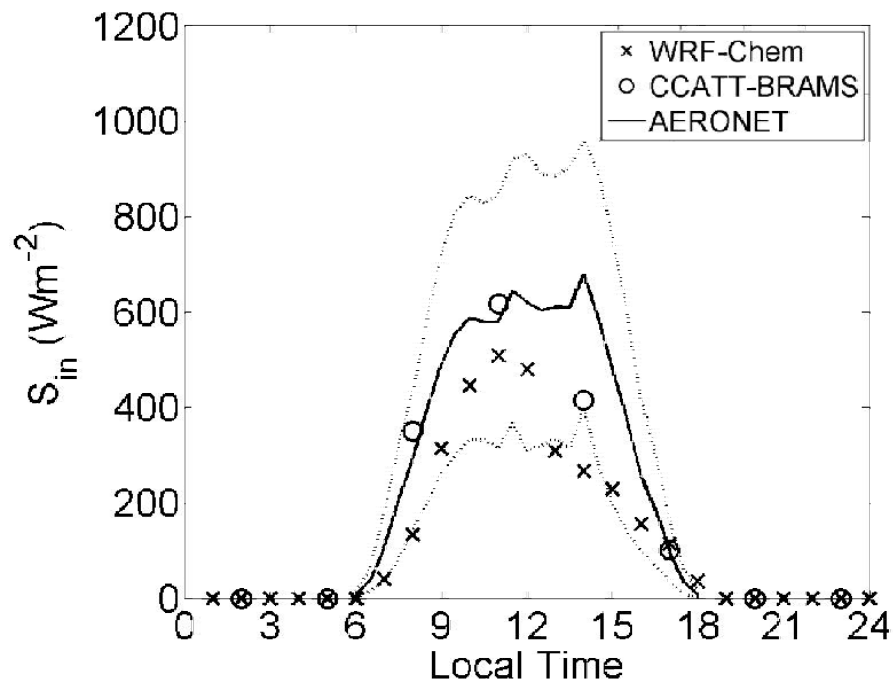
3080

3081

Figure 4. Monthly mean precipitation (mm h^{-1}) on the 35-km resolution domain (dark gray line) for November 2008 from (a) TRMM 3B43, (b) CCATT-BRAMS and (c) WRF-Chem and for May 2009 from (d) TRMM 3B43, (e) CCATT-BRAMS and (f) WRF-Chem. The subregions for precipitation comparison are indicated by black lines.

Excluido: 5

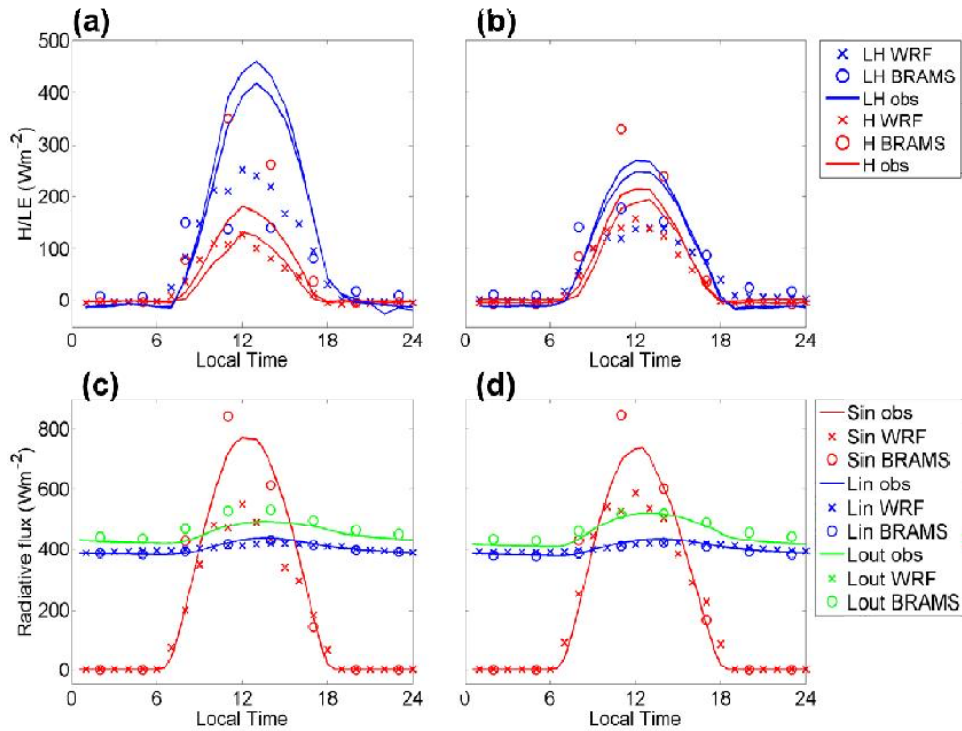
Excluido: Same as Fig. 4, but for May 2009.



3087

3088 | Figure 5. Mean daily cycle of surface incident shortwave radiation from the Manaus
 3089 AERONET site (solid line, dotted line denotes one standard deviation), WRF-Chem
 3090 (crosses) and CCATT-BRAMS (circles) for the BARCA A period (October-November
 3091 2008).

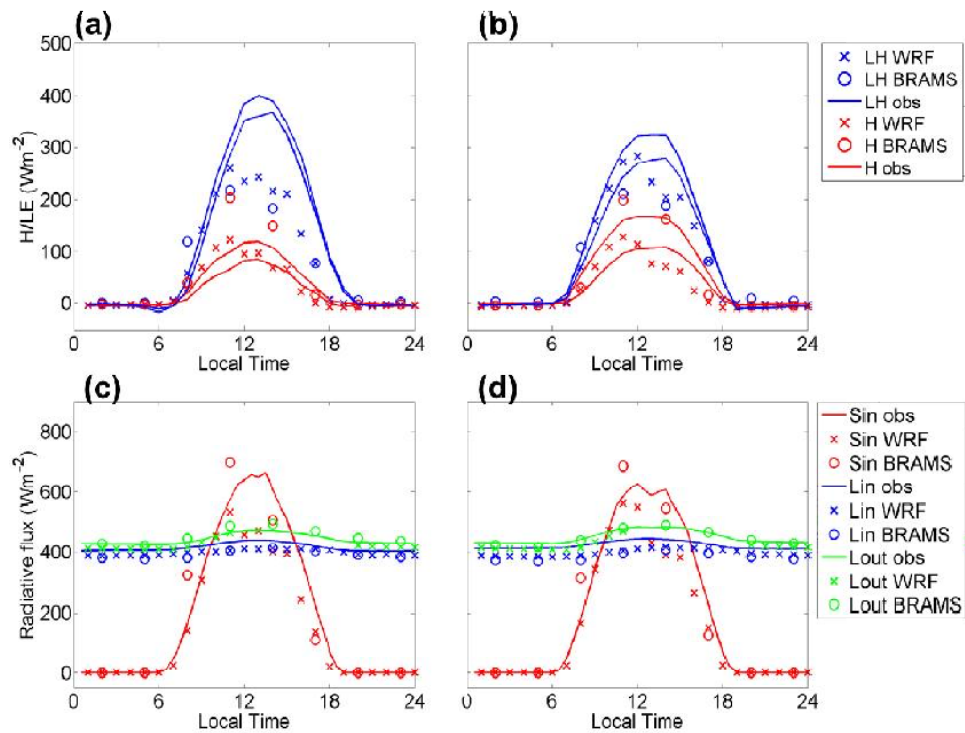
Excluído: 6



3094

3095 Figure 6. Mean daily cycles of surface (a) latent (LE) and sensible (H) heat and (c)
 3096 incident shortwave (S_{in}) and incoming (L_{in}) and outgoing (L_{out}) longwave radiation
 3097 fluxes for a forest site and (b) heat and (d) radiation fluxes for a pasture site, comparing
 3098 observations (solid lines) from von Randow et al. (2004) for the dry-to-wet transition
 3099 season (July-September 1999-2000) and from WRF-Chem (crosses) and CCATT-
 3100 BRAMS (circles) for the BARCA A period (October-November 2008).

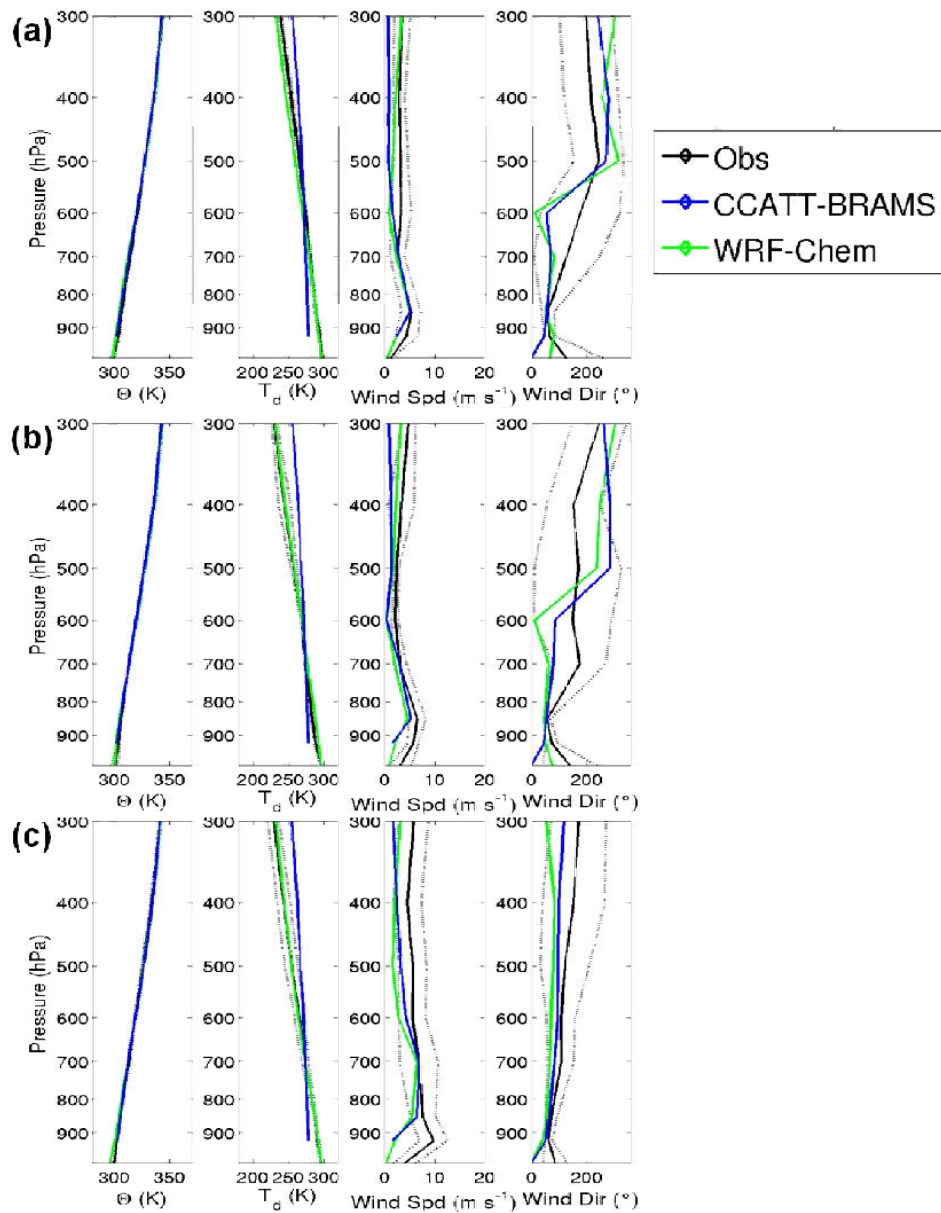
Excluído: 7



3102

3103 Figure 7. Mean daily cycles of surface (a) latent (LE) and sensible (H) heat and (c)
 3104 incident shortwave (S_{in}) and incoming (L_{in}) and outgoing (L_{out}) longwave radiation
 3105 fluxes for a forest site and (b) heat and (d) radiation fluxes for a pasture site, comparing
 3106 observations (solid lines) from von Randow et al. (2004) for the wet-to-dry transition
 3107 season (February-March 1999, January-March 2000) and from WRF-Chem (crosses)
 3108 and CCATT-BRAMS (circles) for the BARCA B period (April-May 2009).

Excluído: 8

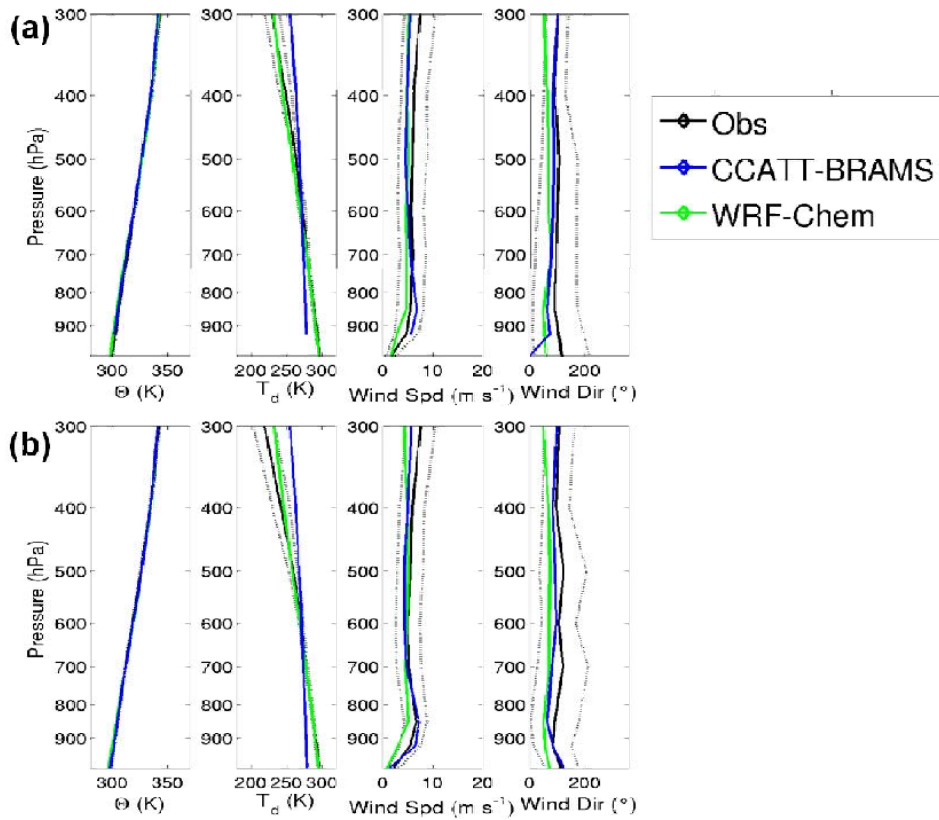


3110

3111 | Figure 8. Mean vertical profiles at Manaus from radiosoundings (black, gray line
 3112 | denotes one standard deviation), CCATT-BRAMS (blue) and WRF-Chem (green) for
 3113 | October-November 2008 at (a) 0:00, (b) 12:00 and (c) 18:00 UTC.

Excluído: 9

Excluído: Z



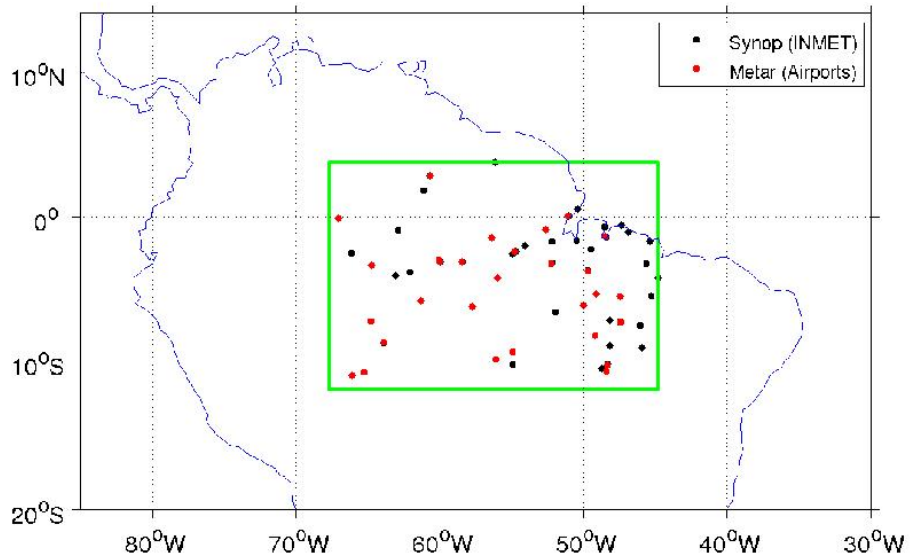
3116

3117 | Figure 9. Mean vertical profiles at Manaus from radiosoundings (black, gray line
 3118 | denotes one standard deviation), CCATT-BRAMS (blue) and WRF-Chem (green) for
 3119 | April-May 2009 at (a) 0:00 and (b) 12:00 UTC.

Excluído: 10

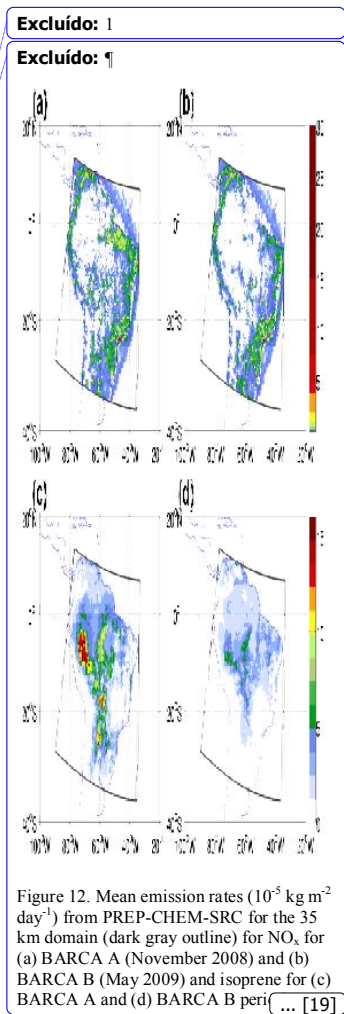
Excluído:

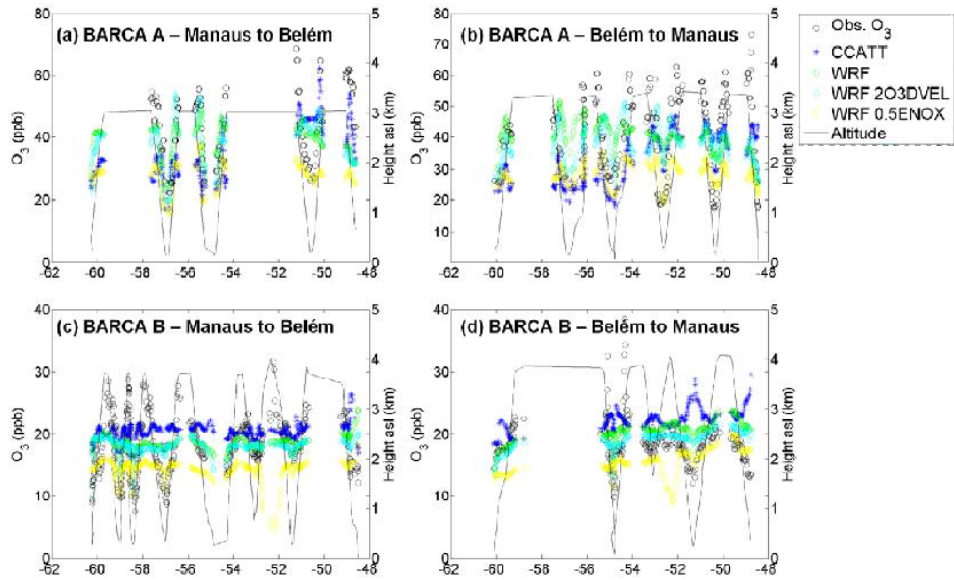
Excluído: Z



3124

3125 | Figure 10. Locations of surface meteorological stations for model evaluation.





Excluído: -----Quebra de página-----
 ¶
 -----Quebra de página-----
 ¶

3146 Figure 11. O_3 as observed (black circles) and simulated with CCATT-BRAMS (blue
 3147 stars) and WRF-Chem (base case – green diamonds, 2DEPVEL – cyan circles and
 3148 0.5ENOX – yellow squares) from BARCA flights (a) from Manaus to Belém on 18
 3149 November 2008, (b) Belém to Manaus on 19 November 2008, (c) Manaus to Belém on
 3150 21 May 2009 and (d) Belém to Manaus on 23 November 2009.

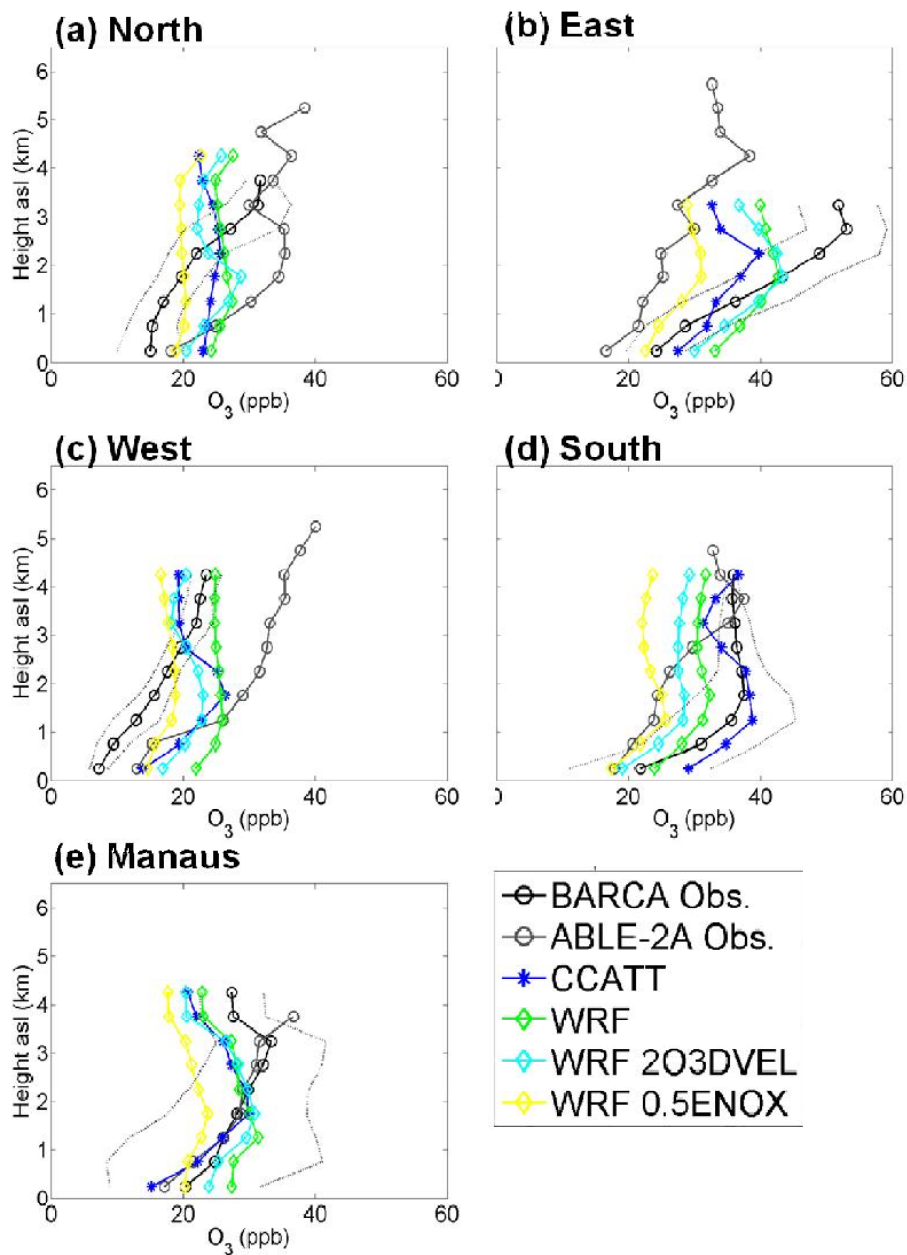
Excluído: 7

Excluído: 18,

Excluído: 19,

Excluído: 21,

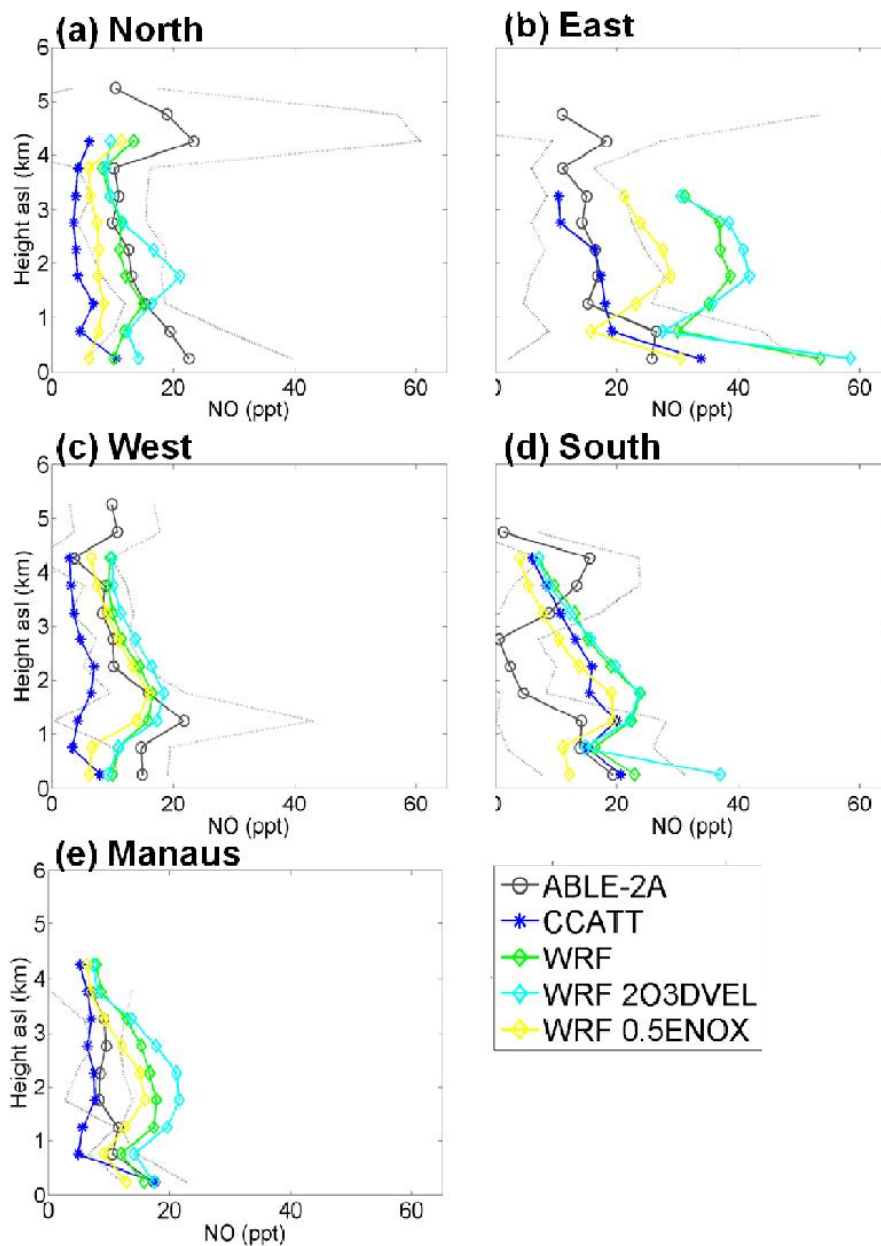
Excluído: 23,



3161

3162 | Figure 12. Mean vertical O_3 profiles for BARCA A flights for observations (black, gray
 3163 | line denotes one standard deviation), CCATT-BRAMS (blue) and WRF-Chem (base
 3164 | case – green, 2DEPVEL – cyan and 0.5ENOX – yellow) simulations by region: (a)
 3165 | north, (b) east, (c) west, (d) south and (e) around Manaus. ABLE-2A observations
 3166 | (gray) from the same regions are included for comparison.

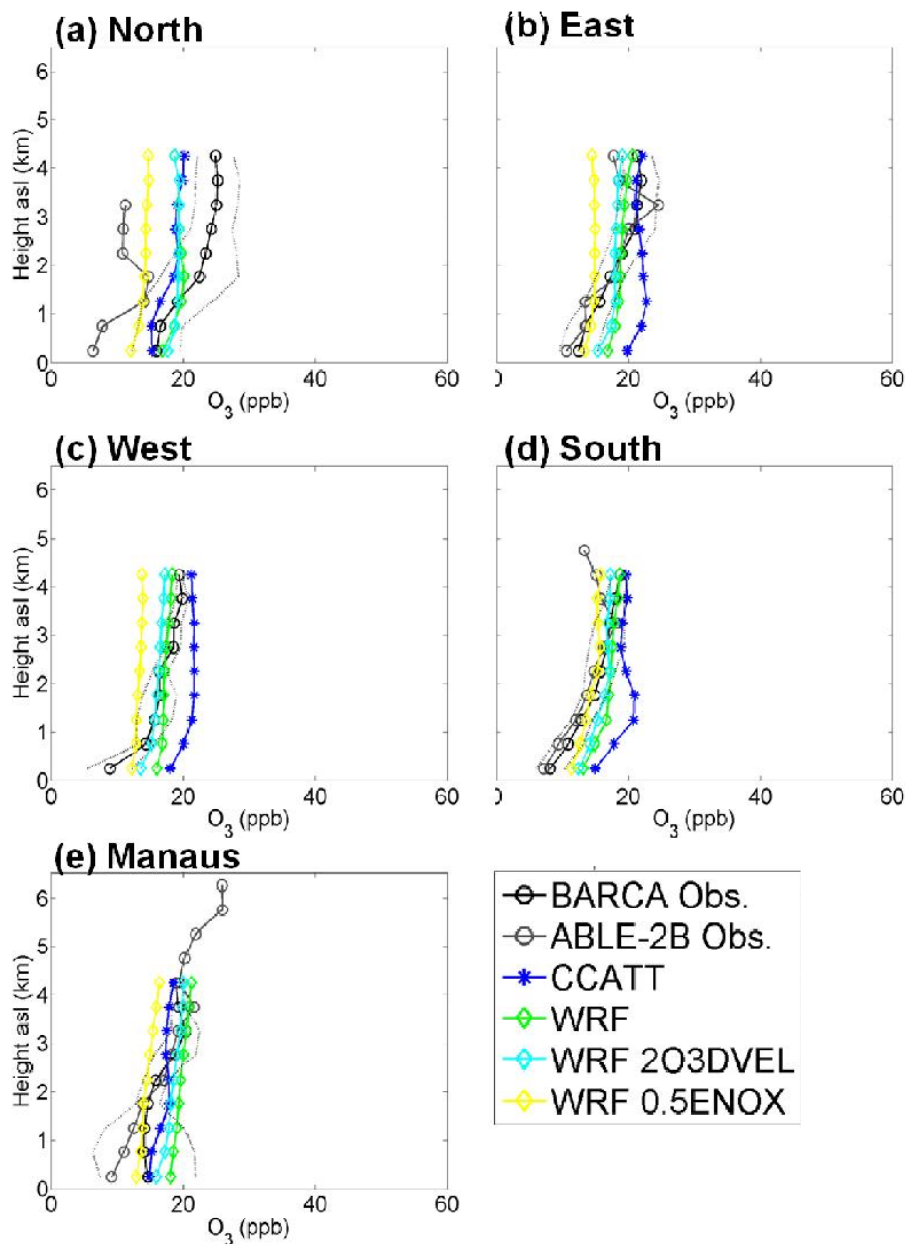
Excluído: 8



3168

3169 | Figure 13. Mean vertical NO profiles corresponding to BARCA A flights for CCATT-
 3170 BRAMS (blue) and WRF-Chem (base case – green, 2DEPVEL – cyan and 0.5ENOX –
 3171 yellow) simulations by region: (a) north, (b) east, (c) west, (d) south and (e) around
 3172 Manaus. ABLE-2A observations (gray) from the same regions are included for
 3173 comparison.

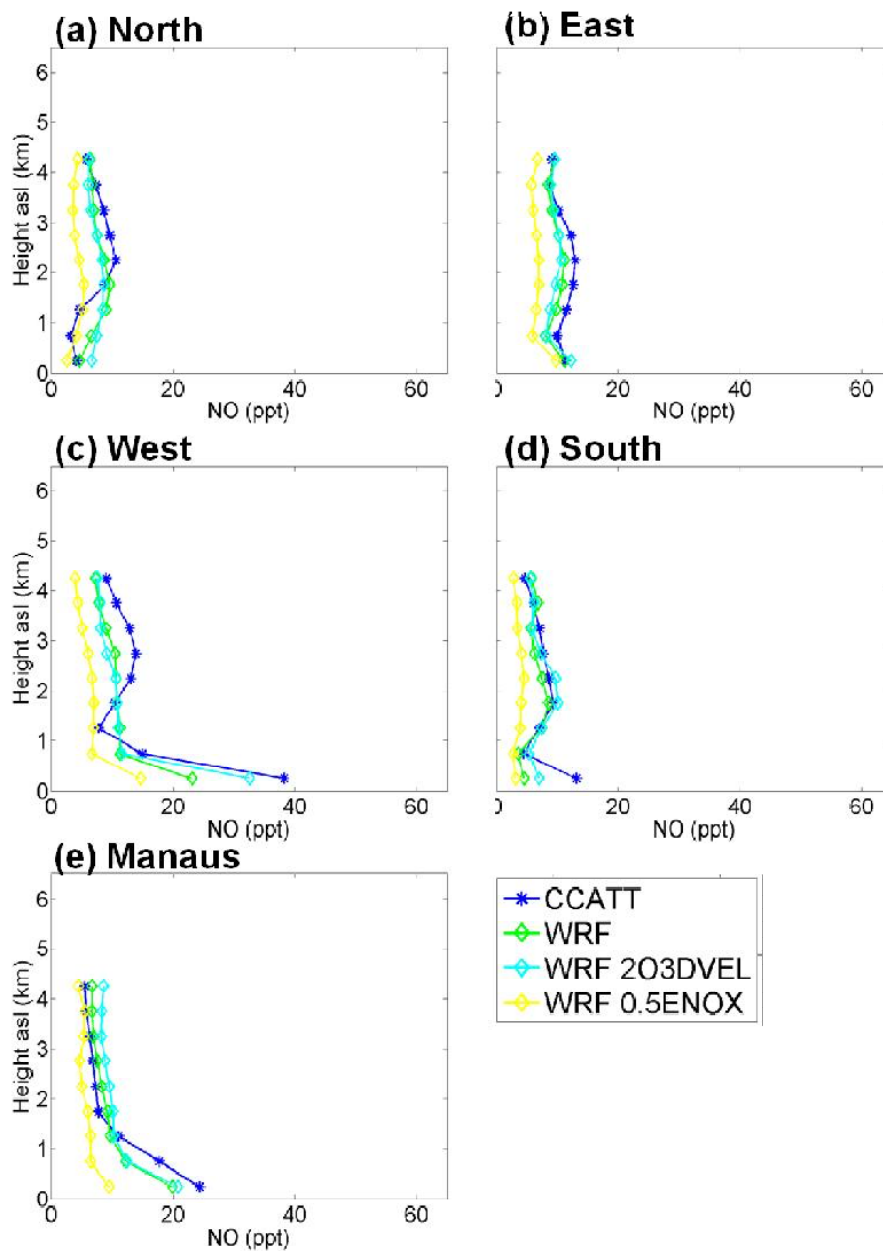
Excluído: 9



3175

3176 Figure 14. Mean vertical O_3 profiles for BARCA B flights for observations (black, gray
 3177 line denotes one standard deviation), CCATT-BRAMS (blue) and WRF-Chem (base
 3178 case – green, 2DEPVEL – cyan and 0.5ENOX – yellow) simulations by region: (a)
 3179 north, (b) east, (c) west, (d) south and (e) around Manaus. ABL-2A observations
 3180 (gray) from the same regions are included for comparison.

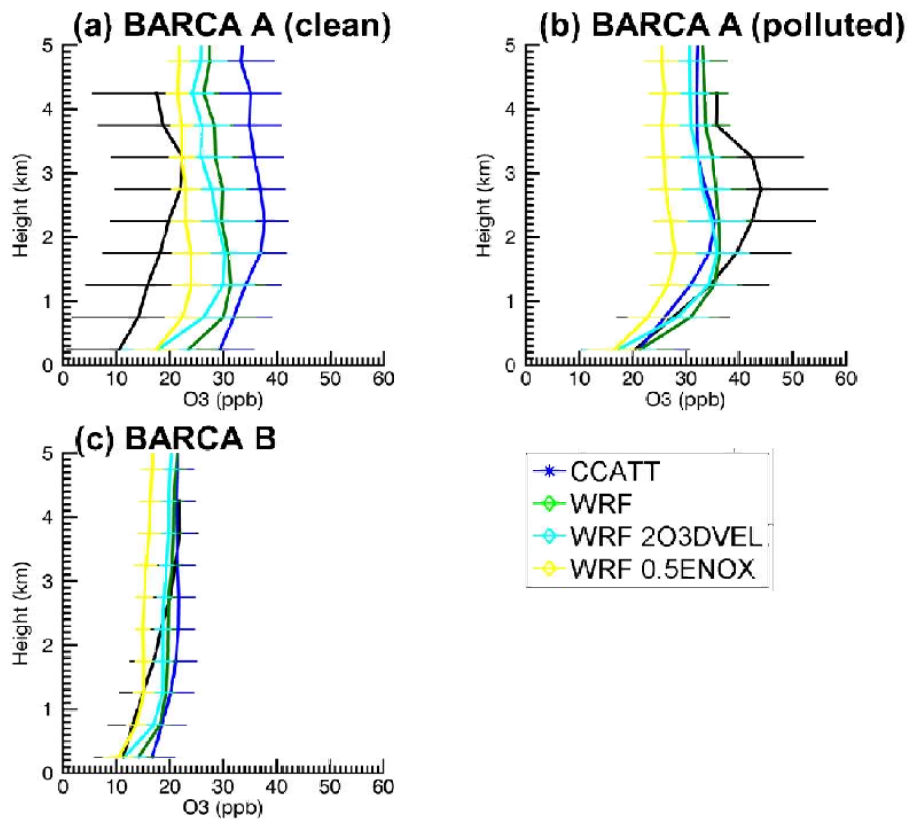
Excluído: 20



3182

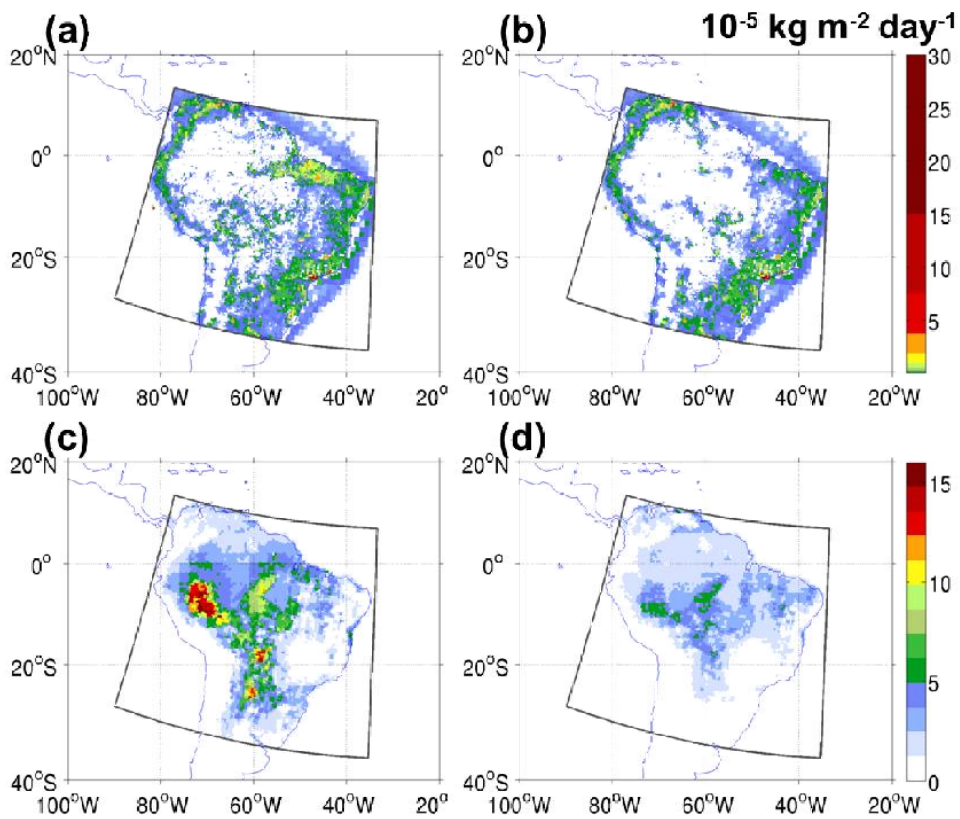
3183 Figure 15. Mean vertical NO profiles corresponding to BARCA B flights for CCATT-
 3184 BRAMS (blue) and WRF-Chem (base case – green, 2DEPVEL – cyan and 0.5ENOX –
 3185 yellow) simulations by region: (a) north, (b) east, (c) west, (d) south and (e) around
 3186 Manaus.

Excluído: 21



3188

3189 Figure 16. O₃ as observed (black circles) and simulated with CCATT-BRAMS (blue
 3190 stars) and WRF-Chem (base case – green diamonds, 2DEPVEL – cyan circles and
 3191 0.5ENOX – yellow squares) during (a) BARCA A, clean conditions (west, north and
 3192 around Manaus regions), (b) BARCA A, polluted conditions (east and south regions)
 3193 and (c) BARCA B.

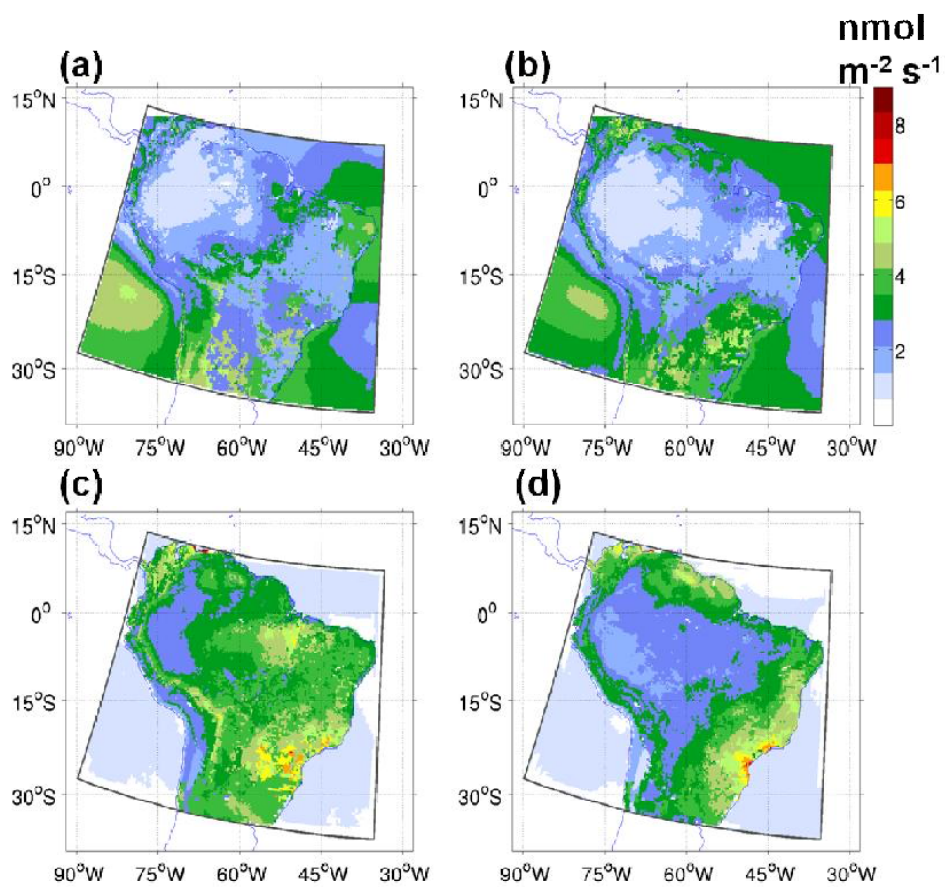


3194

3195 Figure 17. Mean emission rates ($10^{-5} \text{ kg m}^{-2} \text{ d}^{-1}$) from PREP-CHEM-SRC for the 35 km

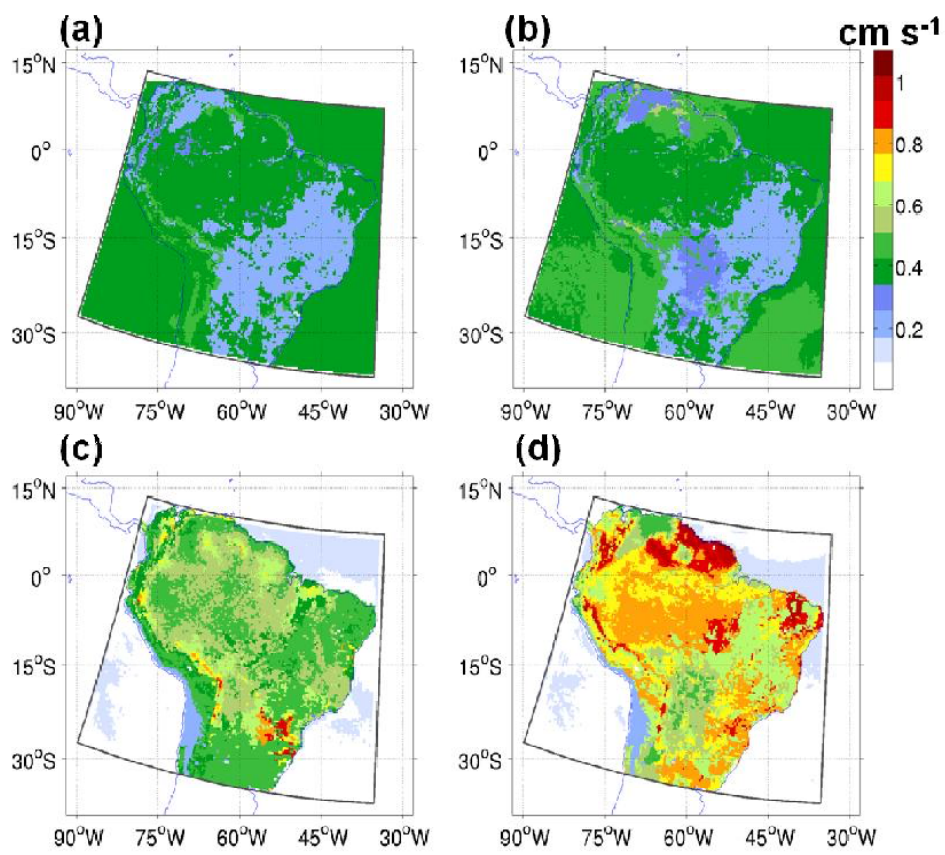
3196 domain (dark gray outline) for NO_x for (a) BARCA A (November 2008) and (b)

3197 BARCA B (May 2009) and isoprene for (c) BARCA A and (d) BARCA B periods.



3198

3199 Figure 18. Average O₃ dry deposition flux (nmol m⁻² s⁻¹) as simulated on the 35 km
 3200 resolution domain (dark gray outline) by the CCATT-BRAMS model for (a) November
 3201 2008 and (b) May 2009 and by the WRF-Chem model for (c) November 2008 and (d)
 3202 May 2009.

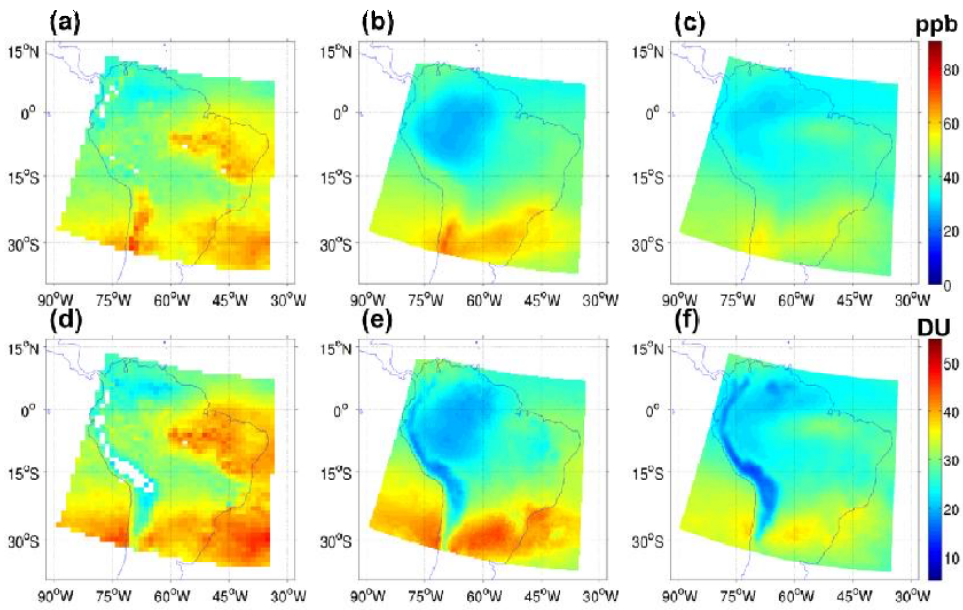


3203

3204

3205

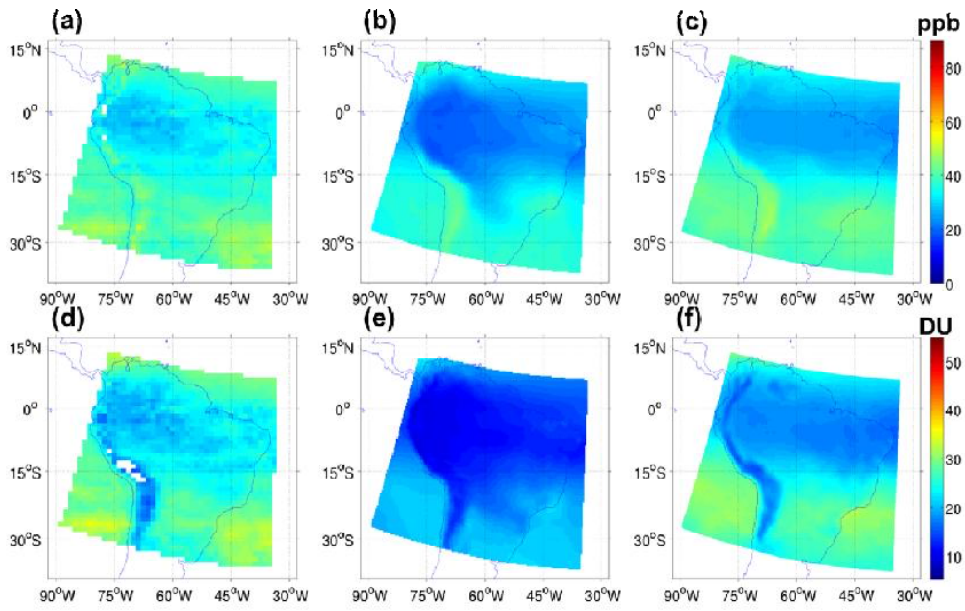
Figure 19. Same as Fig. 18, but daytime (11:00-21:00 UTC) median deposition velocity (cm s⁻¹).



3206

3207 Figure 20. Mean tropospheric O₃ (ppb) on the 35 km domain from (a) OMI/MLS, (b)
 3208 CCATT-BRAMS and (c) WRF-Chem and total tropospheric column O₃ (Dobson units)
 3209 from (d) OMI/MLS, (e) CCATT-BRAMS and (f) WRF-Chem for November 2008.

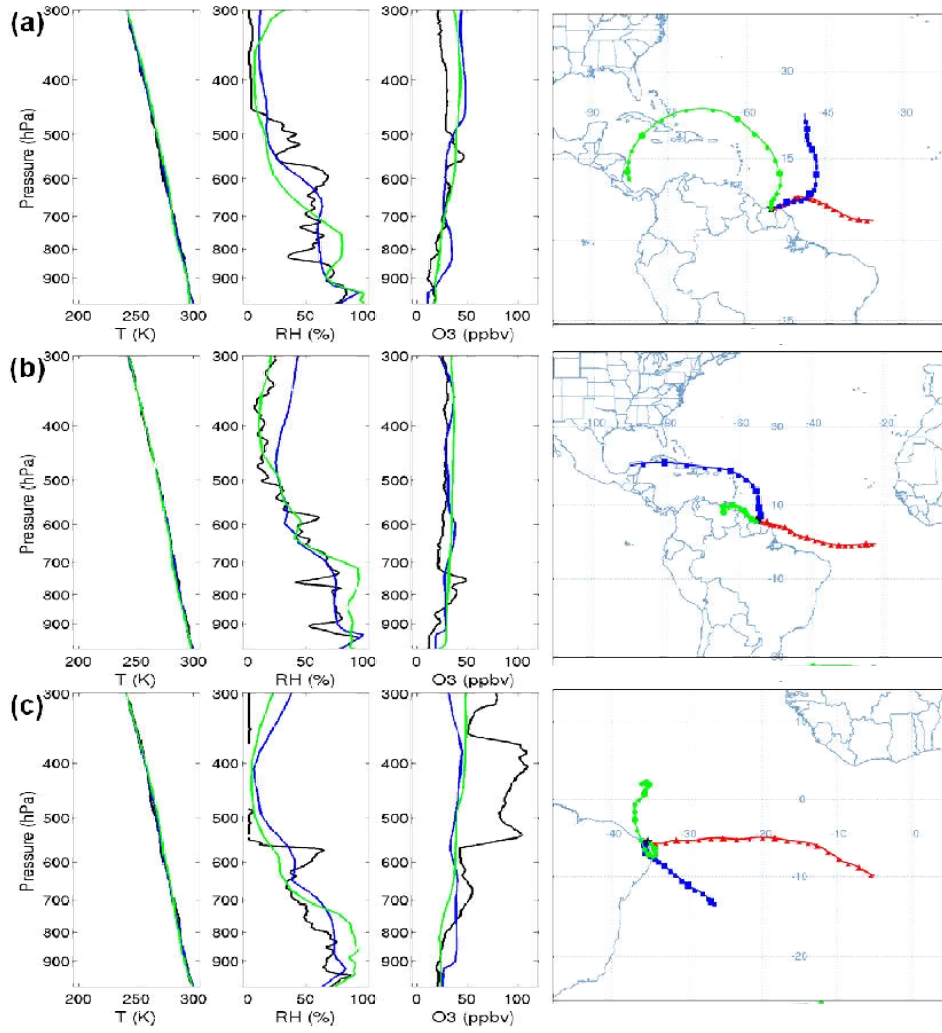
3210



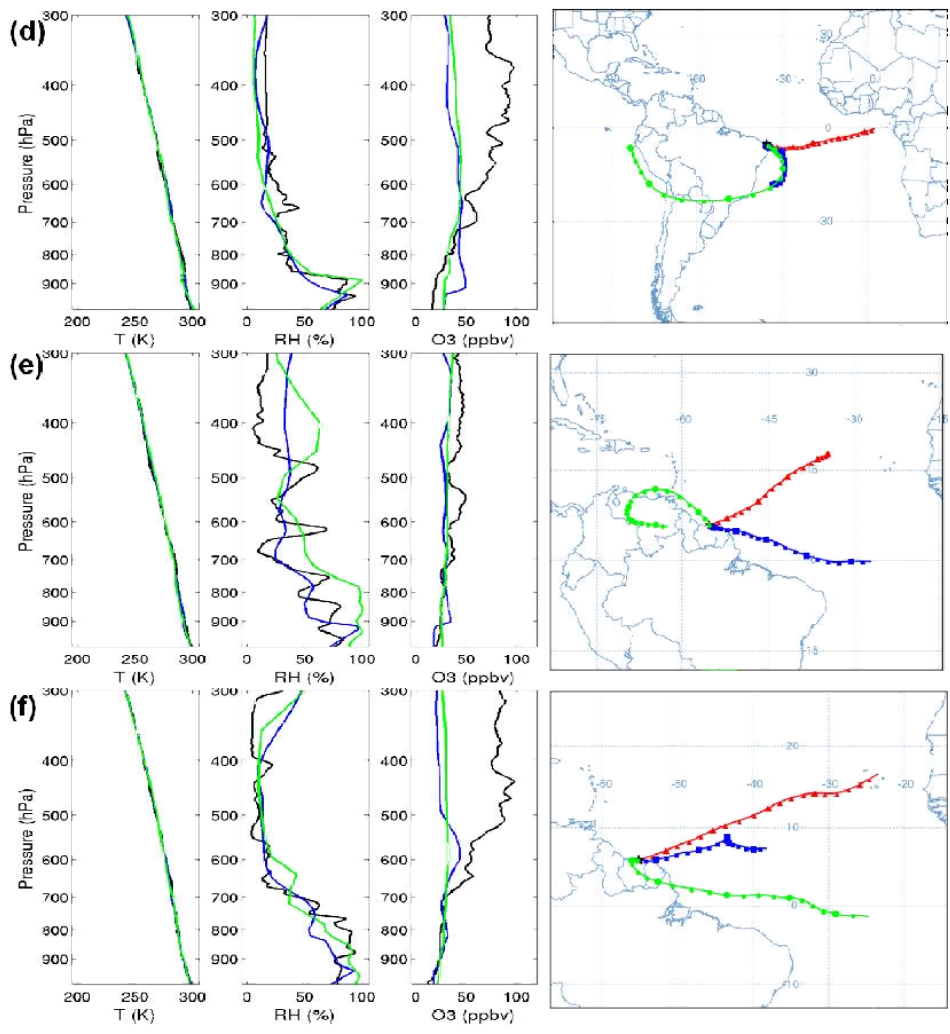
3211

3212 Figure 21. Same as Fig. 20, but for May 2009.

3213



3214



3215

3216 Figure 22. Vertical profiles of potential temperature, relative humidity, and O₃ from
 3217 SHADOZ soundings (black), CCATT-BRAMS (blue) and WRF-Chem (green) and
 3218 HYSPLIT back trajectories at 13:00 UTC, at 1500 m (~850 hPa, red), 6000 m (~470
 3219 hPa, blue) and 9000 m (~310 hPa, green) for: Paramaribo on (a) 6 November and (b) 25
 3220 November 2008, Natal on (c) 7 November, and (d) November 19 2008 and Paramaribo
 3221 on (e) 4 May and (f) 11 May 2009.

Excluído: Z

Excluído: 6

Excluído: 25,

Excluído: 7

It is interesting to compare BARCA data to observations from the NASA Amazon Boundary Layer Experiments ABLE campaigns (ABLE-2A and -2B), which took place during the dry season of 1985 and wet-to-dry transition of 1987. Andreae et al. (2012) showed that CO mixing ratios were about 10 ppb higher during ABLE-2B than in BARCA B everywhere except the southern region, reflecting the global trend towards decreasing CO emissions since the 1980s, particularly in the Northern Hemisphere. The CO comparison also showed a similar enhancement of 10–20 ppb in the lowest 1 km above the surface, attributed to diffuse biogenic sources, and also indicated that the much higher enhancements during the dry season in BARCA A must be due to anthropogenic or biomass burning inputs. The O₃ comparison is expected to yield information in long-term trends in O₃ production in the Amazon Basin, as well as the relative importance of biogenic, urban and fire sources.

Section 1.3 reviews previous observational and remote sensing studies of O₃ distributions and seasonality in the Amazon. Section 2 describes

, as well as the setup of the CCATT-BRAMS and WRF-Chem simulations

Previous studies of O₃ in the Amazon

Analyses of satellite, aircraft and ground-based observations of O₃ over Amazônia since the 1980s have demonstrated the influence of long-range transport of African biomass burning and Northern Hemisphere inputs, local fire sources, NO soil and biogenic VOC emissions, and convective transport on spatial and seasonal variability in O₃. In particular, data from the ABLE-2B aircraft and ground campaign during the 1987 wet-to-dry transition season offers the opportunity to compare the regional O₃ distribution across decades.

Several studies of satellite data have reported a seasonal O₃ maximum in the tropical Southern Hemisphere, largely associated with long-range transport of African fire emissions or lightning NO_x sources. Fishman and Larsen (1987) combined data from 1979-1980 from the Total Ozone

Mapping Spectrometer (TOMS) and the Stratospheric Aerosol and Gas Experiment (SAGE) instruments to construct a climatology of tropospheric O₃ from 15°N to 15°S. They attributed the most elevated O₃ from 60°W to 60°E to biomass burning sources. Thompson et al. (1996) integrated TOMS satellite O₃ data with observations from the Transport and Atmospheric Chemistry near the Equator-Atlantic (TRACE-A) and the southern African Fire-Atmosphere Research Initiative (SAFARI) 1992 experiments. They showed a seasonal maximum in tropospheric O₃ in the south Atlantic, with the highest values (> 90 ppb) between 0-25°S. Back and forward trajectories attributed this elevated O₃ to transport of O₃ from fires in southern Africa by mid-level easterlies or recirculations, with little South American contribution. In Brazil, O₃ was seen to be lofted by deep convective transport, and then transported by high-level westerlies. However, from 0-10°S most of the O₃ was from Africa, since there was a delay of 1-2 months from peak African biomass burning to the O₃ maximum at the coastal site of Natal. O₃ production from the surface to 4 km was estimated to be 15 ppb O₃ per day, with a lower but nonzero rate in the upper troposphere. Using remote sensing observations of fire and lightning flash counts and NO₂, Edwards et al. (2003) identified an early-year tropical Atlantic tropospheric O₃ maximum in January 2001 with two peaks, the first in the lower troposphere from northern hemisphere fires and the second in the southern tropical Atlantic mid-troposphere from lightning NO_x.

For the Amazon region, observations of O₃ and other trace gases were made in several aircraft and ground-based campaigns. These observations identified background (absent of urban and fire influence) O₃ values of around 20 ppb originating from soil NO emissions, decreasing to very low values (~ 5 ppb) at night due to O₃ deposition to the forest. However, nighttime values can be increased due to convective downdrafts, and free troposphere enhancements from biomass burning sources are seen.

The earliest O₃ measurements over the Amazon Basin were made during aircraft campaigns in the dry seasons 1979 and 1980 (Crutzen et al., 1985). Mixing ratios of 20-30 ppb and 40-50 ppb were observed in the boundary layer and the free troposphere, respectively, and elevated O₃ was attributed to photochemical reactions and biomass burning. During the dry season (July-August 1985), the Amazon Boundary Layer Experiment (ABLE-2A) integrated aircraft, ground-based and satellite observations to study the processes affecting the chemical composition in mixed layer over Amazonia (Harriss et al., 1988). Jacob and Wofsy (1988) used a photochemical model

of the Amazonian boundary layer to study the diurnal cycle of isoprene, NO_y and O_3 during ABLE-2A. They found that photochemical production spurred by NO emissions from soils increased daytime O_3 to about 20 ppb. However, at night, dry deposition to the forest caused O_3 to drop below 5 ppb. Model results were consistent with the NO values of 25-60 ppt observed in the lower boundary layer over central Amazonia (Torres and Buchan, 1988). Isoprene emissions were found to have little effect on O_3 levels, as the oxidation of CO would produce sufficient HO_x to generate 20 ppb of O_3 . However, O_3 production in the model was highly sensitive to NO_x emissions, and downward transport from the free troposphere became the dominant source of O_3 in the PBL when NO emissions were decreased below the average value of $44 \pm 14 \mu\text{g N m}^{-2} \text{h}^{-1}$ NO measured by Kaplan et al. (1988). Lidar observations during ABLE-2A showed highly variable O_3 levels, with some small regions with up to 30-40 ppb, attributed to variable NO flux from the canopy (Browell et al., 1988). ABLE-2B was conducted during the wet-to-dry transition season (April-May 1987) (Harriss et al., 1990). Periodic inputs from the Northern Hemisphere were found to be a pollution source over Amazonia, and dry deposition in the region provides a significant sink in the global O_3 budget.

Aircraft measurements from TRACE-A over the South Atlantic in the 1992 dry season attributed high O_3 (> 100 ppb) in the upper troposphere to photochemical production from convectively lofted Brazilian biomass burning emissions. Elevated O_3 (> 75 ppb) originated in lower altitude (< 6 km) plumes from African fires (Browell et al., 1996). During the Smoke, Clouds, and Radiation-Brazil (SCAR-B) campaign (Kaufman et al., 1998), elevated ozone was observed in ozone soundings, launched at Cuiabá from 16 August - 10 September 1995. Elevated ozone was attributed to both local biomass burning pollution and recirculation of urban emissions from SE Brazil. Aerosol backscatter coefficient measurements aboard the ER-2 aircraft during two flights between Cuiabá and Vilhena confirmed the co-occurrence of layers of elevated O_3 with smoke (Longo et al., 1999).

As part of ABLE-2, near-continuous surface O_3 measurements (1.5 m above the surface) showed daytime maximum of 5.7 and 3.7 ppb in a clearing and forest, respectively, and measurements in a tower in a clearing showed an increasing gradient of O_3 with height, up to 6.9 ppb at 15 m above the surface (Kirchhoff et al., 1990). Furthermore, 20 ozonesondes launched in the clearing showed typical mixing ratios of 40 ppb from 500–300 hPa, with values about 10 ppb lower in the wet than dry season.

Observations of O₃, NO_x and CO at a pasture site in the state of Rondônia and forest sites in the states of Pará and Amazonas showed elevated (3x) O₃ and NO₂ levels in the dry-to-wet transition season at the pasture site due to the influence of biomass burning. This was shown by correlations with black carbon and aerosol number concentrations at the surface. On the other hand, NO levels were much lower in the dry-to-wet transition season due to the conversion of NO₂ to NO favored by elevated levels of VOCs, O₃, and radicals, and by higher temperatures. In addition, nighttime ozone was increased in the wet season by transport of ozone-rich cold air from the mid- and upper-troposphere by convective downdrafts, as shown by an anti-correlation of O₃ with equivalent potential temperature (Cordova et al., 2003).

During the LBA-CLAIRE-98 experiment (Andreae et al., 2001) in March 1998, elevated levels of trace gases and biomass burning aerosol were observed at high altitudes (> 9 km) during a flight off the coast of Suriname. Model simulations of CO transport later confirmed the measurements to be the outflow of a deep convective system which had transported biomass burning emissions originating from the northern Amazon (Freitas et al., 2000; Andreae et al., 2001; Gevaerd et al., 2006). During the same experiment, trace gases and CCN spectra were also measured continuously at a ground station in Balbina, near Manaus (Zhou et al., 2002). During the experiment, air masses with origin over undisturbed rainforest and little anthropogenic influence, were sampled at Balbina, yielding O₃ values always less than 20 ppb. Photochemical production of O₃ of up to 15 ppb h⁻¹ was detected via aircraft transects in the Manaus urban plumes (Kuhn et al. 2010). Most of the VOC reactivity was provided by isoprene emissions from the surrounding rainforest, and NO_x emissions suppressed O₃ production close to urban sources, but stimulated it downwind.

Observations at a pasture site in Rondônia in January–February 1999 during the LBA Wet Season Atmospheric Mesoscale Campaign (WETAMC) showed that downward convective transport events increased nighttime surface O₃ up to 30 ppb, compared to a background of 3–5 ppb (Betts et al., 2002). During the LBA-EUSTACH experiments, CCN and trace gases (including O₃, NO_x and VOCs) were measured at forest and pasture sites in Rondônia in the wet-to-dry (27 April–29 May 1999) and dry-to-wet (12 September–27 October 1999) seasons (Andreae et al., 2002; Rummel et al., 2007). The observations showed VOC (isoprene, formaldehyde,

acetaldehyde, acetic and formic acid) concentrations 4-5 times higher in the dry than wet-to-dry transition season as a result of both enhanced biogenic emissions and photochemical decomposition due to increased solar radiation. In addition, VOC and O₃ concentrations peaked in the afternoon (around 15:00 LT) in both seasons and at both sites. Peak O₃ rose from ca. 15 to almost 60 ppb from the wet to dry-to-wet transition season. During the Amazonian Aerosol Characterization Experiment (AMAZE-08), O₃ was measured at the TT34 tower site from 14 February–14 March 2008 (Martin et al., 2010), with observed values of 1-20 ppb (Ebbon et al., 2011). The Tropical Composition, Clouds and Climate Coupling (TC4) experiment, based in Costa Rica in July and August of 2007, involved coordinated flights, including one over the Colombian Amazon, with the NASA ER-2, WB-57 and DC-8 aircraft to study convective processes in the ITCZ region (Toon et al., 2010). Using low ozone as an indicator of convective transport of boundary layer air, a maximum convective outflow height of 10-11 km was estimated (Avery et al., 2010). A flight in the boundary layer over the Columbian Amazon on August 8, 2007 measured O₃ of 10-20 ppb (Jimenez, personal communication, November 12, 2012).

Thus, satellite observations enable the attribution of tropical O₃ maxima to biomass burning and lightning NO_x sources, while ground-based measurements allow the identification of key surface processes in the Amazon Basin affecting O₃ amounts. These processes include O₃ production from soil NO_x emissions and removal via dry deposition to the forest canopy. Aircraft campaigns complete the suite of observations, allowing the examination of convective lofting of surface emissions, with biomass burning emissions of particular importance on the regional scale.

Simulations of BARCA A and B were conducted with the Chemistry Coupled Aerosol-Tracer Transport model to the Brazilian developments on the Regional Atmospheric Modeling System (CCATT-BRAMS; Longo et al., 2013; Freitas et al., 2009) and Weather Research and Forecasting with Chemistry (WRF-Chem; Grell et al., 2005) coupled chemistry and meteorology models. The model physics and chemistry options that were used are listed in Table 1. Both models used a two-way nested grid configuration, with a 140 km grid covering Africa and South America (southwest corner: 60°S, 100°W, northeast corner: 20°N, 50°W), to encompass the cross-Atlantic transport of biomass burning emissions from Africa, and a 35-km resolution grid

covering most of South America (southwest corner: 35°S 85°W, northeast corner: 15°N, 30°W), as depicted in Fig. 3.

The simulations were initialized on 1 October 2008 00:00 UTC and 1 April 2009 00:00 UTC for BARCA A and B, respectively. Boundary conditions and analysis nudging on the outer domain were given by the NCEP GFS analysis (<http://rda.ucar.edu/datasets/ds083.2/>) with a 6 hourly time resolution and 1° × 1° spatial resolution. Chemistry initial and boundary conditions were provided by 6 hourly analyses from the Model of Atmospheric Chemistry at Large Scale (Modélisation de la Chimie Atmosphérique Grande Echelle, MOCAGE) global model (Peuch et al., 1999) with a T42 (~ 2.8°) spatial resolution. Sea surface temperature was provided by the NOAA Optimum Interpolation (OI) Sea Surface Temperature (SST) V2 (available at <http://www.esrl.noaa.gov/psd/data/gridded/data.noaa.oisst.v2.html>) with 1° × 1° spatial resolution. Soil moisture was initialized with the TRMM-based soil moisture operational product (GPNR) developed by Gevaerd and Freitas (2006).

The PBL parameterization in CCATT-BRAMS is based on Mellor and Yamada (1982), while in WRF-Chem the Mellor-Yamada-Janjic (MYJ; Janjić, 1994) scheme was used. In CCATT-BRAMS, shallow and deep convection are parameterized based on the mass-flux approach of Grell and Dévényi (2002). CCATT-BRAMS also uses the Turbulent Kinetic Energy (TKE) from the Planetary Boundary Layer (PBL) scheme to determine if convection will be triggered within a grid cell. In WRF-Chem the Grell 3D (G3) scheme was used, which includes subsidence spreading of convective outflow into neighboring grid cells. The Noah land surface model (Koren et al., 1999) was used in WRF-Chem and the Land Ecosystem–Atmosphere Feedback model v.2 (LEAF-2; Walko et al., 2000) was utilized in CCATT-BRAMS. Land use was provided by the United States Geological Survey (USGS) global 1 km vegetation dataset, updated with a land cover map for the Brazilian Legal Amazon Region for use in meteorological models (PROVEG) (Sestini et al., 2003). PROVEG is based on the Thematic Mapper (TM) Landsat images with spatial resolution of 90 m × 90 m from the year 2000 and deforestation data from the Amazon Deforestation Monitoring Program (PRODES) for the year 1997. For WRF-Chem, albedo and greenness fraction were calculated offline using the updated vegetation dataset, Moderate Resolution Imaging Spectroradiometer (MODIS) Normalized Difference Vegetation Index (NDVI) data from the year 2002–2002 and vegetation parameters from the LEAF-2 land surface model as implemented in CCATT-BRAMS.

Emissions were generated with PREP-CHEM-SRC (Freitas et al., 2011) Version 1.2. Fire emissions were estimated from GOES, AVHRR and MODIS fire count data using the Brazilian Biomass Burning Emission Model (3BEM; Longo et al., 2009).

Anthropogenic emissions were estimated from the RETRO, GOCART and EDGAR v4.0 global databases updated with South American inventories (Alonso et al., 2010). Biogenic emissions were provided by a monthly climatology for the year 2000 produced with the Model of Emissions of Gases and Aerosols from Nature (MEGAN; Guenther et al., 2006). In WRF-Chem, the same Gaussian diurnal cycle with peak at 15:00 UTC (11:00 LT) is applied to both anthropogenic and biogenic emissions, while in CCATT-BRAMS the diurnal cycle of biogenic emissions follows the solar radiation cycle. In both models, the biomass burning daily cycle peaks at 18:00 UTC (15:00 LT). In both CCATT-BRAMS and WRF-Chem, the Regional Atmospheric Chemistry Mechanism (RACM) was used (Stockwell et al., 1997). In WRF-Chem, the Goddard Chemistry Aerosol Radiation and Transport (GOCART; Chin et al., 2002) aerosol scheme was used with aerosol direct radiative effects. CCATT-BRAMS has a smoke aerosol scheme with intensive optical properties (extinction efficiency, single scattering albedo and asymmetry parameter) calculated in an offline Mie code based on observations of climatological size distribution and complex refractive index from AERONET sites in the southern Amazon (Rosario et al., 2011, 2013). CCATT-BRAMS includes scavenging of soluble species in the convective scheme following Berge (1993), as described in Freitas et al. (2005), where the wet removal rates are a function of the precipitation rate, liquid water content and precipitable water. In the cloud microphysics scheme the wet deposition follows Barth et al. (2001), whereby low solubility species partition into the liquid phase according to Henry's Law and high solubility species by diffusion-limited mass transfer. In WRF-Chem, at the convective-parameterizing scale, a constant fraction of gas and aerosol species in convective updrafts are removed (complete removal for sulfur dioxide – SO_2 , sulfate – H_2SO_4 , ammonium – NH_3 , nitric acid – HNO_3 and sea salt; no removal for hydrophobic organic (OC) and black carbon (BC) and dimethyl sulfide (DMS); and 50% removal for all other aerosol species). On the other hand, no wet scavenging is included for cloud water and precipitation resolved by the microphysics scheme, because this option is not currently available in WRF-Chem for the RACM chemical mechanism.

The CCATT-BRAMS simulations also employ a lightning NO_x parameterization based on convective cloud top height (Stockwell et al., 1999). In WRF-Chem, wet deposition and lightning production of NO_x were not considered, because these parameterizations have not yet been evaluated for the Amazon region. Uncertainties remain about the scavenging efficiencies of soluble species by deep convective storms. Simulations of an idealized thunderstorm by several cloud-resolving models yielded varying results for CH_2O , H_2O_2 and HNO_3 in convective outflow due to differing microphysics and assumptions about retention of chemical species during cloud drop freezing (Barth et

al., 2007). In the tropics, over continents, lightning production is comparable to other sources of NO_x , including biomass burning and soil release, and it is the primary source over oceans (Bond et al. 2002). Since lightning NO_x production peaks in the upper troposphere, it could be an important contributor to ozone production. The roles of wet deposition and lightning NO_x production will be more closely examined in future modeling studies of tropospheric chemistry in the Amazon.

For model results evaluation, the mean vertical O_3 profiles for observations, CCATT-BRAMS and WRF-Chem were calculated for the regions to the west, north, south, east, and around Manaus. Horizontal flight legs were excluded from analysis to eliminate the influence of plumes in the boundary layer. To calculate the mean simulated profiles, the four grid points closest in latitude and longitude to each observation were determined at the two model hours that bracket the observations. At each of these grid points and hours, vertical profiles were extracted from the model output and then linearly interpolated to the observed GPS height. The four points from each time were averaged, weighting by the inverse distance to the observed longitude and latitude. Finally, the prior and posterior hour values were averaged with appropriate weights. Thus, 16 model points were used with spatial and temporal weights to obtain each model value for comparison to observations. The observed and model time series were then separated into five regions to the west, north, east, and south of Manaus, and in the region of Manaus itself. The mean value and standard deviation were calculated for each region and 500 m vertical bin.

Mean precipitation during the dry-to-wet (November 2008) and wet-to-dry (May 2009) transition seasons was calculated for the TRMM 3B43 data and the CCATT-BRAMS and WRF-Chem models for three regions: the Amazon ($15^\circ\text{S} - 10^\circ\text{N}$, $50^\circ\text{W} - 80^\circ\text{W}$), northeast Brazil ($15^\circ\text{S} - 0^\circ\text{N}$, $35^\circ\text{W} - 50^\circ\text{W}$), and southeast South America ($15^\circ\text{S} - 35^\circ\text{S}$, $35^\circ\text{W} - 65^\circ\text{W}$). The values are listed in Table 2. The mean precipitation on the 35-km resolution domain for the two months is shown in Figs. 3 and 4, respectively, as well as the delineations of the subregion boxes. The signs of NE-SE differences are correctly modeled by both models during both seasons, i.e., the NE is drier than the SE during November, and vice-versa during May. For the Amazon, CCATT-BRAMS slightly underestimates the precipitation rates in both seasons, but the rate in WRF-Chem is about twice that of TRMM 3B43. The models were also evaluated against TRMM 3B42 3-hourly precipitation rates at the 78 surface station locations in the Amazon (see Table 3). Both models had a positive bias in both seasons, but WRF-Chem had a higher bias and RMSE than CCATT-BRAMS.

, although the mean precipitation rates are slightly lower (CCATT-BRAMS) and substantially higher (WRF-Chem) than the TRMM retrievals in the Amazon region.

Peak shortwave radiation is slightly overestimated by both models, which may be related to low cloudiness (convection is triggering too early) or AOD (too much aerosol wet removal). This will increase O₃ production from photolysis, as well as increase surface temperature and evaporation. Although biogenic emissions are not coupled with meteorology in these simulations, this may increase biogenic emissions in future studies that include online biogenic emissions. WRF-Chem predicts a nearly constant Bowen ratio at forest and pasture sites. This indicates that the Noah land surface model is not properly representing the impact of conversion of forest to pasture and the resulting increase in sensible heat flux.

In the dry-to-wet transition season, for both CCATT-BRAMS and WRF-Chem, the mean daily cycle of surface incident shortwave radiation calculated for the Manaus AERONET site for October–November 2008, falls within one standard deviation of the mean AERONET observations (Fig. 6), but is closer to the upper limit, possibly due to underestimated cloudiness or AOD in the models. For the forest and pasture sites, both models represent the daily cycles of incident shortwave and ingoing and outgoing longwave radiation, although incident shortwave is slightly overestimated (by 50–100 W m⁻²) at peak (Fig. 7). During the wet-to-dry transition season, both models overestimate peak incident shortwave radiation by about 100 W m⁻² (Fig. 8), suggesting that they underestimate cloudiness. Both models represent the daily cycles of incident shortwave and ingoing and outgoing longwave radiation, although incident shortwave is slightly overestimated (by 50–100 W m⁻²) at peak. For both models, CCATT-BRAMS and WRF-Chem, the mean daily cycle of surface incident shortwave radiation calculated for the Manaus AERONET site for Oct.–Nov. 2008, falls within one standard deviation of the mean AERONET observations (Fig. 7), but is closer to the upper limit, possibly due to underestimated cloudiness or AOD in the models.

peak latent heat flux at 13:00 LT is higher at the forest site than at the pasture site (460 W m⁻² vs. 268 W m⁻²) whereas the sensible heat flux shows an opposite difference (180 vs. 215 W m⁻²), due to lower evapotranspiration and higher surface temperatures in the pasture. As a result, the

Both models represent the daily cycles of incident shortwave and ingoing and outgoing longwave radiation, although incident shortwave is slightly overestimated (by 50-100 W m⁻²) at peak. For both models, CCATT-BRAMS and WRF-Chem, the mean daily cycle of surface incident shortwave radiation calculated for the Manaus AERONET site for Oct.-Nov. 2008, falls within one standard deviation of the mean AERONET observations (Fig. 7), but is closer to the upper limit, possibly due to underestimated cloudiness or AOD in the models.

as for the dry-to-wet transition, peak latent heat flux at 13:00 LT is higher at the forest site than at the pasture site (401 W m⁻² vs. 324 W m⁻²). However, the sensible heat flux is also higher at the pasture site (119 W m⁻² vs. 168 W m⁻²) and

Mean vertical profiles at Manaus from radiosoundings, CCATT-BRAMS and WRF-Chem for October - November 2008 at 0, 12 and 18Z and April - May 2009 at 0 and 12Z are shown in Figs. 9 and 10. For BARCA A, while the temperature profile is well represented by the models, the dew point temperature in CCATT-BRAMS is approximately 10 K too high above 500 hPa and 5 K too low below 500 hPa. The wind speed is overestimated by both models above 500 hPa and underestimated below 500 hPa. For BARCA B, dew point temperature is about 5 K too high in CCATT-BRAMS above 500 hPa. Wind speed is about 2 m s⁻¹ too low above 600 hPa in both models. The models were evaluated against data from 26 METAR (airports) and 52 Synop (INPE) surface meteorological stations, whose locations are depicted in Fig. 11. Values of Root Mean Squared Error (RMSE) and bias for various meteorological parameters for CCATT-BRAMS and WRF-Chem simulations for BARCA A (October - November 2008) and BARCA B (April - May 2009) are shown in Table 3.

surface pressure is underestimated by 1 - 2 hPa. Wind speed is underestimated by CCATT-BRAMS and overestimated by WRF-Chem by 0.1 - 0.6 m s⁻¹, and

Now we summarize the key findings of the model-data meteorological comparison and their implications for the chemistry simulations. The models capture the seasonal spatial distribution of precipitation over northern South America, although the mean

precipitation rates are slightly lower (CCATT-BRAMS) and substantially higher (WRF-Chem) than the TRMM retrievals in the Amazon region. This may indicate errors in the strength and vertical distribution of convective transport and the amount of convective wet removal. Peak shortwave radiation is slightly overestimated by both models, which may be related to low cloudiness (convection is triggering too early) or AOD (too much aerosol wet removal). This will increase O₃ production from photolysis, as well as increase surface temperature and evaporation. Although biogenic emissions are not coupled with meteorology in these simulations, this may increase biogenic emissions in future studies that include online biogenic emissions. WRF-Chem predicts a nearly constant Bowen ratio at forest and pasture sites. This indicates that the Noah land surface model is not properly representing the impact of conversion of forest to pasture and the resulting increase in sensible heat flux.

Página 35: [15] Movido para a página 35 (Mover #6)

12/10/2014 15:42:00

mbela

The models generally show good agreement with soundings, but excess moisture in CCATT-BRAMS above 500 hPa may stimulate excess O₃ production.

Página 39: [16] Movido para a página 39 (Mover #3)

12/10/2014 15:22:00

mbela

The mean tropospheric and total tropospheric column O₃ from OMI/MLS, CCATT-BRAMS and WRF-Chem for November 2008 and May 2009 are shown in Figs. 15 and 16, respectively. The models significantly underestimate the total columns from satellite and middle altitudes from BARCA. For both BARCA A and B, the models represent the pattern of lower O₃ over the Amazon and higher values over northeast Brazil (BARCA A only) and at 30°S, although the values are strongly underestimated. In November 2008, OMI/MLS mean tropospheric O₃ concentrations show an inflow of elevated O₃ (mean ca. 55 ppb, total 40-45 DU) on the northeast Brazilian coast due to cross-Atlantic transport from biomass burning in southern and sub-Saharan Africa. Additionally, a band of elevated O₃ (mean 55-60 ppb, total 35-40 DU) passes over the South American continent at around 30°S, also from cross-Atlantic transport. During this month, Northern Hemisphere O₃ levels to the north of South America are relatively low (mean 35-40 ppb, total 25-30 DU). On the other hand, the tropospheric ozone distribution in May 2009 (Fig. 16) is characterized by a band of low ozone extending over the Amazon Basin and northeast Brazil between 10°S and 10°N (mean 25-35 ppb, total 20-25 DU). In addition, lightly elevated values at around 30°S,

primarily over the oceans (40-55 ppb, 30-35 DU) and higher ozone in the Northern Hemisphere (mean 50-55 ppb, total 35-40 DU north of 10°N). Both models capture the overall distribution (inflow in NE Brazil in Nov. 2008, lower values over the Amazon Basin, elevated at 30°S) but values are underestimated relative to OMI/MLS.

However, the BARCA observations are generally lower than the models in the boundary layer, indicating that the satellites appear here to be dominated by the middle troposphere and long-range transport. An example of observed and simulated O₃ during the flight legs between Manaus and Belém in BARCA A and B is shown in Fig. 17. While the models capture the pattern of increasing O₃ values with height, the models underestimate elevated O₃ values from 2.5-4.5 km, and overestimate low values near the surface (1-1.5 km). The models also do not reproduce the variability in the high values, likely due to the aircraft intersection of biomass burning plumes. This is expected given the coarse horizontal grid resolution. Thus, mean profiles are analyzed in order to study differences among the regions and seasons and to assess the models' abilities to capture the impacts of such small-scale processes on regional O₃ distributions.

The mean vertical O₃ profiles for observations, CCATT-BRAMS and WRF-Chem for the regions to the west, north, south, east and around Manaus are shown for BARCA A and B in Figs. 18 and 20, respectively, and NO profiles corresponding to the aircraft tracks are depicted in Figs. 19 and 21, respectively. Mean profiles from longitudinal surveys over Amazônia of O₃ during ABLE-2A (Browell et al., 1988) and ABLE-2B (Harriss et al., 1990) and NO during ABLE-2A (Torres and Buchan, 1988) are included for comparison. In BARCA B, O₃ values were at or near background values in all regions, ranging from 8 - 15 ppb at the surface to 2 - 15 ppb at 4-4.5 km, and the models are generally within 5-10 ppb of the observations. During BARCA A, while the W region still had low O₃ values (5 ppb at the surface to 20 ppb at 4-4.5 km), the N, S and M regions ranged from 15-20 ppb at the surface to 30-35 ppb at 4-4.5 km, and the E region presented the most elevated values, from 25-55 ppb. ABLE-2A O₃ profiles are similar in all regions, ranging from 15-20 ppb near the surface to 30-40 ppb from 4-6 km, so that the BARCA values are higher in the fire-influenced east and south regions, lower in

the north and west regions, and very similar around Manaus. The profiles from ABLE-2B are within one standard deviation of the BARCA B measurements, except for the north region, where they are lower (5-15 ppb). These results suggest an increasing influence of fire emissions to the east and south of Manaus, but that O₃ in clean regions has not changed much.

Both models generally overestimate O₃ from 1-2 km and underestimate O₃ from 3-4.5 km. As seen in the CO results shown in Andreae et al. (2012), the model profiles have steeper slopes than the observations, except in the polluted south, possibly due to excessive vertical mixing of precursors. In addition, the models may be missing sources of O₃ and/or precursors at 3-4.5 km in the model inflow boundary conditions. In general the models overestimate O₃ in the PBL compared to aircraft measurements, but underestimate the total column values relative to the OMI/MLS satellite product. This suggests that the total column values in Amazonia are dominated by global pollution from Africa, rather than local O₃ production from biomass burning.

4.3.2

Página 39: [18] Movido para a página 40 (Mover #2)
12/10/2014 15:19:00

mbela

The excess O₃ in the PBL in the models could be due to either a low deposition sink, as O₃ dry deposition velocities in the models are about half of observed values, or excessive model sensitivity to NO_x emissions, or both. Two additional simulations were conducted with WRF-Chem to evaluate the model sensitivity to these processes: (1) doubling the calculated deposition velocity for O₃ only (2DEPVEL) and (2) halving the NO_x surface emission rates (0.5ENOX). The O₃ profiles corresponding to BARCA flights for these two simulations are also included in Figs. 18 and 20. The corresponding NO profiles from all model simulations as well as a mean profile over Amazônia from ABLE-2A are depicted in Figs. 19 and 21. The 0.5ENOX simulation reduces O₃ more than 2DEPVEL throughout the entire profile. In the dry-to-wet transition, 2DEPVEL reduces O₃ in the lower PBL by about 25%, while 0.5ENOX decreases O₃ by around 40%, and in the wet-to-dry-transition the reductions are about 10% and 30%, respectively. In general the 0.5ENOX O₃ profiles are lower than observed in the first 500 m above the surface, but they provide the best representation of the data for the north and west regions in the dry-to-wet transition. They also provide a similarly good fit as 2DEPVEL for the east, Manaus and south regions, while in the wet-to-dry transition 0.5ENOX is closer to the observed value from 0-500 m in all regions except the north. During BARCA A, NO in all WRF-Chem simulations in the north, west, and Manaus

regions is 10-15 ppt from 0-500 m above the surface, increasing to a maximum of 20-50 ppt at 2 km agl, and is generally lower than the ABLE-2A observations in the PBL. In the east and south, where biomass burning influence was seen, NO in 0-500 m agl increased from 20-50 ppt in the base simulation to 35-60 ppt in 2DEPVEL due to decreased O₃ and conversion of NO to NO₂, and was generally within one standard deviation of the ABLE-2A measurements in the PBL. In BARCA B, NO simulated by WRF-Chem is very low, 5-10 ppt in the entire profile, except for the west region, where a mean NO of 30 ppt is seen from 0-500 m a.g.l. This is again due to very low O₃, and for the Manaus region, where anthropogenic NO_x sources may have contributed to NO values of 20 ppt. These results suggest that adjustment of dry deposition parameterizations are needed to increase O₃ deposition velocities by about a factor of two in agreement with ground observations. Future research will compare simulated NO_x fields with observations from more recent field campaigns, as the results of these simulations also suggest that O₃ in WRF-Chem is very sensitive to NO_x emissions.

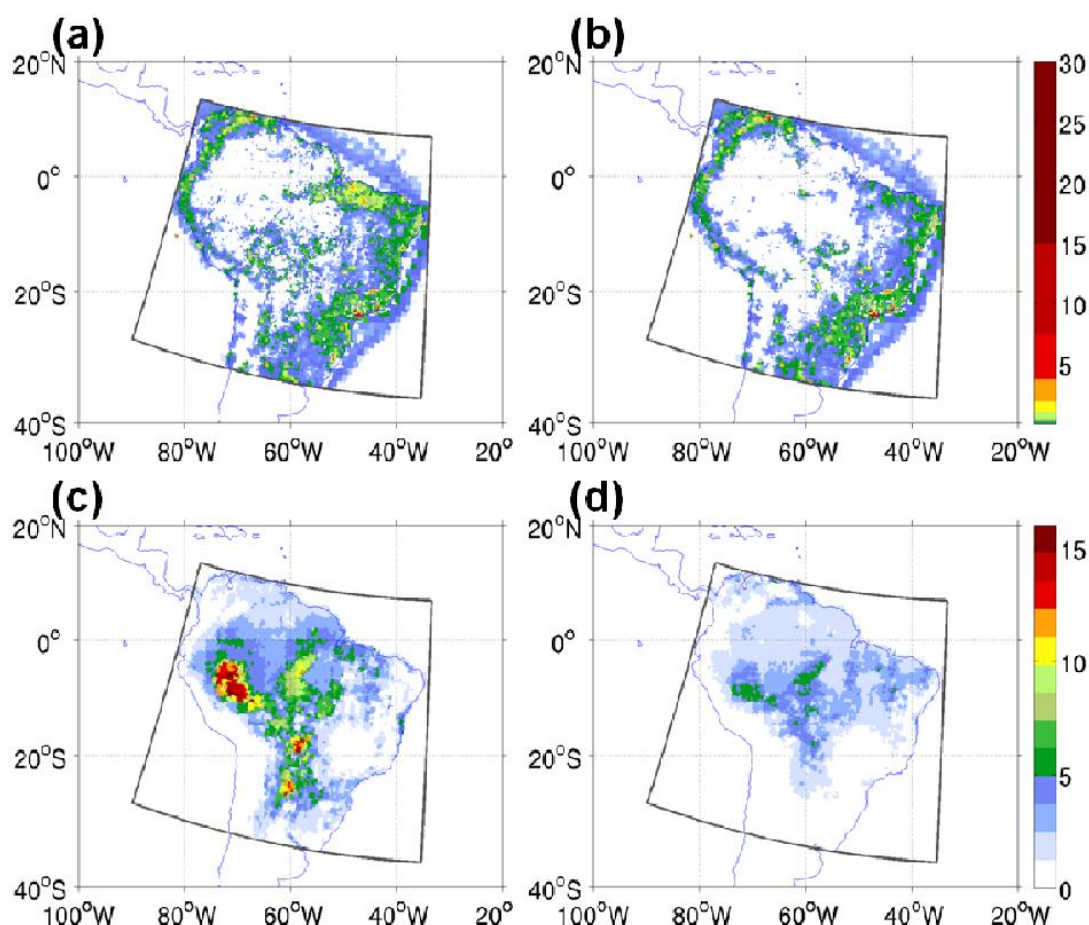


Figure 12. Mean emission rates (10^{-5} kg m⁻² day⁻¹) from PREP-CHEM-SRC for the 35 km domain (dark gray outline) for NO_x for (a) BARCA A (November 2008) and (b) BARCA B (May 2009) and isoprene for (c) BARCA A and (d) BARCA B periods.

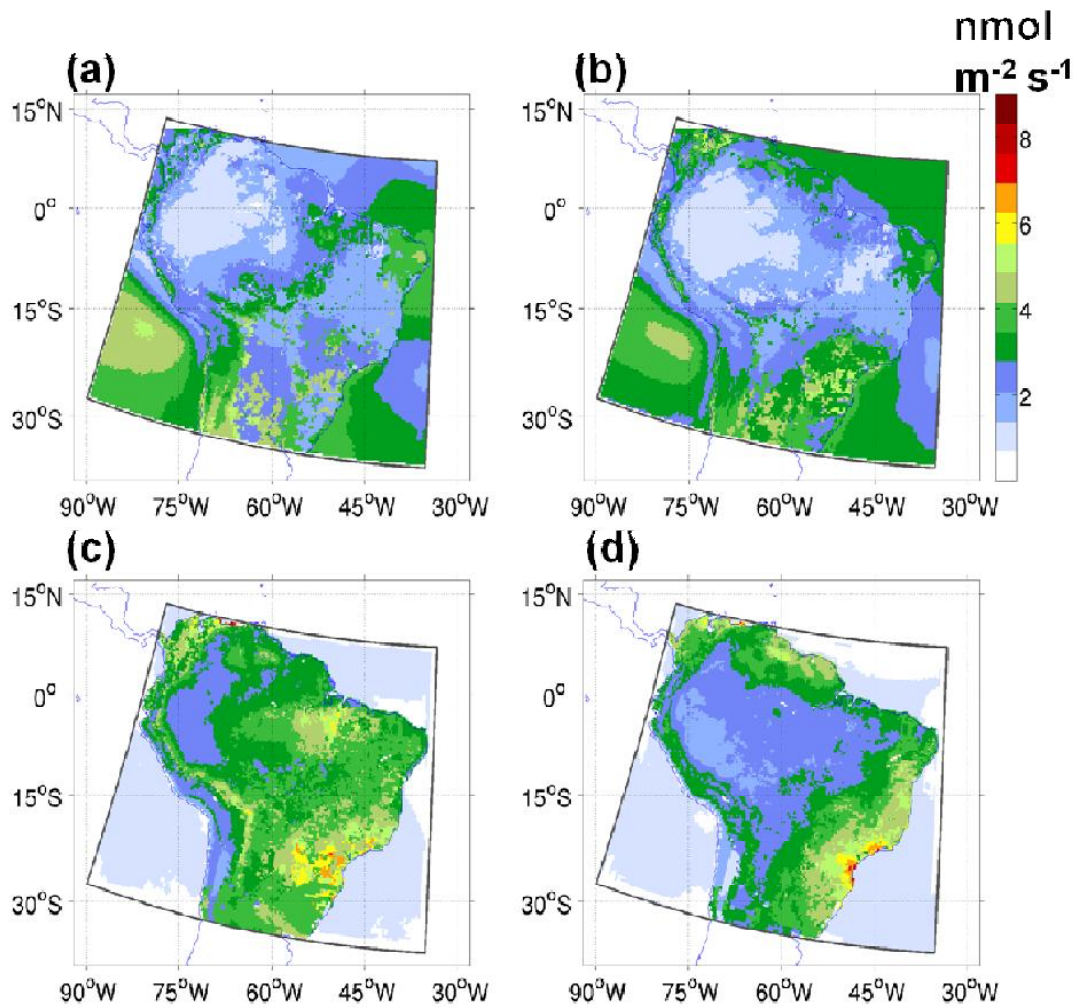


Figure 13. Average O₃ dry deposition flux ($\text{nmol m}^{-2} \text{s}^{-1}$) as simulated on the 35 km resolution domain (dark gray outline) by the CCATT-BRAMS model for (a) November 2008 and (b) May 2009 and by the WRF-Chem model for (c) November 2008 and (d) May 2009.

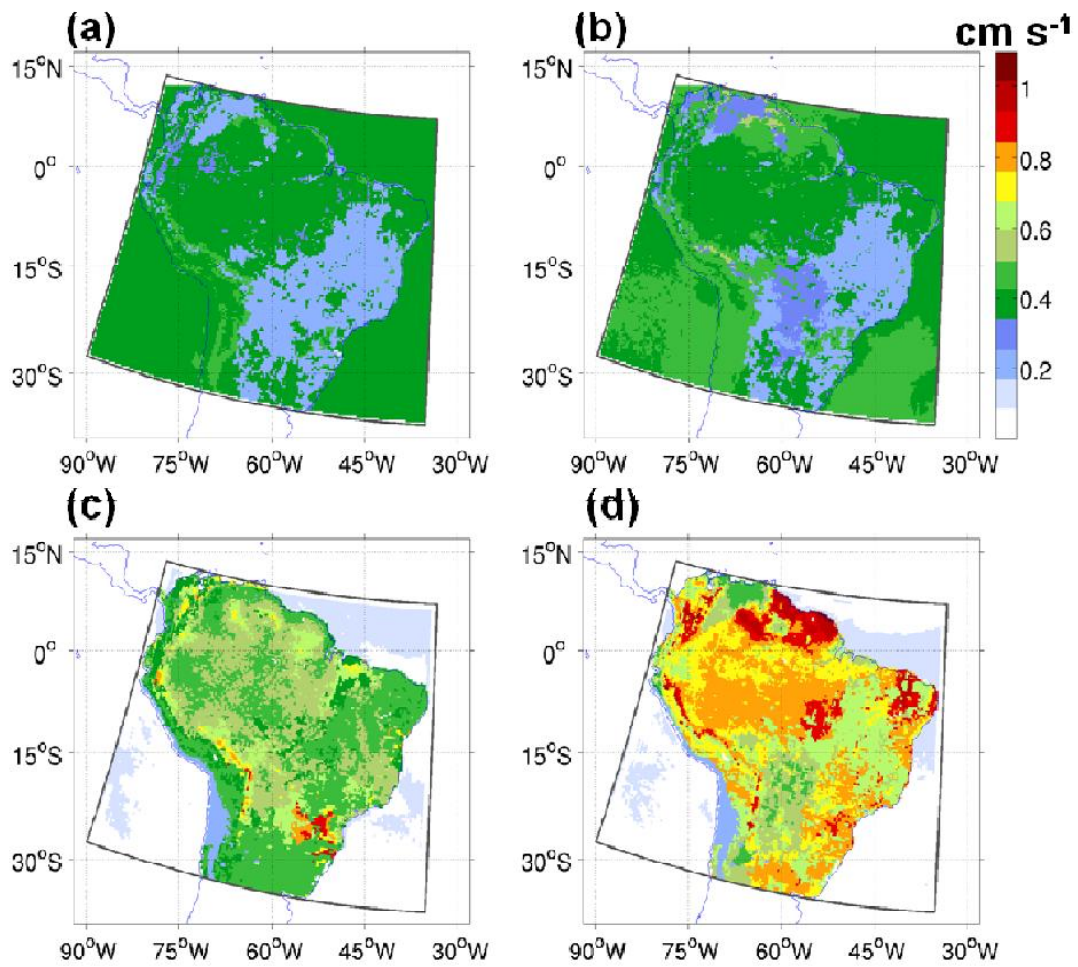


Figure 14. Same as Fig. 13, but daytime (11:00-21:00 UTC) median deposition velocity (cm s^{-1}).

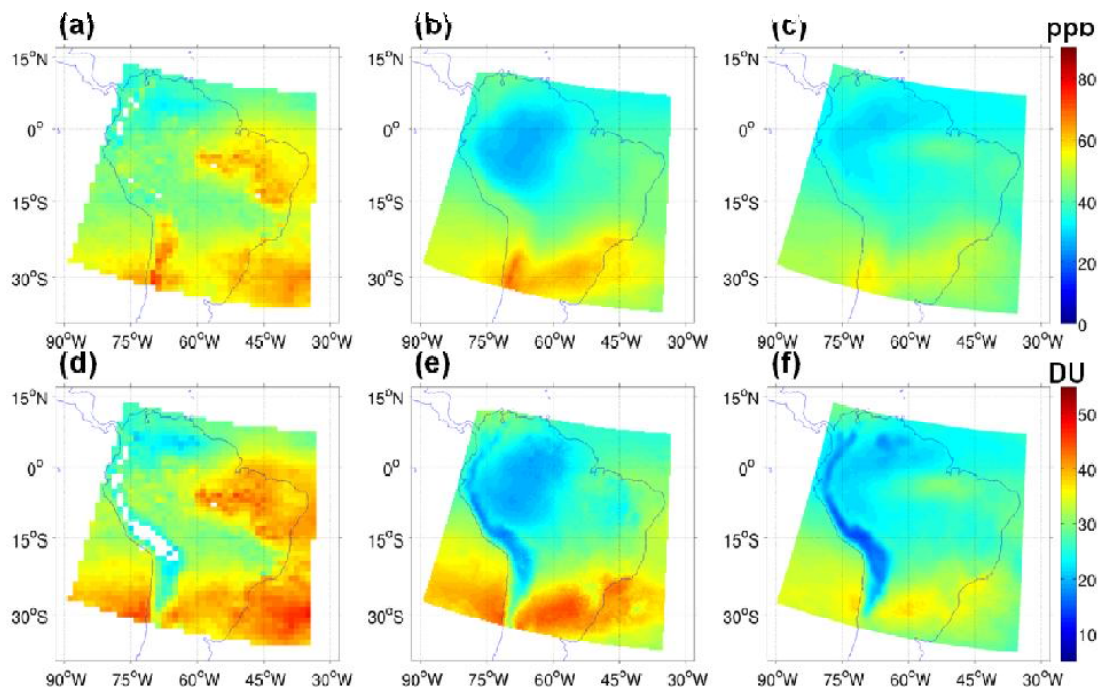


Figure 15. Mean tropospheric O₃ (ppb) on the 35 km domain from (a) OMI/MLS, (b) CCATT-BRAMS and (c) WRF-Chem and total tropospheric column O₃ (Dobson units) from (d) OMI/MLS, (e) CCATT-BRAMS and (f) WRF-Chem for November 2008.

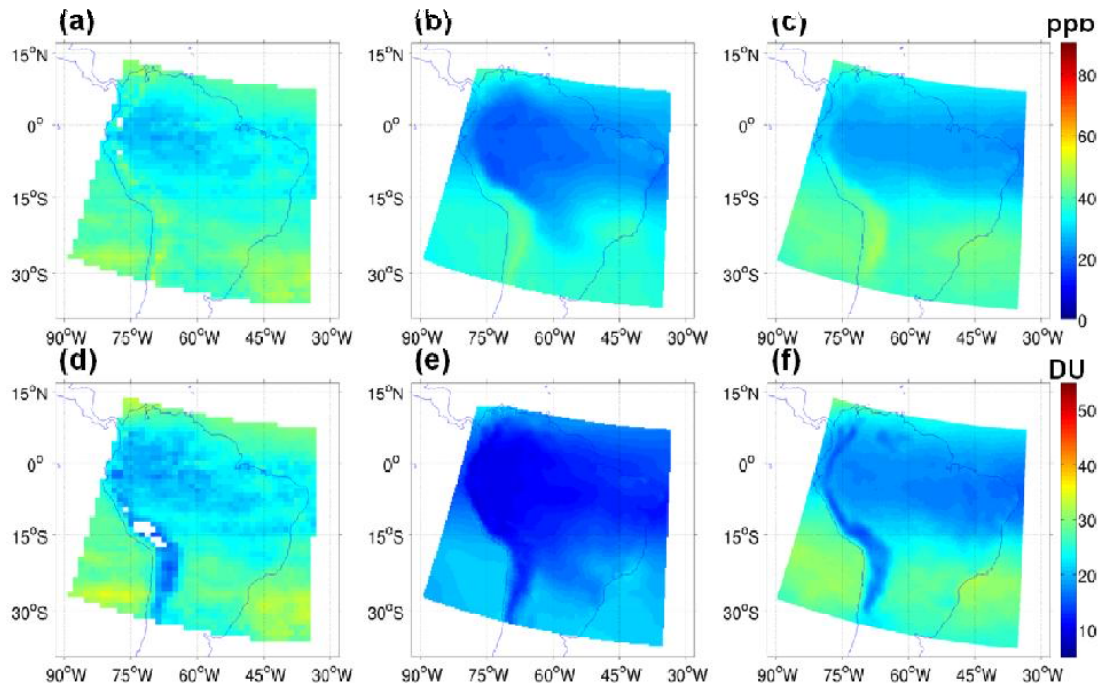


Figure 16. Same as Fig. 15, but for May 2009.